
Investigation of the Impact of Magnesium Implants on the Proteomes of Bone Cells and Bone Tissue

Dissertation with the aim of achieving a doctoral degree
at the Faculty of Mathematics, Informatics and Natural Sciences

Department of Chemistry
University of Hamburg

submitted by

Maryam Omid

from Tehran, Iran

Hamburg

2017

**The following evaluators recommend the admission of the
dissertation:**

Prof. Dr. Hartmut Schlüter

Prof. Dr. Dr. Christian Betzel

Date of disputation:

28.04.2017

This work was done from 2012 until 2016 in the department of clinical chemistry at Universitätsklinikum Hamburg-Eppendorf (UKE) in the working group of Prof. Dr. Hartmut Schlüter.

Dedicated to my lovely parents...

Abstract

Bio-absorbable magnesium (Mg)-based implants offer various superiorities over conventional implants as they get degraded during corrosion thereby avoiding a removal surgery. Furthermore, the osteoinductive properties of Mg and its corrosion products may improve bone formation. In this study, the response of osteoblasts and bone tissues towards Mg-implants and conventional implants at proteome level was compared.

In the first part of this study, the impact of magnesium and titanium implants on the proteomes of cultured osteoblasts was studied via label-free quantification proteomics.

The data show: firstly the number of regulated proteins in the presence of Mg-discs was higher than Ti- compared to control; and secondly Mg- implant may be advantageous for bone remodeling & fracture healing. Furthermore, regulation of 3 proteins in response to Mg-discs was advantageous for cell viability. However, one protein was up-regulated in cellular response to oxidative stress. Overall, the impact of Mg on osteoblasts is more advantageous than the response to Ti regarding bone healing and cell viability.

In the second part of this study, the effect of Mg-implants on the proteome of mice bone tissue was compared to steel (S)-implant as a control in 7, 14, 21, and 133 days after implantation. The extraction of proteins from formalin-fixed plastic embedded- bone sections was performed according to a novel method, followed by label-free quantification proteomics. The results showed a higher change in the proteome of mice bone in response to Mg- compared to S-implants two weeks after implantation. Many of the regulated proteins in the presence of Mg-implants compared to S-implants have a positive effect on bone formation while a few negatively regulate bone formation. Some of the proteins related to inflammatory reaction were significantly regulated after 14 days. After 133 days there was no difference any more compared to the control. In contrast coagulation factor X (FX) was down-regulated in the group of Mg-implant mice even after 133 days, after the Mg-implants have disappeared. This phenomenon should be addressed in future experiments.

Zusammenfassung

Bioresorbierbare, Magnesium- (Mg-)basierte Implantate bieten verschiedene Überlegenheit gegenüber herkömmlichen Implantaten, da sie während der Korrosion abgebaut werden, wodurch eine operative Entfernung des Implantats vermieden wird. Mg-Implantate und seine Korrosionsprodukte haben osteoinduktive Eigenschaften, die für die Knochenheilung vorteilhaft sein könnte. In dieser Studie wurde die Reaktion von Knochenzellen (hier Osteoblasten) und Knochengewebe auf bioresorbierbaren sowie konventionellen Implantaten auf der Proteomebene verglichen, um die Frage zu beantworten, welchen systemischen Einfluss Mg-Implantate und seine Korrosionsprodukte auf Knochengewebe hat.

Im ersten Teil dieser Studie wurde der Einfluss von Magnesium- und Titan-Implantaten auf kultivierte Osteoblasten untersucht. Die Proteine wurden aus den Zellen extrahiert mit einer markierungsfreien quantitativen Proteomanalyse analysiert. Die Ergebnisse zeigen, dass die Anzahl der regulierten Proteine in Gegenwart von Mg-Implantaten höher lag als die von Ti-Implantaten und dass das Mg-Implantat die Regenerierung des Knochengewebes unterstützt. Darüber hinaus sind 3 regulierte Proteine bei Mg-Implantaten für die Zellviabilität vom Vorteil. Allerdings wurde ein Protein beim zellulären oxidativen Stress hochreguliert. Insgesamt ist der Einfluss von Mg-Implantaten im Vergleich zu Ti-Implantaten auf Osteoblasten vorteilhafter bezüglich der Knochenheilung und der Zellviabilität.

Im zweiten Teil dieser Studie wurde die Wirkung von Mg-Implantaten auf das Proteom des Mäuse-Knochengewebes mit der Wirkung von Stahl- (Steel/St)-Implantaten als Kontrolle in 7, 14, 21 und 133 Tage nach dem Implantieren verglichen. Die Proteinextraktion aus formalin-fixierten, kunststoff-eingebetteten Knochenschnitten erfolgte mit einer neu entwickelten Methode. Die Proteome wurden mit einer markierungsfreien Methode quantifiziert.

Nach zwei Wochen zeigten die Mäuseknochen mit Mg-Implantaten eine deutlich größere Veränderung als die Mäuseknochen mit St-Implantaten. Viele der durch die Anwesenheit von Mg regulierten Proteine haben einen positiven Effekt auf die Knochenbildung, während die Zahl der regulierten Proteine klein ist, die mit einer für die Knochenbildung ungünstigen Eigenschaft assoziiert sind.

Die Konzentrationen einiger Proteine mit Funktionen im Bereich von Entzündungsreaktionen waren nach 14 Tagen signifikant verändert.

Nach 133 Tagen wurden von diesen Proteinen keine Unterschiede mehr gemessen. Die Konzentration des Koagulationsfaktor X (FX) war in der Gruppe der Mg-Implantat-Mäuse zu allen Zeitpunkten signifikant erniedrigt. Diese Beobachtung muss in zukünftigen Experimenten genauer untersucht werden, um sicher zu stellen, dass von Mg-Implantaten keine unerwünschten Wirkungen ausgehen.

List of published papers:

1. Kwiatkowski, M., Wurlitzer, M., Krutilin, A., Kiani, P., Nimer, R., **Omidi, M.**, Mannaa, A., Bussmann, T., Bartkowiak, K., Kruber, S., Uschold, S., Steffen, P., Lübberstedt, J., Küpker, N., Petersen, H., Knecht, R., Hansen, N.O., Zarrine-Afsar, A., Robertson, W.D., Miller, R.J., Schlüter, H. (2016) Homogenization of tissues via picosecond-infrared laser (PIRL) ablation: Giving a closer view on the in-vivo composition of protein species as compared to mechanical homogenization. *J Proteomics*. 16 (134):193-202.
2. Kwiatkowski, M., Wurlitzer, M., **Omidi, M.**, Ren, L., Kruber, S., Nimer, R., Robertson, W.D., Horst, A., Miller, R.J., Schlüter, H. (2015) Ultrafast extraction of proteins from tissues using desorption by impulsive vibrational excitation. *Angew Chem Int Ed Engl*. 54(1):285-8.
3. Steurer, S., Singer, J.M., Rink, M., Chun, F., Dahlem, R., Simon, R., Burandt, E., Stahl, P., Terracciano, L., Schlomm, T., Wagner, W., Höppner, W., **Omidi, M.**, Kraus, O., Kwiatkowski, M., Doh, O., Fisch, M., Soave, A., Sauter, G., Wurlitzer, M., Schlüter, H., Minner, S. (2014) MALDI imaging-based identification of prognostically relevant signals in bladder cancer using large-scale tissue microarrays. *Urol Oncol*. 32(8):1225-33.
4. Quaas, A., Bahar, A.S., von Loga, K., Seddiqi, A.S., Singer, J.M., **Omidi, M.**, Kraus, O., Kwiatkowski, M., Trusch, M., Minner, S., Burandt, E., Stahl, P., Wilczak, W., Wurlitzer, M., Simon, R., Sauter, G., Marx, A., Schlüter, H. (2013) MALDI imaging on large-scale tissue microarrays identifies molecular features associated with tumour phenotype in oesophageal cancer. *Histopathology*. 63(4): 455-62.
5. Richter, V., Kwiatkowski, M., **Omidi, M.**, Omidi, A., Robertson, W.D., Schlüter, H., (2013) Review: Mass spectrometric analysis of protein species of biologics. *Pharmaceutical Bioprocessing*. 1 (4): 381-404.

List of published conference abstracts:

1. **Omidi, M.**, Gasser, A., Hesse, E., Weinberg, A., Willumeit, R., Schlüter, H. (August 2014) Proteomic approaches for studying bone tissue sections. *eCM Journal*. 28(3):72.
2. Schlüter, H., **Omidi, M.**, A Burmester, A., Willumeit, R. (August 2014) Application of proteomics for investigating the impact of magnesium implants on bone tissue. *eCM Journal*. 28(3):51.

Oral Presentation:

1. **Omidi, M.**, Burmester, A., Kiani, P., Kwiatkowski, M., Luthringer, B., Willumeit, R., Schlüter, H. (August 2015) Investigation the impact of magnesium-implants compared to titanium-implant on protein composition in cultured osteoblast by label free quantification. 7th Symposium on Biodegradable Metals, Riva Marina Resort, Carovigno, Italy.

Poster presentations:

1. **Omidi, M.**, Burmester, A., Schütz, D., Wurlitzer, M., Kwiatkowski, M., Luthringer, B., Willumeit-Römer, R., Schlüter, H. (Feb-March 2016) Application of proteomics on bone cells in response to Mg-alloys compared to Ti-Implants. 49. Annual meeting of the German Society of Mass Spectrometry (DGMS), Hamburg, Germany.
 2. **Omidi, M.**, Burmester, A., Kiani, P., Kwiatkowski, M., Luthringer, B., Willumeit, R., Schlüter, H. (August 2015) Investigation the impact of magnesium-implants compared to titanium-implant on protein composition in cultured osteoblast by label free quantification. 7th Symposium on Biodegradable Metals, Riva Marina Resort, Carovigno, Italy.
 3. Schlüter, H., **Omidi, M.**, Kwiatkowski, M., Wurlitzer, M., Burmester, A., Luthringer, B., Römer-Willumeit, R. (August 2015) Analysis of the response of bone cells towards magnesium alloys by proteomics. 7th Symposium on Biodegradable Metals, Riva Marina Resort, Carovigno, Italy.
 4. **Omidi, M.**, Burmester, A., Kiani, P., Kwiatkowski, M., Luthringer, B., Willumeit, R., Schlüter, H. (March 2015) Proteomic study of the impact of Magnesium implants on osteoblasts. Annual meeting of the German Society of Mass Spectrometry (DGMS), Wuppertal, Germany.
 5. **Omidi, M.**, Gasser, A., Hesse, E., Weinberg, A., Willumeit, R., Schlüter, H. (August 2014) Proteomic approaches for studying bone tissue sections. 6th Symposium on Biodegradable Metals, Maratea, Italy.
 6. Schlüter, H., **Omidi, M.**, A Burmester, A., Willumeit, R. (August 2014) Application of proteomics for investigating the impact of magnesium implants on bone tissue. 6th Symposium on Biodegradable Metals, Maratea, Italy.
 7. **Omidi, M.**, Kraus, O., Wurlitzer, M., Kwiatkowski, M., Schlüter, H. (March 2014) Development a method for identification of protein in formalin-fixed paraffin embedded tissues. Annual meeting of the German Society of Mass Spectrometry (DGMS), Frankfurt, Germany.
 8. **Omidi, M.**, Gasser, A., Hesse, E., Schlüter, H. (March 2013) MALDI Mass Spectrometry Imaging of Bone Tissue. Annual meeting of the German Society of Mass Spectrometry (DGMS), Berlin, Germany.
-
-

Table of contents

List of abbreviations	I
1 Introduction	1
<hr/>	
1.1 Magnesium	1
1.2 Bioadsorbable implants	2
1.3 Bone and bone cells	3
1.4 Inflammation	4
1.5 Proteomics	5
1.5.1 Mass spectrometry-based proteomics	5
1.5.2 Labeling and label free mass spectrometry approaches	6
2 Aim of the study	9
3 Materials and methods	10
<hr/>	
3.1 Chemicals	10
3.2 Biomaterials	11
3.3 Equipments	11
3.4 Softwares	12
3.5 Sample preparation prior to Mass spectrometry analysis	13
3.5.1 Sample preparation for <i>in vitro</i> analysis	13
3.5.1.1 Cell culture and cell preparation	13
3.5.1.2 Protein extraction	14
3.5.1.3 In solution tryptic digestion	15
3.5.1.4 Desalting of tryptic digested Peptide from osteoblasts in the presence and absence of Mg/Ti-discs	16
3.5.1.5 LC-MS/MS analysis	16
3.5.2 Sample preparation for <i>in vivo</i> experiment	18
3.5.2.1 Mice bone: preparation & implantation	18
3.5.2.2 Method establishment and optimization for an <i>in situ</i> digestion and protein identification from formalin-fixed plastic embedded tissues	19
3.6 LC-MS/MS analysis	21
<hr/>	
	X

3.7	<i>Data analysis</i>	22
4	<i>Results and discussion</i>	23
4.1	<i>Proteome analysis of osteoblasts incubated with Mg& Ti-discs</i>	23
4.1.1	<i>Clustering of identified proteins from osteoblasts in the presence of Mg/Ti-Discs</i>	23
4.1.2	<i>Clustering of identified proteins of osteoblasts which were incubated with Mg& Ti-disc</i>	24
4.1.3	<i>Clustering of the regulated proteins of osteoblasts which were incubated with Mg& Ti-discs</i>	31
4.1.3.1	<i>Regulated proteins involved in bone development</i>	31
4.1.3.1.1	<i>Up-regulated proteins which are involved in bone development</i>	31
4.1.3.1.1.1	<i>Down-regulated proteins which are involved in bone development</i>	34
4.1.3.2	<i>Regulated proteins involved in energy metabolism</i>	36
4.1.3.3	<i>Regulated proteins involved involved in apoptosis</i>	37
4.1.3.4	<i>Regulated proteins involved in the response to oxidative stress</i>	38
4.2	<i>Establishment of a method for protein extraction and identification from formalin-fixed plastic embedded tissues</i>	38
4.3	<i>Proteome analysis of implanted mouse bone tissue sections with Mg& S-Implants</i>	40
4.3.1	<i>Clustering of identified proteins from mice bone tissue in the presence of Mg/S-Implant</i>	41
4.3.2	<i>Clustering of the regulated proteins from mice bone tissue in the presence of Mg/St-Implant</i>	42
4.3.3	<i>Regulated proteins in bone cells and bone tissues (in vivo) under the influence of bio-adsorbable and conventional implants</i>	50
4.3.3.1	<i>Regulated proteins involved in bone remodeling</i>	50
4.3.3.1.1	<i>Regulated proteins which are involved in bone development</i>	50
4.3.3.2	<i>Regulated blood proteins in the mouse bone tissue</i>	85
4.3.3.3	<i>Regulated proteins in the mouse bone tissues which are involved in inflammatory reaction</i>	88
5	<i>Conclusion and outlook</i>	92

6	<i>References</i>	94
7	<i>Risk and safety statement</i>	112
8	<i>Acknowledgement</i>	116
9	<i>Declaration</i>	117

List of figures

Fig. 1	Mg-corrosion reaction in aqueous environments [33]	3
Fig. 2	The schematic view of bottom-up mass spectrometry approach [65].	6
Fig. 3	Schematic proteomic workflow of label-free Vs labeling approaches [74].	8
Fig. 4	The workflow of sample preparation & data processing in the <i>in vitro</i> experiment	13
Fig. 5	The workflow of sample preparation & data processing in the <i>in vivo</i> experiment	18
Fig. 6	The number of identified proteins in osteoblasts in the presence of Mg/Ti-Disc is sorted due to their location in the cells.	24
Fig. 7	Heat-map and hierarchical clustering of the up- and down-regulated proteins (FDR= 0.01; S0= 0.1, min. fold-change of 2) in cultured osteoblast after 7 days incubation with Mg-disc compared to control of the same time based on the mean values of the biological replicates(normalized on Control -0).	25
Fig. 8	Heat-map and hierarchical clustering of the up- and down-regulated proteins (FDR= 0.01; S0= 0.1, min. fold-change of 2) in cultured osteoblast after 7 days incubation with Ti-disc compared to control of the same time based on the mean values of the biological replicates(normalized on Control -0).	26
Fig. 9	The method of sample preparation for LC-MS/MS measurement.	40
Fig. 10	The number of identified proteins in the presence of Mg/S-Implant sorted due to their location in the cells.	42
Fig. 11	Heat-map and hierarchical clustering of the significantly up- and down-regulated proteins (P-value= 0.05; min. fold-change of 2) in 7 days in mice bone tissue in the presence of Mg-Implant compared to S-Implant (as control) based on the mean values of the biological replicates (normalized on S7). Fold changes of these proteins in the other incubation times are shown in the heat map figure as well.	47
Fig. 12	Heat-map and hierarchical clustering of the up- and down-regulated proteins (P-value= 0.05; min. fold-change of 2) in 14 days in mice bone tissue in the presence of Mg-Implant compared to S-Implant (as control) based on the mean values of the biological replicates (normalized on S14). Fold changes of these proteins in the other incubation times are shown in the heat map figure as well.	48
Fig. 13	Heat-map and hierarchical clustering of the up- and down-regulated proteins (P-value= 0.05; min. fold-change of 2) in 133 days in mice bone tissue in the	

	presence of Mg-Implant compared to S-Implant (as control) based on the mean values of the biological replicates (normalized on S133). Fold changes of these proteins in the other incubation times are shown in the heat map figure as well.	49
Fig. 14	Regulation of fibrillin-1 (Fbn1) during the incubation of mice bone with Mg-implant Vs S-Implant during the time.	51
Fig. 15	Regulation of cartilage oligomeric matrix protein (Comp) during the incubation of mice bone with Mg-implant Vs S-Implant during the time.	52
Fig. 16	Regulation of tenascin (Tnc) during the incubation of mice bone with Mg-implant Vs S-Implant during the time.	53
Fig. 17	Regulation of low-density lipoprotein receptor-related protein 1 (Lrp1) during the incubation of mice bone with Mg-implant Vs S-Implant during the time.	54
Fig. 18	Regulation of nuclease-sensitive element-binding protein 1 or Y-box binding protein-1 (Ybx1) during the incubation of mice bone with Mg-implant Vs S-Implant during the time.	55
Fig. 19	Regulation of tropomyosin alpha-4 chain (Tpm4) during the incubation of mice bone with Mg-implant Vs S-Implant during the time.	56
Fig. 20	Regulation of keratocan (Kera) during the incubation of mice bone with Mg-implant Vs S-Implant during the time.	57
Fig. 21	Regulation of periostin (Postn) during the incubation of mice bone with Mg-implant Vs S-Implant during the time.	58
Fig. 22	Regulation of aggrecan core protein (Acan) during the incubation of mice bone with Mg-implant Vs S-Implant during the time	59
Fig. 23	Regulation of 3-hydroxyacyl-CoA dehydrogenase type-2 (Hsd17b10) during the incubation of mice bone with Mg-implant Vs S-Implant during the time	60
Fig. 24	Regulation of V-type proton ATPase subunit B (ATP6V1B2) during the incubation of mice bone with Mg-implant Vs S-Implant during the time	61
Fig. 25	Regulation of matrilin-3 (Matn3) during the incubation of mice bone with Mg-implant Vs S-Implant during the time	62
Fig. 26	Regulation of lactadherin (Mfge8) during the incubation of mice bone with Mg-implant Vs S-Implant during the time.	63
Fig. 27	Regulation of alkaline phosphatase, tissue-nonspecific isozyme (Alpl) during the incubation of mice bone with Mg-implant Vs S-Implant during the time.	64
Fig. 28	Regulation of chitinase-like protein 3 (Chil3) during the incubation of mice bone with Mg-implant Vs S-Implant during the time	65

Fig. 29	Regulation of plastin-3 (Pls3) during the incubation of mice bone with Mg-implant Vs S-Implant during the time	66
Fig. 30	Regulation of HSP47 or serpin-H1 (Serpinh1) during the incubation of mice bone with Mg-implant Vs S-Implant during the time	67
Fig. 31	Regulation of hyaluronan and proteoglycan link protein 1 (Hapln1) during the incubation of mice bone with Mg-implant Vs S-Implant during the time	68
Fig. 32	Regulation of epidermal growth factor receptor (Egfr) during the incubation of mice bone with Mg-implant Vs S-Implant during the time	69
Fig. 33	Regulation of collagen alpha-1(XI) chain (Col11a1) during the incubation of mice bone with Mg-implant Vs S-Implant during the time	70
Fig. 34	Regulation of collagen alpha-1(IX) chain (Col9a1) during the incubation of mice bone with Mg-implant Vs S-Implant during the time	71
Fig. 35	Regulation of V-type proton ATPase catalytic subunit A (Atp6v1a) during the incubation of mice bone with Mg-implant Vs S-Implant during the time	72
Fig. 36	Regulation of creatine kinase B-type (Ckb) during the incubation of mice bone with Mg-implant Vs S-Implant during the time	73
Fig. 37	Regulation of clusterin (Clu) during the incubation of mice bone with Mg-implant Vs S-Implant during the time	74
Fig. 38	Regulation of carbonic anhydrase 2 (CA2) during the incubation of mice bone with Mg-implant Vs S-Implant during the time	75
Fig. 39	Regulation of osteopontin (Spp1) or OPN during the incubation of mice bone with Mg-implant Vs S-Implant during the time	76
Fig. 40	Regulation of alpha-2-HS-glycoprotein (Ahsg) during the incubation of mice bone with Mg-implant Vs S-Implant during the time.	77
Fig. 41	Regulation of calmodulin (Calm1) during the incubation of mice bone with Mg-implant Vs S-Implant during the time.	78
Fig. 42	Regulation of 40S ribosomal protein S23 (Rps23) during the incubation of mice bone with Mg-implant Vs S-Implant during the time	79
Fig. 43	Regulation of selenium-binding protein (Selenbp) during the incubation of mice bone with Mg-implant Vs S-Implant during the time	80
Fig. 44	Regulation of DNA (cytosine-5)-methyltransferase 1 (Dnmt1) during the incubation of mice bone with Mg-implant Vs S-Implant during the time	81
Fig. 45	Regulation of neutrophil elastase (Elane) during the incubation of mice bone with Mg-implant Vs S-Implant during the time	82
Fig. 46	Regulation of 10 kDa heat shock protein, mitochondrial (Hspe1) during the incubation of mice bone with Mg-implant Vs S-Implant during the time	83

Fig. 47	Regulation of DNA replication licensing factor MCM2 during the incubation of mice bone with Mg-implant Vs S-Implant during the time	84
Fig. 48	Regulation of DNA replication licensing factor MCM7 during the incubation of mice bone with Mg-implant Vs S-Implant during the time	84
Fig. 49	Regulation of prothrombin (F2) during the incubation of mice bone with Mg-implant Vs S-Implant during the time	87
Fig. 50	Regulation of coagulation factor X (F10) during the incubation of mice bone with Mg-implant Vs S-Implant during the time	88
Fig. 51	Regulation of hemopexin (Hpx) during the incubation of mice bone with Mg-implant Vs S-Implant during the time.	89
Fig. 52	Regulation of transient receptor potential ankyrin-1 (ANK1) during the incubation of mice bone with Mg-implant Vs S-Implant during the time.	90
Fig. 53	Regulation of S100-A9 (s100a9) during the incubation of mice bone with Mg-implant Vs S-Implant during the time.	91

List of tables

Table 1	List of chemicals	10
Table 2	List of biomaterials	11
Table 3	List of Equipment	11
Table 4	List of softwares	12
Table 5	Lysis buffer composition	14
Table 6	In solution digestion buffer compositions	15
Table 7	Buffer composition for desalting	16
Table 8	De-plastification of mice bone tissue and in situ tryptic digestion buffer compositions	19
Table 9	Significantly regulated proteins in osteoblasts in the presence of Mg-discs compared to control after 7 days incubation.	27
Table 10	Significantly regulated proteins in osteoblasts in the presence of Ti-discs compared to control after 7 days incubation.	30
Table 11	Significantly regulated proteins in mice bone in the presence of Mg-Implant compared to S-Implant in 7days after implantation.	44
Table 12	Significantly regulated proteins in mice bone in the presence of Mg-Implant compared to S-Implant in 14 days after implantation.	45
Table 13	Significantly regulated protein in mice bone in the presence of Mg-Implant compared to S-Implant in 21days after implantation.	46
Table 14	Significantly regulated proteins in mice bone in the presence of Mg-Implant compared to S-Implant in 133days after implantation.	46

List of abbreviations

Mg	Magnesium
Ti	Titanium
S	Stainless steel
MS	Mass spectrometer
MS/MS	Tandem mass spectrometry
LFQ	label free quantification
µL	microliter
g	Gram
mM	milli Molar
mg	milli gram
mL	milliliter
°C	degree Celsius
<i>et al.</i>	<i>et alii</i>
kDa	kilo Dalton
H ₂ O	Water
ACN	Acetonitrile
FA	Formic acid
TFA	Trifluoroacetic acid
DDT	Dithiothreitol
IAA	Iodoacetamide
PMSF	Phenylmethylsulfonyl fluorid
HPLC	High pressure liquid chromatography
HCD	Higher-energy collisional dissociation
LC	Liquid Chromatography
LC-MS/MS	Liquid chromatography tandem-mass spectrometry
AmBiCa	Ammonium bicarbonate
X g	times gravity
rpm	rotations per minute
KO	Knockout
H ₂ O ₂	Hydrogen peroxide
ROS	reactive oxygen species

1 Introduction

1.1 Magnesium

Magnesium (Mg), a co-factor for more than 300 enzymes [1], is the second most abundant intracellular cation (Mg^{2+}) and the fourth most abundant mineral (after calcium, potassium, and sodium) in the human body [1, 2]. Mg plays significant roles in cell growth and energy metabolism mainly as a co-factor for phosphoryl transferase enzyme [3]. Moreover, around 60% of the Mg in our body is bound to the bone tissue [4, 5], that can be released under the conditions of hypomagnesemia [6]. Mg depletion causes hypomagnesemia, which is related to osteoporosis [7-9]. Recently, scientists observed Mg deficiency and reduction in bone hardness in female patients who suffered from osteoporosis [10, 11]. Also, Schwartz *et al.* found that Mg depletion has a negative effect on the differentiation of bone and cartilage [12]. Furthermore, Mg is known as an essential co-factor activating vitamin D [13, 14]. In post-menopausal women with a deficiency in vitamin D, less amounts of PTH and Mg were found compared to those without a deficiency [12]. Lack of Mg stimulates osteopenia and leads to enhanced skeletal fragility and impaired bone growth [15, 16]. The involvement of hypomagnesemia in various diseases which affect the cardiovascular and neuromuscular system and bone metabolism is well studied [8]. However, a few studies have been focused on the effects of hypermagnesemia, which cause muscle weakness and lethargy arrhythmia [5, 17]. The *in vivo* biodegradation of Mg-based materials is associated with the formation of non-toxic soluble corrosion products in urine which are not harmful; even though excreting the Mg element in urine is rarely observed in hypermagnesemia [18, 19]. The activated form of Mg facilitates the absorption of calcium that causes mineralization, as well [20]. Mg has influences on the bone cell function by playing a role in bone matrix metabolism and mineralization as well as the formation of hydroxyapatite crystals [21]. Jones *et al.* suggested that Mg has an effect on the

modulation of the activation of osteoblast and osteoclast in the bone mineralization process via bone formation [22]. Since Mg plays an important role in the bone health, there is a growing interest in the application of Mg in implantation of bone.

1.2 Bioadsorbable implants

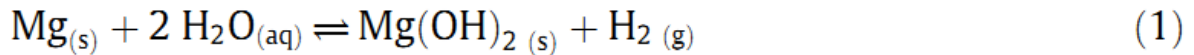
Regarding their mechanical properties, metals are considered to be more appropriate than polymers to use as bone implants [23]. Scientists working in different fields from the material science to biology and medicine try to develop and improve new materials and technologies to produce implants with advanced clinical performance [24]. Polymer implants have insufficient strength and mechanical properties [25]. Moreover conventional implants (non-biodegradable) must be removed when they are no longer needed [26]. The idea of using biodegradable materials in implantation came up with the necessity to remove implants which were used for healing injured tissue in orthopedic and cardiovascular fields [27].

Recently, Mg-based alloys and Mg with the potential of corrosion (degradation) in physiological conditions, gained particular attention for maxillofacial orthopedic applications [26]. Slow and homogenous corrosion of biodegradable implants from materials which do not shed exceedingly large parts of fragments is necessary for manufacturing implants with “desired” cell adhesion [28]. Therefore, chemical and topographical patterning as well as physical and mechanical properties of implant materials are of critical importance to choose the proper implant which leads cell differentiation and colonization [29, 30].

The first effort at using Mg as an implant was made by Lambotte *et al.* in 1907 [31]. They compared pure-Mg plate for fracture healing of the lower leg to a gold plated steel nail. However, the result was not satisfying because of the fast speed of *in vivo* degradation (only 8 days after implantation) which resulted from the production of high amounts of hydrogen gas [31].

The biodegradable implants which are finally replaced with newly formed bone tissue, should have the properties to remain in the body for 12 to 18 weeks by maintaining the mechanical integrity during the healing process of bone tissue [17, 32]. The use of Mg as an orthopedic implant is not yet common owing to a high corrosion rate (low corrosion resistance) which is accompanied by a great production

of hydrogen and alkylation of a solution (Fig. 1) [33]. Magnesium hydroxide ($\text{Mg}(\text{OH})_2$) produced during the corrosion of Mg accumulates on the surface of the implant and forms a slight protective corrosion coating in aqueous condition. This layer reacts with Cl-ions in blood and creates hydrogen gas (H_2) and MgCl_2 which is vastly soluble [33].



This overall reaction may include the following partial reactions:

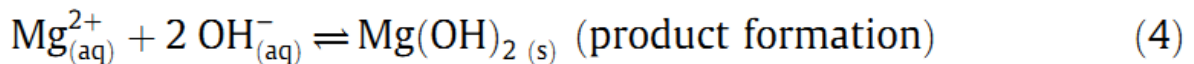
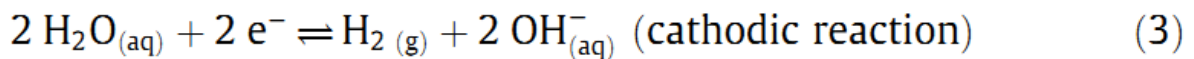
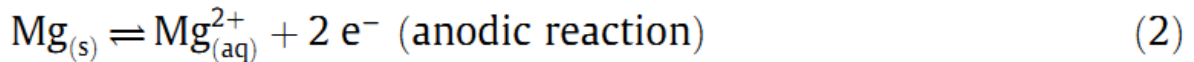


Fig. 1 Mg-corrosion reaction in aqueous environments [33]

1.3 Bone and bone cells

Bone as a living tissue includes cortical bone and trabecular bone parts. Cortical bone surrounds the mesh, dense and hard bone structure known as the “trabecular bone” [33]. Bone cells, osteoblasts, osteoclasts and osteocytes [34], are involved in bone modeling, remodeling and growth [34].

Bone remodelling, which includes bone formation and mineralization by osteoblasts, and mineralized bone deletion by osteoclasts, is a lifetime on-going process [35]. Osteoblasts; bone-forming cells, are responsible for the synthesis, mineralization and release of bone matrix proteins such as type I collagen, the most abundant protein in ECM in bone tissue [35]. On the other hand, osteoclasts; bone resorbing cells, have roles in mineralized bone deletion [36]. Bone cells and (homeopathic) bone marrow cells regulate the whole integrity of bone by several kinds of components, hormones and other proteins [36]. There are interactions between osteoblasts and osteoclasts [37]. Various mechanisms are involved in the control of bone formation/resorption. In case of an imbalance in these processes (bone formation or resorption), bone diseases can occur. [37]. Approximately 90% of the population over 40 years old are

suffering from bone diseases of degenerative bone and joint disease such as osteoarthritis and osteoporosis [38]. Additionally, in Europe and the United States, about 30 % of post-menopausal women suffer from osteoporosis [39, 40].

Diverse types of transcriptional and growth factors are involved in osteogenesis (bone formation) [41]. Extracellular matrix (ECM) is mainly responsible for the regulation of the majority of bone quality properties such as integrity, strength, and stability [35, 42]. 10%-30% of the composition of ECM is proteins mainly type I collagen fibers and non-collagenous proteins; however 70%-90% of it is made up of minerals [36, 43]. Osteoblast differentiation can be modulated by the interactions between ECM proteins and growth factors [35]. Many of non-collagenous ECM proteins play critical roles in bone by generating cellular environment during the cell development and cell morphogenesis [36]; even though the role of many of these proteins in bone formation/resorption has not been clarified yet [36].

1.4 Inflammation

Recent studies showed that magnesium does not trigger any inflammatory reactions [44]. Enhancement in the bone mass of implanted bone tissue with Mg has been reported, as well [32, 45].

Nevertheless, Shive *et al.* observed 3 phases of tissue response after injection of biodegradable microcapsules. Firstly, initiation, resolution, and organization of acute or chronic inflammatory response to the biodegradable material in the first two weeks, which was minimal and with a predominance of monocytes, occurred. Then, in the second phase, monocytes and macrophages were predominant, and the foreign body giant cells were formed from monocytes which were differentiated to macrophages. Finally, in the last phase of the host tissue response, breakdown into small microspheres happened. The time period of the 2nd and 3rd phase depends on the degradation rate of the material [46]. After implantation, inflammation might happen due to a reaction of the body to a foreign material so-called "Foreign body reaction" [47, 48]. The implant material get incontact body fluids during implantation because of damages (wounding) to vascularized tissue, and subsequently the protein layer the surface of material adsorbed [49].

1.5 Proteomics

Proteomics is the study of proteins that includes identification, characterization, and quantification of the full complement of proteins, which are synthesized in a cell, in order to realize the gene and cellular function of proteins [50]. Proteins; as essential biological components of the organism [51], have roles in diverse cellular processes such as metabolism, immune responses and cell adhesion[52]. All the produced and synthesized proteins and those proteins modified after synthesis (via post translational modifications) are called “Proteome” [53, 54]. Proteins can be classified according to many diverse classifications such as classification based on their chemical structure or physiological functions [55].

1.5.1 Mass spectrometry-based proteomics

Mass spectrometry-based proteomics is a suitable and strong technology for analysis (identification and quantification) of complex proteins in the study of the proteome [50, 56-59]. It provides the opportunity of identifying a high range of presented proteins in a complex mixture [50]. In analytical mass spectrometry, ionized analytes and ions are separated in a gas phase according to their mass-to-charge (m/z) ratio which is detected by a mass analyzer [60].

Top-down and bottom-up are two main proteomic approaches based on mass spectrometry [61]. In the top-down approach, non-digested (intact) proteins are analyzed which preserves the native primary structure of proteins such as PTMs [61]. However, in the bottom-up (or shotgun) approach, proteins are firstly digested with an enzyme and then analyzed, which results in losing their primary native structure [61]. Top-down approach is often combined with one or two-dimensional gel electrophoresis (SDS-PAGE or 2DE) [60] which has some disadvantageous such as less sensitivity and less resolution [62]. Due to the drawbacks of the top-down approach like less ability of ionization of large molecules, sample handling, separation and solubilization in a complex sample is more complicated compared to peptides in bottom-up approach; bottom-up method is mostly used [61]. Numerous specific proteases such as trypsin and chymotrypsin can be utilized for protein digestion in proteomics experiments [63, 64]. However, trypsin is the most commonly

used. It functions by cleaving the carboxyl side of arginine and lysine residues [50, 63, 64]. An example of the schematic workflow of a bottom-up proteomic approach is as showed in Fig. 2 [65].

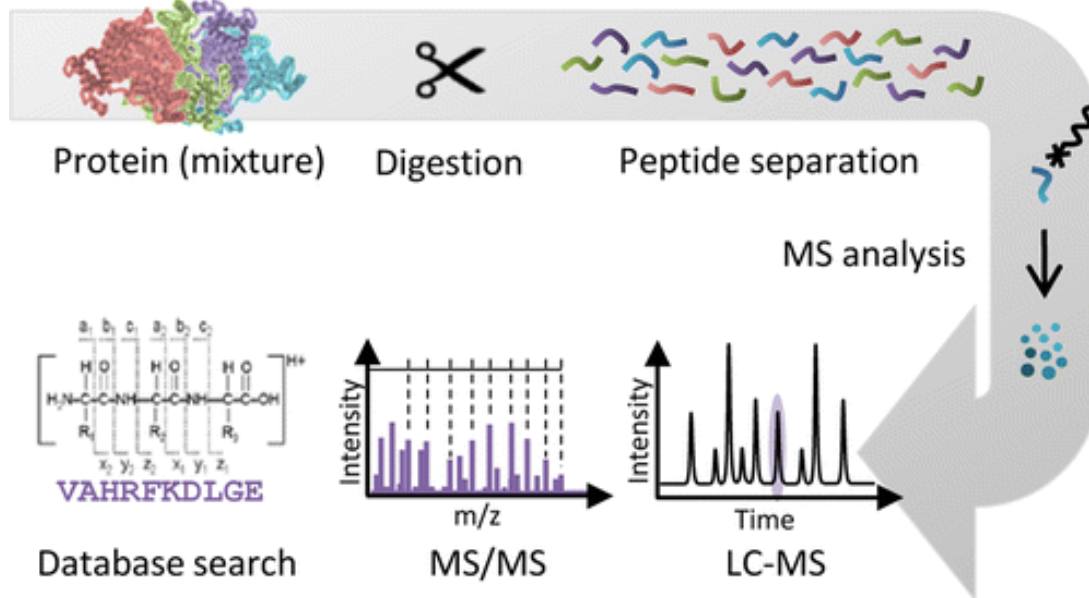


Fig. 2 The schematic view of bottom-up mass spectrometry approach [65].

Comparison between various biologically relevant samples in differential proteomics, gives us an opportunity to get an in depth view of multiple samples, cellular functions and molecular mechanism in the studied cells. Furthermore, besides identification, quantification is one of the important majors which help us to understand the molecular mechanisms in the cell.

1.5.2 Labeling and label free mass spectrometry approaches

In bottom-up mass spectrometry approach, various labeling strategies such as stable isotope labeling on amino acids in cell culture (SILAC), tandem mass tags (TMT), isobaric tags for relative and absolute quantification (iTRAQ), isotope-coded affinity tags (ICAT), and stable isotope labeled peptides can be integrated [62]. The need for using higher sample concentrations and more sample preparation steps makes the labeling techniques more complicated

and imperfect. As a result, the label-free approach got more attention to tackle these problems especially as there is no need to add extra preparation steps [66, 67]. An upside is that label free quantification (LFQ) methods provide the opportunity of comparing as many samples as possible but labelling is quite expensive, so analyzing too many samples becomes less cost effective [67].

On the other hand, Latosinska *et al.* found more protein coverage sequence in LFQ compared to iTRAQ [68]. There are two approaches for LFQ: spectral counting, and measuring the intensity of chromatographic peaks of peptides (intensity-based) [69]. The accuracy of this method is affected by shifting in retention time and mass per charge (m/z). Reproducibility of the liquid chromatography tandem-mass spectrometry (LC-MS/MS) runs is essential to get the best results from label-free quantification especially when measuring the intensity of chromatographic peaks of peptides [70-72].

These advantages of label-free quantification plus the possibility of applying LFQ in clinical samples which cannot be metabolically labeled encouraged us to use this method rather than isotope- or other labeling methods. Furthermore, relative quantification of the complex samples is simplified by the development of label-free and labeling methods [73]. Fig. 3 schematically shows simple proteomics workflows of label-free quantification (LFQ) approach versus labeling [74].

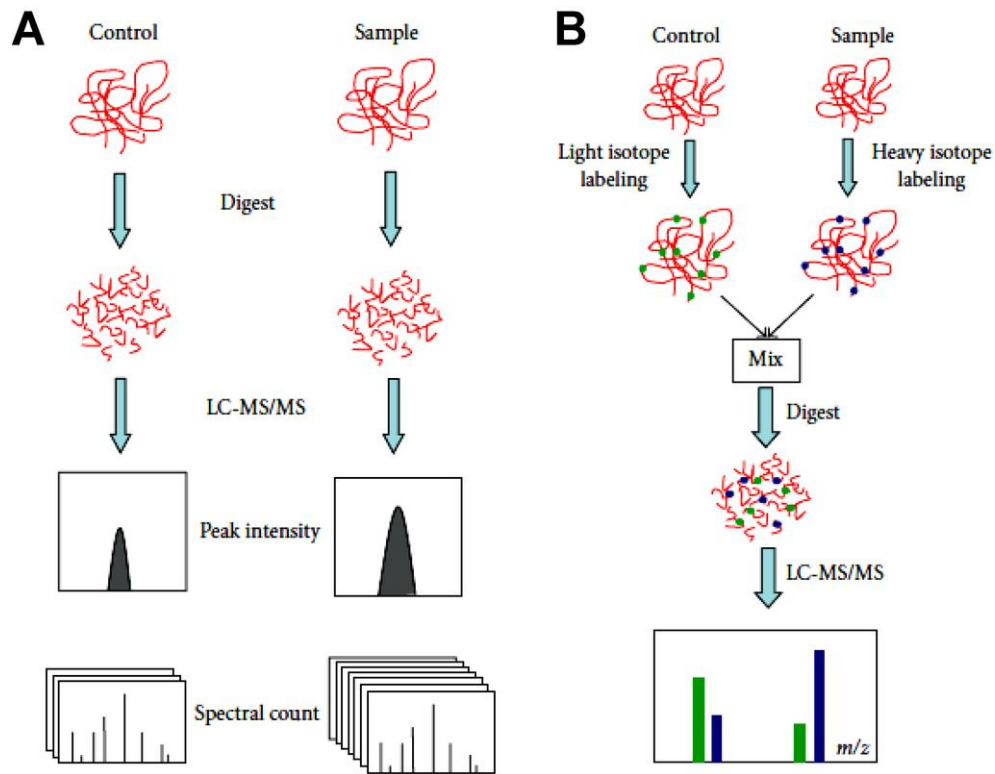


Fig. 3 Schematic proteomic workflow of label-free Vs labeling approaches [74].

2 Aim of the study

Due to the superiorities of Mg-based implants over conventional implants, Mg-implants can be more desirable than conventional permanent metal implants.

The overall aim of this study was to investigate how Mg-implants and its corrosion products affect bone cells and bone healing on the level of proteins compared to conventional implants using proteomic-based approaches.

The study was designed to get an insight about the proteins involved in bone formation/resorption and to find which proteins affect phenotypic changes. Moreover, to answer the question, by which molecular mechanisms the osteoinductive impact of Mg-alloys is affected, the proteomes of bone cells in the absence and presence of Mg were compared.

Since in the study of Mg-based implants for medical applications, cell interaction toward Mg-materials is one of the critical features, another aim was to answer the question: are Mg-implants beneficial for bone healing or are associated with any risks?

3 Materials and methods

3.1 Chemicals

Table 1 List of chemicals

Material and consumables	Supplier
DMEM-GlutaMAX I	Life Technologies (Darmstadt, Germany)
Foetal bovine serum	FBS, PAA Cell Culture Company (Linz, Austria)
Urea	Amersham (Freiburg, Germany)
benzonase	Merck (Darmstadt, Germany)
Phenylmethylsulfonyl fluoride (PMSF)	Fluka Chemika (Buchs, Switzerland)
protease inhibitor	Complete Tablet Mini, EDTA-free (Roche, Mannheim, Germany)
Water (LiChrosolv®)	Merck (Darmstadt, Germany)
Ammonium bicarbonate	Merck (Darmstadt, Germany)
Dithiothreitol	Sigma-Aldrich (Steinheim, Germany)
Iodoacetamide	Sigma-Aldrich (Steinheim, Germany)
Formic acid	Merck (Darmstadt, Germany)
Trifluoroacetic acid	Sigma-Aldrich (Steinheim, Germany)
Acetonitrile (LiChrosolv®)	Merck (Darmstadt, Germany)
Oligo™ R3 Bulk Medium	Applied Biosystems (Darmstadt, Germany)
Methanol (LiChrosolv®)	Merck (Darmstadt, Germany)
Isopropanol	Fluka Chemika (Buchs, Switzerland)
(2-Methoxyethyl)- acetate	Merck (Darmstadt, Germany)
Target retrieval solution pH2	BioGenex (Fremont, CA, USA)
Xylol	ChemSolute®, Th. Geyer (Renningen, Germany)

Trypsin Resuspension buffer	Promega (Mannheim, Germany)
Empore Extraktionsmembran C18	Sigma-Aldrich (Steinheim, Germany)

3.2 Biomaterials

Table 2 List of biomaterials

Biomaterials	Supplier
Cultured human osteoblasts in the presence and absence of Mg/Ti-discs	Prof. Willumeit-Römer group at <i>Helmholtz-Zentrum Geesthacht, Germany</i>
Implanted mice bone tissue with Mg-/St-implansts	Prof. Hesse group at <i>Universitätsklinikum Hamburg-Eppendorf (UKE), Hamburg, Germany</i>
Trypsin	Promega (Mannheim, Germany)

3.3 Equipments

Table 3 List of Equipment

Instruments	supplier
Vacuum pump CVC 2000	Vacuubrand (Wertheim, Germany)
Orbitrap fusion mass spectrometer	Thermo Scientific (Bremen, Germany)
Quadrupole-Orbitrap-System (Q Exactive™)	Thermo Scientific (Bremen, Germany)
Q-TOF Premier	Waters, Manchester, UK
Speed Vac concentrator 5301	Eppendorf AG (Hamburg, Germany)
Thermo mixer 5320	Eppendorf AG (Hamburg, Germany)
Centrifuge 5424	Eppendorf AG (Hamburg, Germany)
Centrifuge 4-16K	Sigma-Aldrich (Steinheim, Germany)
Surgical Disposable Scalple (21)	B.Braun (Tuttlingen, Germany)
Incubator	Heraus instruments (Hanau, Germany)

Freezer (-20 °C)	Liebherr (Kirchdorf an der Iller, Germany)
Freezer (-80 °C)	SANYO (Moriguchi City, Japan)
TissueLyzer II	QIAGEN (USA)
Scale	KERN and Sohn Gmbh (Balingen-Frommern, Germany)
Refrigerator	Gorenje Vertriebs GmbH (München, Germany)

3.4 Softwares

Table 4 List of softwares

Software	Supplier
Xcalibur™ 2.1	Thermo Scientific, Bremen, Germany
Proteome discoverer 2.0	Thermo Scientific, Bremen, Germany
MaxQuant 1.5.2.8	Cox and Mann (Martinsried, Germany)
Microsoft Excel, word, power point 2007 & 2010	Microsoft Corporation
Perseus 1.5..2.6	Cox and Mann (Martinsried, Germany)
Wolfram Mathematica 9.0.1.0	Wolfram Research (Oxfordshire, UK)

3.5 Sample preparation prior to Mass spectrometry analysis

3.5.1 Sample preparation for *in vitro* analysis

Protein extraction from the cells in the first part of this study is schematically showed in Fig. 4 and will be explained in details in the following chapters.

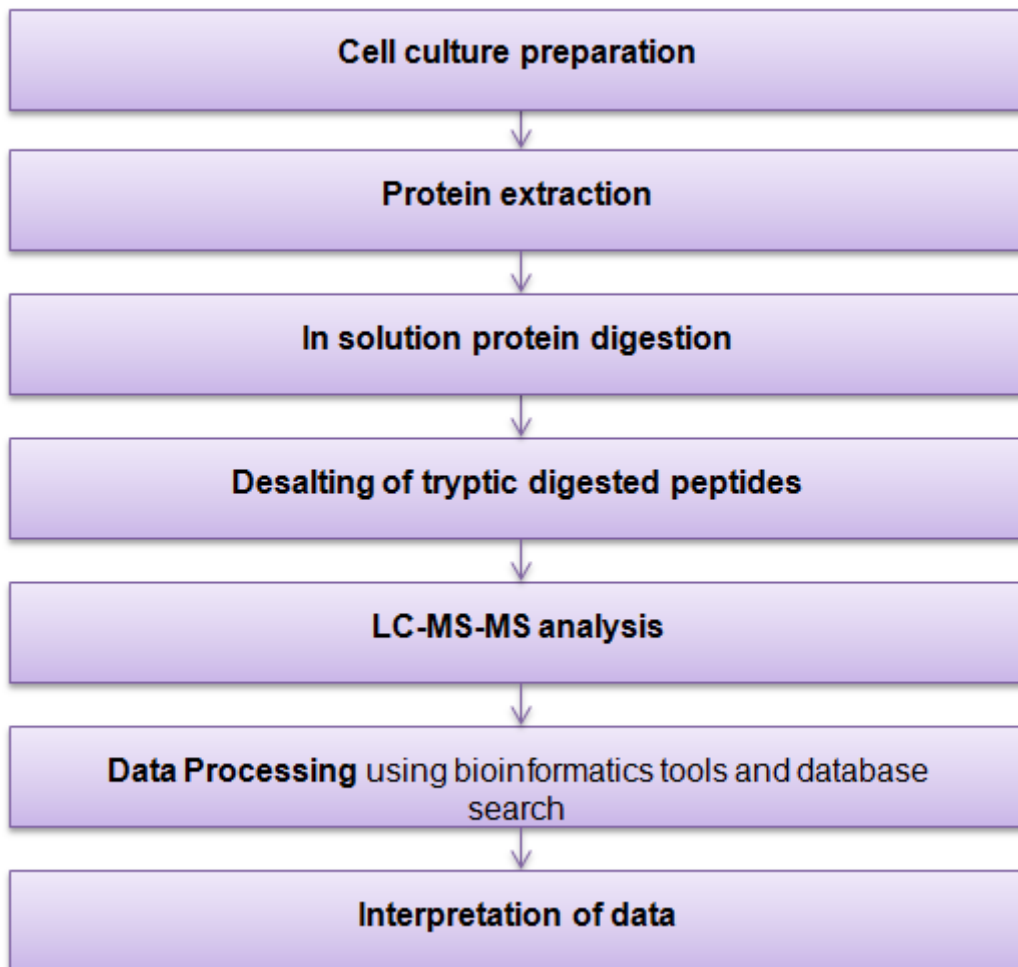


Fig. 4 The workflow of sample preparation & data processing in the *in vitro* experiment.

3.5.1.1 Cell culture and cell preparation

The cells used in this study were obtained from Prof. Willumeit-Romer group at Helmholtz-Zentrum Geesthacht, Germany. Primary human osteoblasts [75] (with the approval of the local ethic committee) were cultured with DMEM-GlutaMAX I (Life Technologies, Darmstadt, Germany) containing 10% (v/v) foetal bovine serum (FBS,

PAA Cell Culture Company, Linz, Austria). Osteoblasts were incubated with pure Mg-discs (10 x 1.5 mm) or Ti-discs (10 x 1 mm) which were pre-incubated with the same conditions as cell culture. Cultured osteoblasts without Mg/Ti metals were used as control groups. Cells were incubated in both conditions (with/without Mg/Ti-Discs) for seven days and the medium was changed in every 2-3 days.

3.5.1.2 Protein extraction

For protein extraction, 500 microliter (μL) of lysis buffer (Table 5) was added to the cell pellets and incubated for 1 hour on ice. Centrifugation was done after this step at 12000 times gravity ($\times g$) for 30 minutes. The supernatants were transferred to new reaction vials and used for further analysis.

Table 5 Lysis buffer composition

Reagent / buffer	Composition	amount
8M Urea	24.024 gram (g) of Urea was dissolved in HPLC-grade water	8 milliliter (ml)
200mM Phenylmethylsulfonyl fluorid (PMSF)	0.035 g in 1mL	50 μL
Benzonase		30 μL
Protease inhibitor ,Complete Tablet Mini, EDTA-free		1 tablet
HPLC-grade water		Up to 10 ml
Required Materials & equipment	Small Centrifuge, scale	

3.5.1.3 In solution tryptic digestion

Table 6 In solution digestion buffer compositions

Reagent / buffer	Composition
6 M urea	5.405g of urea was dissolved in 15 ml HPLC grade-water (H ₂ O)
100 mM Ammonium bicarbonate stock solution (AmBiCa)	0.119g of NH ₄ HCO ₃ was dissolved in 15 ml HPLC grade-H ₂ O
100 mM dithiothreitol (DTT)	15.4 milligram per milliliter (mg/mL) dissolved in 100 mM NH ₄ CO ₃
300 mM Iodoacetamide (IAA)	55.5 mg/mL dissolved in 100 mM NH ₄ CO ₃
Trypsin-Solution	0.25 µg/µL (dissolved in trypsin resuspension buffer)
Required Materials & equipment	Centrifuge Filters, Cut-off 10 kDa, Small Centrifuge, scale Incubator/Heater 56 °C

The extracted proteins (3.5.1.2) were transferred to 10 kilo Dalton (kDa) centrifuge filters. Then, centrifugation was done at 14000 rotations per minute (rpm) at 4 degree Celsius (°C), and for 20 minutes. Proteins were denaturated by adding 500µl of 6M Urea followed by centrifugation at 14000 rpm at 4°C for 25 minutes in order to get less than 50 µL retentate. To guarantee that the buffer was entirely exchanged, the last step was repeated twice. The disulfide bonds were reduced using 1.3 µL of 100 mM dithiothreitol (DTT) and incubated for 10 minutes at 56°C. Further incubation was performed in order to alkylate sulfhydryl groups by adding 1.3 µL of 300 mM iodoacetamide (IAA) for 30 minutes in the dark at room temperature. Then, 425 µL of NaHCO₃ was added to the samples. 2 µg of trypsin solution was added to each sample, and the samples were incubated overnight at 37 °C. Then, tryptic digested peptides were collected in the filtrate in a new tube by centrifugation at 14000 rpm at 4 °C for 25 minutes. Finally, formic acid (FA) was added to the filtrates to a final concentration of 0.2%. Samples were evaporated in a speed vac and stored in -20 °C until further processing.

3.5.1.4 Desalting of tryptic digested Peptide from osteoblasts in the presence and absence of Mg/Ti-discs

Table 7 Buffer composition for desalting

Buffer	Composition
Wash buffer	0.1% TFA in HPLC grade-H ₂ O
Elution buffer	50% ACN, 0.1% TFA in HPLC-water
PorosOligo R3-Solution	4 mg/mL, dissolved in 50% ACN
Required Materials & equipments	Gel-Loader, Small Centrifuge C18-EMPORE-DISC, scale

Desalting of the tryptic digested peptides was performed using PorosOligo R3 reversed phase packing material and C18-EMPORE-DISC. By using a P10-Tip, a small piece of C18-EMPORE-DISC was stamped out with a size of ~6millimeter (mm) and placed at the end of the Gel-Loader by a liquid chromatography (LC)-Capillary. Then it was washed with 20 μ L 100% acetonitrile (ACN) and about 40-50 μ L of the Oligo R3-Solution was added onto the column. Afterward, the column was conditioned and equilibrated respectively by washing with 60 μ L elution buffer, and 60 μ L wash buffer. Then, the sample was dissolved in 60 μ L of 0.1% trifluoroacetic acid (TFA) in high pressure liquid chromatography (HPLC)-grade water (H₂O) and loaded onto the column. Then, the peptides were eluted in 30 μ L of elution buffer. The eluates were dried in a vacuum concentrator.

Then, eluates were evaporated and suspended in 20 μ L 0.1% FA for LC-MS-Analysis. The samples were then centrifuged at 15000 rpm for 10 minutes. Supernatants were used for LC-MS/MS analysis.

3.5.1.5 LC-MS/MS analysis

All the samples were reconstituted in 20 μ L of 0.1% FA, and centrifuged at 15000 rpm for 10 minutes at 4°C prior to analysis by LC-MS/MS.

In order to perform label-free quantification, all the samples were injected twice. The same amount of the samples was injected at first (1 μ L of each sample). According to the base peak chromatogram of the first run, the concentration of the samples was calculated from the intensities of base peak chromatogram. Then, the same concentration of the samples was calculated aiming to injecting the same concentration in the second run for label-free quantification.

LC-MS/MS analysis was performed using a linear trap quadrupole (LTQ) Orbitrap mass spectrometer (MS) (Orbitrap Fusion, Thermo Scientific, Bremen, Germany) coupled via electrospray ionization (ESI)-source to a nano liquid chromatography system (Dionex UltiMate 3000 RSLCnano; Thermo Scientific, Bremen, Germany). Samples were injected onto a trapping column, 300 μ m x 5mm, 5 μ m, 100 \AA , Acclaim PepMap μ -precolumn, C18 material using an autosampler. Buffer A&B were respectively composed of 0.1% FA in HPLC grade water (H_2O) and buffer B; 0.1% FA in ACN. The flow rate during the sample loading on trapping column was 5 μ L/min with 2% buffer B. The flow rate in the whole chromatographic run was 200 nL/min. The tryptic digested peptides were eluted and onto separation column (Acclaim PepMap 100, C18, 75 micrometer(μ m) \times 250 mm, 2 μ m, 100 \AA , Thermo Scientific, Bremen, Germany; nanoAcquity UPLC column, BEH 130 C18, Waters; 75 μ m \times 250 mm, 1.7 μ m, 100 \AA). A gradient elution phase was then performed by increasing the concentration of buffer B to 30% in 90 minutes. The gradient of buffer B was then increased to 70% in 10 minutes, and later 90% in 2 minutes. A holding phase of 90% buffer B lasted 3 minutes, and the ratio was decreased to 2% for 15 minutes for column equilibration. Eluted peptides were ionized by electrospray-ionization with an Orbitrap MS. For operating a data-dependent acquisition mass analysis using top speed mode in the positive ionization mode, the following parameters were used: the m/z scan range 400-1300, with a resolution of 120,000, Higher-energy collisional dissociation (HCD) collision energy of 28%, AGC target of 2.0e5, maximum injection time of 50 ms, including charge states 2-6, mass tolerance of 10 ppm, a minimum intensity of 2.0e5, an isolation width of 1.6 m/z. Ion trap was used as a detector to record MS/MS spectra in a rapid mode with a maximum injection time of 200 ms and an AGC target of 1.0e4.

“The electrospray was generated from a fused-silica emitter (I.D. 10 μ m, New Objective, Woburn, USA) at a capillary voltage of 1650 V”.

3.5.2 Sample preparation for *in vivo* experiment

Proteome analysis of the mice bone, in the second part of our study is schematically showed in Fig. 5 and will be discussed in details in the next chapters. De-plastification and *in situ* protein digestion were optimized during the experiments to obtain the protocol to get the highest yield of the identified proteins.

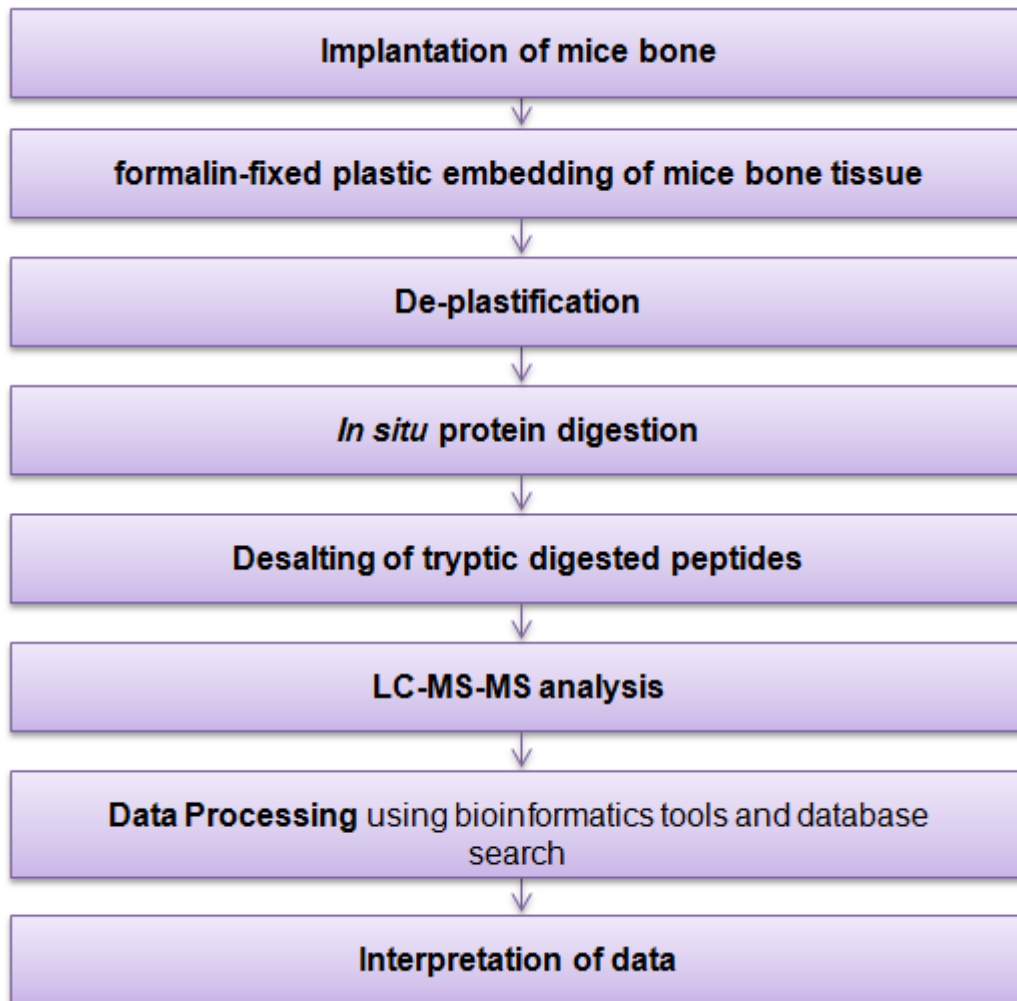


Fig. 5 The workflow of sample preparation & data processing in the *in vivo* experiment

3.5.2.1 Mice bone: preparation & implantation

The bone tissues used in this study were obtained from the group of Prof. Hesse at *Universitätsklinikum Hamburg-Eppendorf* (UKE) (animal protocol according to law has been previously obtained by the group). Ten-week-old male C57Bl/6J wild-type mice were used as *in vivo* model. A Mg₂Ag (2% Ag, wt/wt) or stainless steel (S) pin,

of a diameter of 0.8 mm and a length of 20 mm, was inserted into the distal femur of mice followed by fracturing the femur in the mid-shaft area using a bone cutter. “Implants were moved forward over the fracture into the proximal femur” [45]. Mice with fractured bones and implants were collected in groups at day 7, 14, 21 and 133 post implantation. Steel implants were removed and bones were fixed in 4% buffered formalin, and further processed for embedding in MMA. Consecutive sections were cut in a Leica microtome with section thickness of 5 μm .

3.5.2.2 Method establishment and optimization for an *in situ* digestion and protein identification from formalin-fixed plastic embedded tissues

One of our goals of the *in vivo* study was to develop a standard protocol in order to get the highest yield of identified proteins from bone tissue sections. To achieve this goal a primary workflow [76] was chosen. A new protocol was established and optimized to get the highest yield of identified proteins from formalin-fixed plastic embedded bone tissue owing to the novelty of plastic embedding of bone tissue.

De-plastification of mice bone tissue and *in situ* tryptic digestion

Table 8 De-plastification of mice bone tissue and *in situ* tryptic digestion buffer compositions

Reagent / buffer	Composition
Xylol	100%
(2-Methoxyethyl)-acetate	100%
Isopropanol	100%, 96%, 70%, 30%
Target retrieval solution pH2	In dilution of 1:10
1M AMmBiCa	1.186g of NH_4HCO_3 was dissolved in 15 ml HPLC grade- H_2O
100 mM DTT	15.4 mg/mL (dissolved in 100 mM NH_4CO_3)

300 mM IAA	55.5 mg/mL (dissolved in 100 mM NH ₄ CO ₃)
Trypsin-Solution	0.25 µg/µL (dissolved in trypsin resuspension buffer)
Required Materials:	Clean bench, Small Centrifuge, scalpel Incubator/Heater 65&56 °C

From each time point of Mg₂Ag/Steel-implanted bone, 20 consecutive formalin-fixed plastic embedded bones, which were sliced and mounted on glass slides, were used. All the tissue sections were put for 20 minutes in Xylol (twice). Then, the tissue sections were washed in (2-Methoxyethyl)- acetate for 20 minutes. This step was repeated once, and the tissue sections were rinsed in isopropanol 100%, 96%, 70%, and 30%, for 5 minutes in each step. In order to get rid of formalin, the tissue slices were transferred from the slides into a reaction vial including 1 mL Target retrieval solution pH2 and incubated for 4 hours at 65⁰ C. Centrifugation was done at 12000 x g for 5 minutes and tissues were washed with water twice followed by another centrifugation at 12000 x g for 5 minutes. Then, 900 µL of 100 mM AmBiCa was added to the tissues.

In the next step, bone tissues were homogenized using TissueLyzer II at a frequency of 25.0/s for 3.5 minutes. Then, 50 µL of 100 mM DTT was added to the tissue sections and incubated for 10 minutes at 56°C. After that, 50 µL of 300 mM IAA was added to the tissue sections, and the samples were incubated for 20 minutes in the dark at room temperature. Finally, 5 µg of trypsin solution was added to each sample. Then, the samples were incubated overnight at 37°C. Finally, formic acid (FA) was added to the samples to a final concentration of 0.2%. The samples were centrifuged at 12000 x g for 10 minutes, and the supernatants were transferred to new tubes ⁽¹⁾. 200 µL of 50% ACN was added to the pellet until covering the pellets and put on a mixer for about 1-2 minutes. Then, the samples were centrifuged at 12000 x g for 10 minutes and supernatants were collected in the tubes of supernatants⁽¹⁾.

All the supernatants were dried in the speed vac and stored in -20°C for further processing.

All the samples were dissolved in 20 µL of 0.1% FA, and centrifuged for 5 minutes at 15000 rpm at 4°C. Desalting procedure was the same as performed for the samples from *in vitro* experiments (3.5.1.4).

3.6 LC-MS/MS analysis

Before analysis by LC-MS/MS, all the samples were resuspended in 40 μL of 0.1% FA followed by centrifugation at 15000 rpm for 10 minutes at 4°C.

Similar to the samples from cultured osteoblast with/without Mg-Ti-discs, with the intention of performing label-free quantification, all the samples were injected twice: firstly, they were injected with the same amount (1 μL of each sample).

The concentration of the samples was calculated from the intensities of base peak chromatogram from the first run. Afterwards, all the samples were injected to LC-MS/MS with the same concentration in the second run for label-free quantification.

Tryptic digested peptides were analysed using a nano-flow UPLC-column (nanoAcQUITY, Waters, Manchester, UK) coupled via electrospray ionization (ESI) to Quadrupole-Orbitrap-System (Q Exactive™, Thermo Scientific, Bremen, Deutschland). Samples were injected onto a trapping column, nanoAcquity UPLC column C18, 180 μm \times 20 mm, 5 μm , and 100Å C18 material using an autosampler (Waters, Manchester, UK). During the sample loading phase, the flow rate was 5 $\mu\text{L}/\text{min}$ with 2% buffer B. The ratio of buffer A (0.1% FA in HPLC grade- H_2O): B (0.1% FA in ACN) was 98:2 throughout column equilibration, sample application and wash phases. The flow rate of 250 nL/min was used during the entire chromatographic run. After 5 minutes, gradient elution was performed by increasing the concentration of buffer B to 30% in 90 minutes. In 5 minutes, the gradient of buffer B was increased to 70%, and then 90% in 3 minutes, and held on 90% for 2 minutes. Then, the ratio was decreased to 2% for 0.1 minutes to equilibrate the column and held on 2% for 20 minutes. Eluted peptides were ionized by electrospray-ionization with an Orbitrap MS.

To operate a data-dependent acquisition mass analysis using top speed mode in the positive ionization mode in 125 minutes, the following parameters were used: the m/z scan range 400-1300, with a resolution of 70,000, AGC target of 3.0e6, maximum injection time of 100 ms. MS/MS spectra were obtained from 200-2000 m/z, with an isolation window of 2.0 m/z, with a resolution of 17,500, and NCE of 30, with a maximum injection time of 200 ms and an AGC target of 1.0e4.

3.7 Data analysis

Data analysis and processing were performed using MaxQuant 1.5.2.8 against the SwissProt databases (human database for the samples from the *in vitro* experiment and mice database for the samples from the *in vivo* experiment); and MaxQuant's internal contaminants database. Data processing was performed using the following parameters: a carbamidomethylation on cysteine as a static modification and acetylation of the N-terminus and oxidation of methionines as variable modifications, fragment mass tolerance was set to 0.2 Da and precursor mass tolerance was set to 10 ppm, the minimum ratio count for LFQ was set to 1, peptide-spectrum match (PSM) and protein false discovery rate (FDR) was set to 0.01. For bioinformatic analysis, Perseus 1.5.2.6, Excel 2010, and Mathematica 10.0 were used.

Histograms of the LFQ intensities were plotted in Mathematica and the data of unmatched samples were deleted.

For the data from osteoblasts incubated with/without Mg/Ti, two-sided student 's T-test was done in Perseus in order to compare the data from osteoblasts incubated with Mg/Ti to control (permutation-based FDR of 0.01, $s_0 = 0.1$) followed by performing a second two-sided student 's T-test on incubated cells after 7 days versus control at T0. Finally, by subtracting the treatment against control, data was normalized to control in each group.

For the data from mice bone implanted with Mg/St-implants to control, two-sided student 's T-test was done in Perseus with the aim of comparing the data from the Mg-implanted bone after 7 days versus S-implanted bones after 7 days as control (permutation-based P-value of 0.05). To observe the changes in these significantly regulate proteins in 7 days, a two-sided student's T-test for the other incubation times was done as well. Finally, by subtracting the treatment against control, data was normalized to control in each group.

These steps were repeated to get the significantly regulated proteins in Mg-implanted bone versus S-implanted bone in the other time points (14days, 21 days, and 133 days).

4 Results and discussion

4.1 Proteome analysis of osteoblasts incubated with Mg& Ti-discs

Due to the importance of titanium (Ti) and magnesium ions in bone formation [77], the impact of these two metals on cultured osteoblasts *in vitro* was compared in the first part of this study. To define this impact, extracted proteins from osteoblasts after 7 days incubation with magnesium and titanium discs were digested with trypsin and analyzed by liquid-chromatography coupled to tandem mass spectrometry (LC-MS/MS) for label-free quantification (LFQ) analysis. A total of 357,102 spectra were recorded, yielding ~2100 identified proteins with >12,000 peptides.

4.1.1 Clustering of identified proteins from osteoblasts in the presence of Mg/Ti-Discs

Firstly, all the identified proteins from cultured osteoblasts were clustered based on their location in the cells according to the Gene Ontology (GO) annotation which was downloaded from UniProt (Fig. 6). The number of identified proteins from extracellular (whether extracellular matrix (ECM) or not) membrane, and cytoplasm were more than the other proteins; however, the number of cytoskeletal proteins was less.

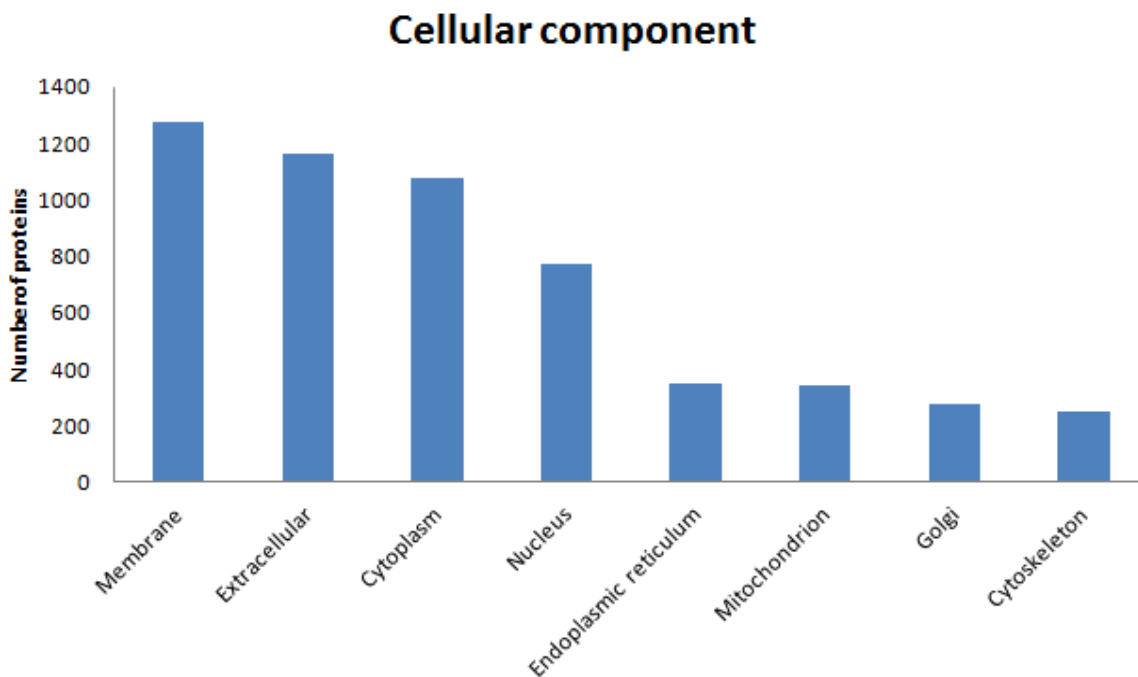


Fig. 6 The number of identified proteins in osteoblasts in the presence of Mg/Ti-Disc is sorted due to their location in the cells.

4.1.2 Clustering of identified proteins of osteoblasts which were incubated with Mg & Ti-disc

The levels of 91 of identified proteins were significantly regulated in response to elevated concentrations of metal discs (Mg&Ti). From the mean value of the regulated proteins which were normalized to control, considerably regulated proteins of osteoblasts in response to biodegradable (Mg) and conventional (Ti) discs, were created and clustered in “heat map” figures (Fig. 7, Fig. 8). These regulated proteins and their fold changes compared to osteoblasts control cells are listed in Table 9 and Table 10.

From this regulated protein list, the level of 38 proteins was increased and 43 proteins was decreased in response to Mg-disc (Fig. 7, Table 9).

On the other hand, 6 proteins were up- and 4 proteins were down-regulated in the presence of Ti-disc (Fig. 8, Table 10). Remarkably, all the up-regulated proteins in response of both metals are in the same subset; however there were no crossings among down-regulated proteins.

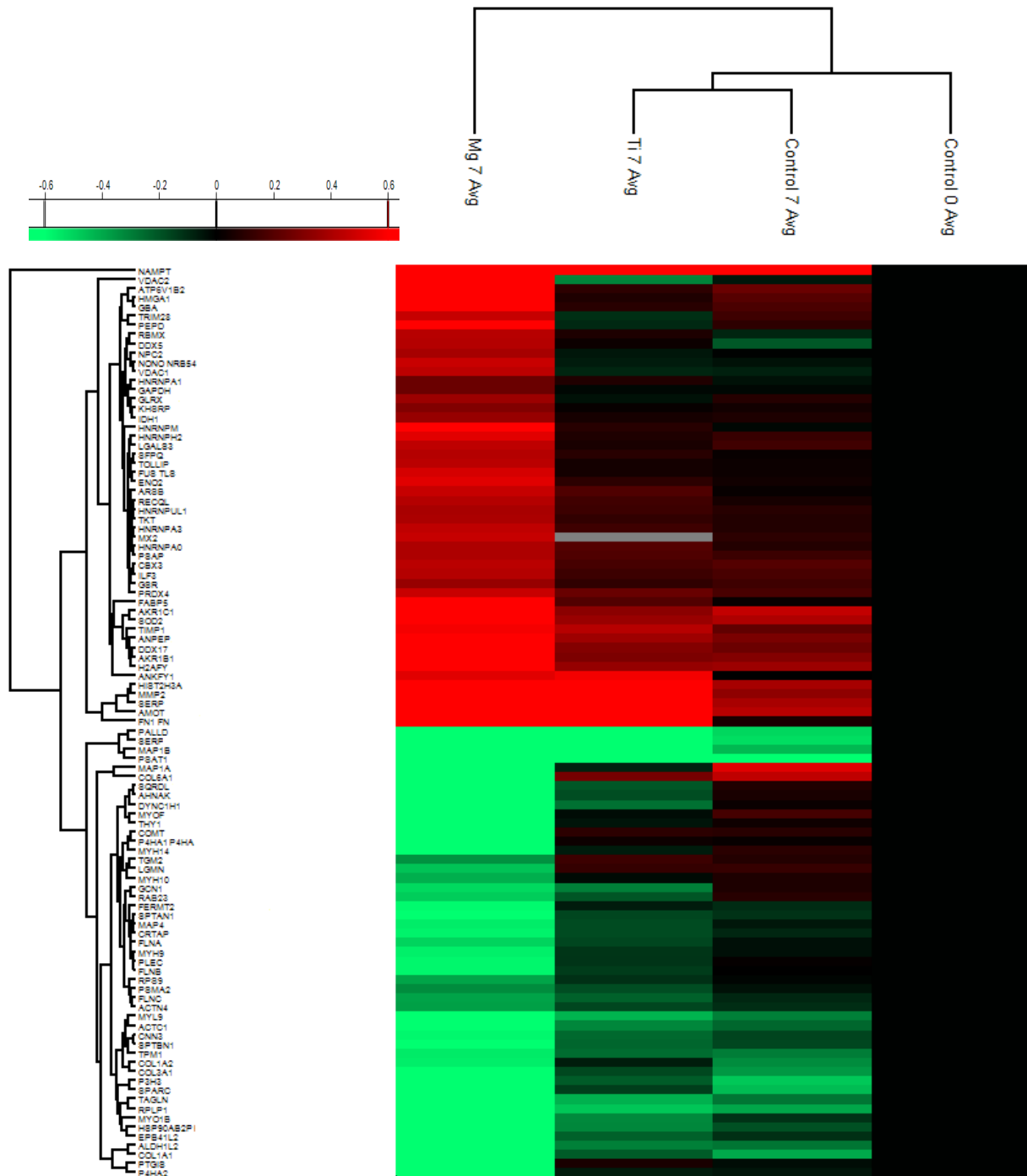


Fig. 7 Heat-map and hierarchical clustering of the up- and down-regulated proteins (FDR= 0.01; S0= 0.1, min. fold-change of 2) in cultured osteoblast after 7days incubation with Mg-disc compared to control of the same time based on the mean values of the biological replicates(normalized on Control -0).

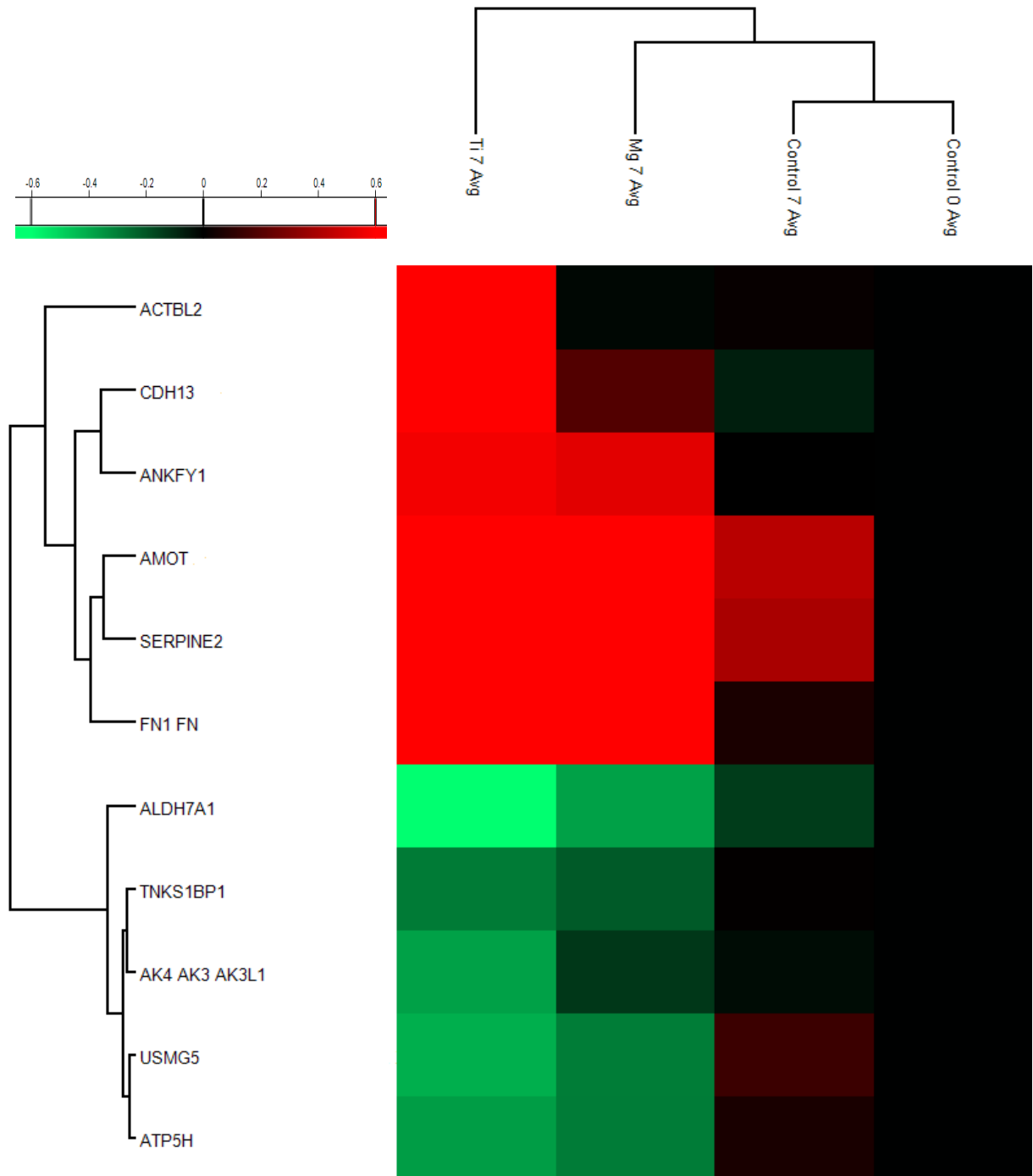


Fig. 8 Heat-map and hierarchical clustering of the up- and down-regulated proteins (FDR= 0.01; S0= 0.1, min. fold-change of 2) in cultured osteoblast after 7days incubation with Ti-disc compared to control of the same time based on the mean values of the biological replicates(normalized on Control -0).

Table 9 Significantly regulated proteins in osteoblasts in the presence of Mg-discs compared to control after 7 days incubation.

Protein names	Fold changes in Mg7 Vs Control7
Microtubule-associated protein 1A (MAP1A)	↓21.42
Prostacyclin synthase (PTGIS)	↓13.69
Collagen alpha-1(VI) chain (COL6A1)	↓11.20
Prolyl 4-hydroxylase subunit alpha-2 (P4HA2)	↓10.28
Unconventional myosin-Ib (MYO1B)	↓9.80
Mitochondrial 10-formyltetrahydrofolate dehydrogenase (ALDH1L2)	↓9.44
Myoferlin (MYOF)	↓9.26
Microtubule-associated protein 1B (MAP1B)	↓8.89
Neuroblast differentiation-associated protein AHNAK (AHNAK)	↓8.16
Sulfide:quinone oxidoreductase (SQRDL)	↓7.57
Collagen alpha-1(I) chain (COL1A1)	↓7.55
Thy-1 membrane glycoprotein (THY1)	↓6.58
Phosphoserine aminotransferase (PSAT1)	↓5.91
Cytoplasmic dynein 1 heavy chain 1 (DYNC1H1)	↓5.72
Heat shock protein 90-beta b (HSP90AB2P)	↓5.48
Catechol O-methyltransferase (COMT)	↓5.16
Myosin-14 (MYH14)	↓5.13
Band 4.1-like protein 2 (EPB41L2)	↓4.88
Prolyl 4-hydroxylase subunit alpha-1 (P4HA1)	↓4.34
Plasminogen activator inhibitor 2 (PAI-2) (SERPINB2)	↓3.97
Plectin (PLEC)	↓3.90
Legumain (LGMN)	↓3.86
eIF-2-alpha kinase activator GCN1 (GCN1)	↓3.81
Filamin-B (FLN-B) (FLNB)	↓3.79
Ras-related protein Rab-23 (RAB23)	↓3.75
Palladin (PALLD)	↓3.50

Myosin-9 (MYH9)	↓3.39
Transgelin (TAGLN)	↓3.32
Microtubule-associated protein 4 (MAP4)	↓3.17
SPARC (SPARC)	↓3.14
Fermitin family homolog 2 (FERMT2)	↓3.05
Spectrin alpha chain, non-erythrocytic 1 (SPTAN1)	↓3.05
Myosin-10 (MYH10)	↓3.03
Cartilage-associated protein (CRTAP)	↓3.03
60S acidic ribosomal protein P1 (RPLP1)	↓2.99
Filamin-A (FLN-A) (FLNA)	↓2.91
Actin, alpha cardiac muscle 1 (ACTC1)	↓2.89
Spectrin beta chain (SPTBN1)	↓2.73
Protein-glutamine gamma-glutamyltransferase 2 (TGM2)	↓2.66
Calponin-3 (CNN3)	↓2.64
40S ribosomal protein S9 (RPS9)	↓2.40
Prolyl 3-hydroxylase 3 (P3H3)	↓2.29
Myosin regulatory light polypeptide 9 (MYL9)	↓2.15
Heterogeneous nuclear ribonucleoprotein U-like protein 1 (HNRNPUL1)	↑2.02
Transcription intermediary factor 1-beta (TIF1-beta) (TRIM28)	↑2.08
Aldose reductase (AKR1B1)	↑2.08
Transketolase (TK) (TKT)	↑2.09
Heterogeneous nuclear ribonucleoprotein A0 (HNRNPA0)	↑2.09
Metalloproteinase inhibitor 1 (TIMP1) (TIMP1)	↑2.23
Interferon-induced GTP-binding protein Mx2 (MX2)	↑2.29
Superoxide dismutase [Mn] (SOD2)	↑2.30
ATP-dependent DNA helicase Q1 (RECQL)	↑2.33
Heterogeneous nuclear ribonucleoprotein A3	↑2.36

(HNRNPA3)	
Nicotinamide phosphoribosyltransferase	↑2.40
(NAMPT)	
Epididymal secretory protein E1 (NPC2)	↑2.46
Splicing factor, proline- and glutamine-rich	↑2.51
(SFPQ)	
Heterogeneous nuclear ribonucleoprotein H2	↑2.52
(HNRNPH2)	
Probable ATP-dependent RNA helicase DDX17	↑2.54
(DDX17)	
Toll-interacting protein (TOLLIP) (TOLLIP)	↑2.57
Aldo-keto reductase (AKR1C1)	↑2.64
High mobility group protein HMG-I/HMG-Y	↑2.66
(HMGA1)	
Glia-derived nexin (SERPINE2)	↑2.70
Glucosylceramidase (GBA)	↑2.73
Aminopeptidase N (ANPEP)	↑2.79
Arylsulfatase B (ARSB)	↑2.81
RNA-binding protein FUS (FUS)	↑2.98
Gamma-enolase (ENO2)	↑3.09
V-type proton ATPase subunit B, brain isoform	↑3.16
(ATP6V1B2)	
Xaa-Pro dipeptidase (PEPD)	↑3.21
Non-POU (p54nrb) (NONO)	↑3.22
RNA-binding motif protein (RBMX)	↑3.29
Voltage-dependent anion-selective channel	↑3.30
protein 1 (VDAC1)	
Rabankyrin-5 (ANKFY1)	↑3.39
Histone H3.2 (Histone H3/m) (Histone H3/o)	↑3.61
(HIST2H3A;HIST2H3C)	
Heterogeneous nuclear ribonucleoprotein M	↑4.25
(HNRNPM)	
Probable ATP-dependent RNA helicase DDX5	↑4.28

(DDX5)	
72 kDa type IV collagenase (MMP2)	↑4.47
Angiomotin (AMOT)	↑6.93
Fatty acid-binding protein (FABP5)	↑7.34
Fibronectin (FN) (FN1)	↑8.88
Voltage-dependent anion-selective channel protein 2 (VDAC2)	↑10.54

Table 10 Significantly regulated proteins in osteoblasts in the presence of Ti-discs compared to control after 7 days incubation.

Protein name	Fold changes in Ti7 Vs Control7
Up-regulated during skeletal muscle growth protein 5(USMG5)	↓3.57
Alpha-aminoadipic semialdehyde dehydrogenase (ALDH7A1)	↓3.44
ATP synthase subunit d (ATP5H)	↓2.68
Adenylate kinase 4 (AK4)	↓2.24
Glia-derived nexin (SERPINE2)	↑2.00
Angiomotin (AMOT)	↑2.35
Rabankyrin-5 (ANKFY1)	↑3.72
Cadherin-13 (CDH13)	↑9.75
Fibronectin (FN1)	↑14.59
Beta-actin-like protein 2 (ACTBL2)	↑53.88

4.1.3 Clustering of the regulated proteins of osteoblasts which were incubated with Mg& Ti-discs

Checking the molecular function and their involvement in various biological processes of the regulated proteins in UniProt gave a general overview about proteins. In many cases this information is so basic and does not provide a deep insight to find the importance of a special protein in diverse biological pathways.

Hence, all the regulated proteins were searched one after each in 'PubMed' and 'Web of Science'. By searching for the function of the regulated proteins in PubMed search, the number of proteins which are involved in the diverse biological process was higher than the GO-annotation downloaded from UniProt. This was thus more reliable than the UniProt search. For the final data interpretation, regulated proteins were clustered based on their involvement in bone development, energy metabolism, apoptosis and response to oxidative stress.

4.1.3.1 Regulated proteins involved in bone development

Bone remodeling is a life-time process which includes bone formation and resorption. Bone-forming cells, osteoblasts, play strong roles in bone formation. In contrast, osteoclasts play roles in bone resorption [35, 36]. Various types of transcriptional and growth factors are involved in the bone healing process[41]. Since osteoblasts are greatly responsible for bone remodeling, the regulated proteins which have functions in bone development will be discussed in this chapter. 25 of the regulated protein in response to Mg/Ti-discs were involved in bone development.14 were up- and 11 were down-regulated.

4.1.3.1.1 Up-regulated proteins which are involved in bone development

Fibronectin-1 (FN1), a critical component of extracellular matrix [78], was strongly up-regulated in the presence of both Mg- and Ti-discs (Fig. 7, Fig. 8, Table 9, Table 10) Fibronectin is a collagen binding protein [79, 80], and one of the major extracellular matrix components [78]. It regulates osteoblasts adhesion of extracellular matrix components [78, 81, 82]. Furthermore, fibronectin plays a role in matrix mineralization [82]. Therefore, an increase in the amount of fibronectin 1 is beneficial regarding bone formation.

Matrix-metalloproteinase-2 (MMP2), from the family of zinc-dependent enzyme [83, 84], was considerably up-regulated in the presence of Mg-discs (Fig. 7, Table 9). The members of matrix metalloproteinase family (MMPs) are involved in the remodeling of ECM [85, 86]. In order to improve of skeleton, MMP2 plays a role in the degradation of bioactive molecules [83, 84]. A mutation in the gene coding for MMP2 has been found in cases of Multicentric osteolysis which a rare genetic disorder. This disease results in bone resorption and this could be due to the deficiency of MMP2 [87]. Thus, MMP2 up-regulation under the influence of M-disc could be advantageous for bone formation.

Another significantly up-regulated protein in the presence of Mg-disc was fibroblast collagenase inhibitor (TIMP1) (Fig. 7, Table 9). The family members of natural tissue inhibitors of matrix metalloproteinase, which TIMP1 belongs to it, regulate ECM degradation. They prevent vascular wall degradation by inhibiting the activity of matrix metalloproteinases (MMPs) [88-90]. Since down-regulation of TIMP-1 causes an extreme rate of degradation of ECM [90], increasing the amount of this protein in the presence of Mg-implant can be beneficial for bone formation *in vivo*.

DEAD box protein 5 (DDX5) or P68, was another up-regulated protein in the presence of Mg-disc (Fig. 7, Table 9). Due to the role of this protein as a co-activator for RUNX2 in the development of osteoblast (essential for the maturation of osteoblasts) [91], up-regulation of this protein might be helpful for bone.

Enhancement of the amount of heterogeneous nuclear ribonucleoprotein G (hnRNP-G), which belongs to heterogeneous nuclear ribonucleoproteins [92, 93] in the presence of Mg-disc was observed (Fig. 7, Table 9). Foster *et al.* mentioned that hnRNP-G was up-regulated throughout osteoblast differentiation [94]. Regarding the beneficial role of hnRNP-G in osteoblast differentiation, up-regulation of this protein in the presence of Mg-Disc might be beneficial for bone.

Aminopeptidase N (ANPEP; CD13) is a surface marker of adipose-derived mesenchymal stem cells (AMSCs) and deciduous tooth stem cells (DTSCs) [95]. It was considerably increased under the influence of Mg-discs (Fig. 7, Table 9). AMSCs synthesize aminopeptidase N via its differentiation to osteoblasts [95]. Therefore, the impact of Mg-disc on the increasing the amount of this protein can be effective for bone formation.

The amount of nicotinamide phosphoribosyltransferase (NAMPT) was enhanced in the presence of Mg-discs (Fig. 7, Table 9). Regarding the negative effect of the NAMPT-deficiency in osteoblast differentiation [96], the impact of Mg-discs on the up-regulation of this protein might help bone during OB differentiation.

The amount of prostacyclin synthase (PGI2) from the family of prostaglandins was reduced in the presence of Mg-discs (Fig. 7, Table 9). This protein has a function in regulating the production of prostacyclin [97], which enhances osteoblast differentiation and matrix mineralization in osteoblasts via enhancement of β -catenin [98]. Deficiency of PGI2 causes age-dependent symptoms. In young mice, reduction of bone mineral density and bone mass was observed, whereas enhancement of bone mineral density and bone mass occurred in adult mice [97, 99]. Therefore, using Mg-implants might cause an adverse effect on the bone mass in children. It is recommendable to check the amount of this protein *in vivo*.

Another significantly up-regulated protein under the influence of Mg was prolylase (PEPD) (Fig. 7, Table 9). Prolidase plays a critical role in collagen metabolism [100], and the lack of this protein causes bone mass and bone strength deterioration [100]. Thus, it can be concluded that Mg-implant should be beneficial for bone healing regarding its positive influence on the regulation of prolylase.

The nuclear binding protein, NONO (p54(nrb)) [101], was also significantly enhanced in the cultured osteoblasts which were incubated with Mg-discs (Fig. 7, Table 9) compared to Ti-discs and control cells. During chondrogenesis, NONO has a role in the transcription of mRNA of Col2a1 as well as its processing by interacting with Sox9 [101]. Hence, Mg-induced up-regulation of NONO it can be can be supportive for new bone formation.

The level of arylsulfatase B (ARSB) was also enhanced in the presence of Mg-discs (Fig. 7, Table 9). Vairo *et al.* mentioned that in ARSB-deficiency, glycosaminoglycans (GAGs) are not broken down. This causes an accumulation of glycosaminoglycans (GAGs) which leads to bone dysplasia [102]. Thus, an increase in the amount of this protein under the influence of Mg-implants might prevent GAG accumulation and thus quite positive for health of bone.

A further up-regulated protein in the presence of Mg-disc was proton-pumping V-type ATPase (ATP6V1B2) (Fig. 7, Table 9). It is a multisubunit protein which is highly expressed in ameloblasts [103]. It aids in lysosomal acidification and hence its'

importance in enamel development [103, 104]. A deficiency of this protein has been observed in cases of osteoporosis. Therefore, the up-regulation of this protein in the presence of Mg-Implants can be beneficial for the maturation of bone maturation.

Glucosylceramidase (GBA) is a macrophage-targeted enzyme [105, 106] which was enhanced in the cultured osteoblasts in the presence of Mg-discs (Fig. 7, Table 9). The lack of GBA causes Gaucher's disease, which is a common disorder in sphingolipid storage, and leads to osteoporosis as well [105, 106]. Regarding the positive effect of Mg on the regulation of this protein, enhancement of bone formation might occur.

The level of angiominin (AMOT) was significantly increased in the presence of both Mg&Ti- discs (Fig. 7, Fig. 8, Table 9, Table 10). The amount of this protein, which is a member of the cadherin-11/ β -catenin/p120 complex, was enhanced in osteosarcoma in a study by Niu *et al.* [107], thus, up-regulation of this protein in the presence of both metals seems not beneficial for bone.

4.1.3.1.1.2 Down-regulated proteins which are involved in bone development

The level of paladin (PALLD) was also significantly decreased in the presence of Mg-discs (Fig. 7, Table 9). Up-regulation of paladin, which is an actin-linked protein and has a function in cytoskeleton organization, was observed in osteogenic differentiation of (adipose-derived adult) ADASC. However, its reduction does not have a negative effect on osteogenesis, it had a negative effect on actin-stress fibers [108]. Although down-regulation of this protein in the presence of Mg-implant causes reduction of actin stress fibers, it does not affect osteogenesis *in vivo*.

Another down-regulated protein in cultured osteoblasts in the presence of Mg-discs was an active binding protein [109, 110], filamin A (FLNA) (Fig. 7, Table 9). Filamin A plays a critical role in osteoclastogenesis [109]. In a study on filamin-deficient mice, the collagen density was high with less structural organization unlike wild-type mice [110]. Thus, down-regulation of filamin A under the influence of Mg-implant can be beneficial for bone formation *in vivo* (by inhibiting bone resorption during fracture healing).

The level of osteonectin (SPARC), which has a critical function in bone remodeling by stimulating the activation of plasminogen [111], was considerably decreased in the presence of Mg-discs (Fig. 7, Table 9). Proteolysis of ECM occurs when plasminogen

binds to collagen in the presence of osteonectin [111]. Not activating plasminogen by plasminogen activator can suppress the proteolysis of non-collagenous proteins in non-mineralized bone. Decreasing the amount of plasminogen activator was seen to increase bone formation [112]. Hence, reduction of osteonectin, a type of plasminogen activator, in the presence of Mg-implant might be helpful for bone health.

Transgelin (TAGLN, SM22), another actin binding protein, was down-regulated in the presence of Mg-discs (Fig. 7, Table 9). This protein inhibits the production of matrix-metalloproteinase-9 (MMP-9) which is a type of collagenase [113, 114]; however in our results, MMP-9 was not affected by this change regardless. Due to this, in the presence of Mg-implant bone formation is not directly affected by down-regulation of transgelin.

The *in vivo* substrate for osteopontin (one of the key proteins in bone), transglutaminase-2 (TGM2), [115] was significantly reduced in the presence of Mg-discs (Fig. 7, Table 9). Concerning the positive effect of this protein in increasing the Ca-dependent binding of collagen and osteopontin [115]; it is recommendable to check regulation of this protein *in vivo*. However, down-regulation of transglutaminase-2 in the presence of Mg-discs might be disadvantageous for bone regeneration.

Another down-regulated protein in the presence of Mg-discs was the osteoclast inhibitory peptide 2 (OIP-2), legumain (LGMN) (Fig. 7, Table 9). Treatment of bone marrow culture with Ab-legumain has been found to be beneficial for the formation of osteoclasts [116]. Hence, down-regulation of this protein under the influence of Mg-implant does not seem beneficial for bone health; hence checking its regulation in the *in vivo* study with Mg-implant is necessary.

Prolyl 4-hydroxylase subunit alpha-2 (P4HA2), which is critical in the biosynthesis of collagen [117, 118] was also down-regulated in the presence of Mg-discs (Fig. 7, Table 9). Regarding the importance of this protein in cartilage development [117], its reduction in the presence of Mg-implant might affect the strength of bone.

Two proteins from the leprecan family Cartilage-associated protein (CRTAP) and prolyl 3-hydroxylase 3 (P3H3) [119] were down-regulated in the presence of Mg-discs (Fig. 7, Table 9). The members of the leprecan family have functions in bone development and collagen helix formation [120, 121]. Alteration of the gene coding for CRTAP has

been observed in diseases like osteogenesis imperfecta [119, 122, 123]. Thus, down-regulation of these two proteins in the presence of Mg-implant seems disadvantageous for bone renewal.

Another member of actin-binding proteins, calponin-3 (CNN3) [124, 125], was down-regulated in the presence of Mg-discs as well (Fig. 7, Table 9). Reduction of this protein was observed in osteoarthritic joints [124]. The strength of newly formed bone might be negatively affected by down-regulation of this protein under the influence of Mg-implants.

COL1A1 and COL6A1 were significantly down-regulated in the presence of Mg-discs (Fig. 7, Table 9). COL1A1 plays a role in the modulation of bone mass [126]. COL1A1-deficiency is observed in osteogenesis imperfecta (an inborn bone disease which is associated with bone fragility) [127]. COL6A1 has a function in encapsulating chondrocytes, and it is present in “pericellular matrix” (PCM) and its deficiency affects the mechanical properties of bone [128]. Therefore, down-regulation of collagens seems harmful to bone strength.

The level of ATP synthase subunit d (ATP5) was significantly decreased in the presence of Ti-discs (Fig. 8, Table 10). The amount of this protein found to reduce in a study by Hong *et al.*, when they treat MC3T3-E1 cells with DEX which suppresses the differentiation & proliferation of osteoblast [129]. While ATP5 was not significantly regulated in the presence of Mg-discs, it can be concluded that osteoblast differentiation was not suppressed by Mg-discs regarding this protein. However, it is affected by Ti.

4.1.3.2 Regulated proteins involved in energy metabolism

Bone requires energy for mineralization and remodeling,... [130-133]. Therefore, further investigation was performed by clustering regulated proteins based on their participation in energy metabolism. Two of up-regulated proteins in the presence of Mg-discs were found in this category (Fig. 7, Table 9).

1) Fatty acid-binding protein 5 (FABP5), which has a high affinity to polyunsaturated fatty acids (PUFA) [134, 135] and aids in their transportation [136, 137]. The lack of PUFAs leads to osteoporosis [134, 135].

2) Aldose reductase (AKR1B1), which belongs to aldo-keto-reductase family, has a role in the polyol pathway in glucose metabolism [138, 139]. It also regulates oxidant stress in the cells via lipid peroxidation [140] as well as in inflammatory reactions in cancer and asthma [138].

Consequently, up-regulation of these energy metabolism related proteins might be because of increased activity of osteoblasts in the presence of Mg-discs and the energy requirements of the cells. Furthermore, Mg-implants might keep cells from toxic responses by up-regulating Aldose reductase.

4.1.3.3 Regulated proteins involved involved in apoptosis

An increase in bone mass has been observed by suppressing apoptosis in osteoblasts due to increase in osteoblast activity as mentioned by Moriishi *et al.* [141]. Therefore, in the next step, regulated proteins which are involved in programmed cell death, “apoptosis” were clustered. 7 of the regulated proteins in the presence of Mg/Ti-discs compared to control cells have roles in the apoptotic process. Four of them were up-regulated in the presence of Mg-discs; 1 was down- and 1 was up-regulated in the presence of Ti-discs.

Increasing the amount of voltage-dependent anion channel proteins (VDAC1 and VDAC2) in the presence of Mg-discs (Fig. 7, Table 9) might be beneficial for bone cells due to: the role of VDAC1 in inhibiting cells proliferation and apoptosis [142] and the role of VDAC2 in reducing apoptosis [143].

Also, up-regulation of transcription intermediary factor 1-beta (TIF1-beta) or “TRIM28” under the influence of Mg (Fig. 7, Table 9) may support bone cells. In TIF1-deficient mice apoptosis was stimulated.[144]. Therefore TRIM 28 can be considered to favor the viability of cells.

The level of heterogeneous nuclear ribonucleoprotein U-like protein 1 (HNRNPUL1) was enhanced in the presence of Mg-discs (Fig. 7, Table 9). HNRNPUL1 increases cell viability via its critical role in the response of cells towards the signalling of DNA-double strand breaks [145]. Thus, its up-regulation might be beneficial for bone cells. Also, up-regulation of cadherin-13 (CDH13), from adhesion transmembrane proteins [146-148], in osteoblasts in response to Ti-discs (Fig. 8, Table 10) might be beneficial

for cells by improving cell adhesion. Cadherin-13 suppresses neovascularization which is known to increase metastasis in many types of cancer [146-148].

With alpha-amino adipic semialdehyde dehydrogenase (ALDH7A1), a decrease in the presence of Ti-discs (Fig. 8, Table 10) might be associated with negative effects on bone. This protein plays a role in cells against hyperosmotic stress-induced apoptosis and also aids in aldehyde detoxification to prevent oxidative stress. [149].

4.1.3.4 Regulated proteins involved in the response to oxidative stress

Oxidative stress is known to be dependent on oxidant-antioxidant balance within cells and the anti-oxidant system under physiological conditions controls the levels of reactive oxygen species (ROS) by acting as free radical “scavengers” [150]. It has been noticed that approximately 2% of mitochondrial oxygen reduction results in superoxide anion (O_2^-) or Hydrogen peroxide (H_2O_2) [151, 152] which can affect bone remodeling. Due to this, regulated proteins related to oxidative stress were also clustered.

Superoxide dismutase (SOD2), the only one protein among the regulated proteins which takes part in this category, was up-regulated in osteoblasts in the presence of Mg-discs (Fig. 7, Table 9). SOD2 in its effort to get rid of the superoxide produces H_2O_2 which is also a ROS though less damaging. However, H_2O_2 stimulates both osteoclastogenesis and the activity of mature osteoclasts bone resorption even more than O_2^- [153-155].

4.2 Establishment of a method for protein extraction and identification from formalin-fixed plastic embedded tissues

Owing to the long-term stability and high rate of preserving formalin fixed paraffin embedded (FFPE) tissues, formalin fixation and embedding the tissues in paraffin, is a typical method for fixation and preservation of the tissues [156]. However, extraction of the proteins from formalin fixed tissues is not simple because of the chemical changes in the proteins of tissues [157-159]. Therefore, tissues need another step to eliminate formalin before protein extraction. In addition, in classical

embedding procedures such as paraffin embedding, changes in tissue composition (especially protein composition), tissue shrinkage, and difficulties in tissue sectioning (which depends on the hardness of tissue) have been observed [160, 161]. Nevertheless, in resin-embedding mixtures such as methacrylates, which are nowadays used, preserving the morphology of tissues compared to classical embedding methods is expected [162].

The widely used technique in experimental animal studies and clinical medicine for embedding bone tissue is Methylmethacrylate (MMA) embedding. Due to the advantages of embedding bone in Methylmethacrylate (MMA), such as higher quality in histological view, and easy removal from bone sections, MMA is widely used for embedding bone tissue in animal studies and clinical medicine[163].

Embedding hard tissue in plastic prevents the bone tissue from fragility during the cutting process and makes the slicing process with microtome easier; however getting rid of the plastic and formalin prior to the protein extraction is needed.

Regarding the novelty of plastic embedding of bone tissue, a new method for the extraction of the proteins from formalin-fixed plastic embedded tissues was established and optimized. Therefore, a novel technique for the extraction of proteins from MMA-embedded tissues was established to get the highest yield of extracted proteins from bone tissue.

For this new method, firstly the previous method which was developed for the extraction of proteins from Paraffin-embedded formalin-fixed bone tissue [76] was used with some changes in the first step of washing and de-plastification of tissues. Then, to improve the extraction method, the duration of incubation of the de-plastification step and mouse bone tissues in target retrieval solution was increased. The bone tissues were homogenized using TissueLyzer II (QIAGEN) at a frequency of 25.0/s in 3.5 minutes followed by tryptic digestion. All the samples were desalted and measured by LC-MS/MS (Fig. 9). Finally, in the final improved extraction method, from formalin-fixed plastic embedded mouse bone tissue sections, 1393 proteins, and more than 9500 peptides were identified with ~378000 recorded spectra, which show the final method seems quite optimal to follow.

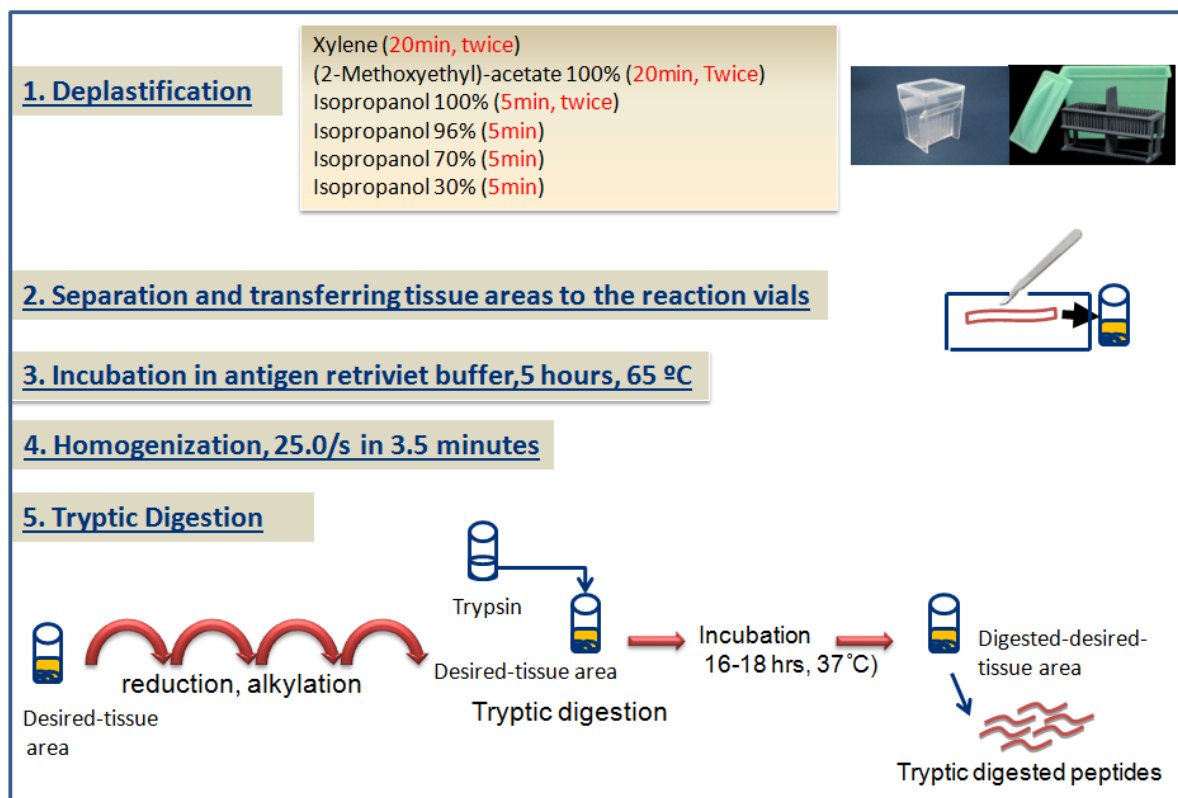


Fig. 9 The method of sample preparation for LC-MS/MS measurement.

4.3 Proteome analysis of implanted mouse bone tissue sections with Mg& S-Implants

Mg-based alloys are promising materials to apply as biodegradable implants in biomedical applications due to their physiochemical properties (mechanical properties and biodegradability) [164-167]. Owing to the impression Mg-alloys application for biomedical research, the study of primary stability and suitable biodegradability of them in respect to bone healing is necessary [33]. To study the influence of Mg-implant on bone tissue *in vivo*, the impact of bio-absorbable Mg-Implant (Mg₂Ag-nails) on the protein composition of open midshaft bi-cortical femoral fracture model in mice [45] was investigated in the second part of this study. Mg₂Ag-nail compared to other Mg-based implants does not affect the osmolality and environmental PH in about 1.7 years of degradation time [168, 169].

From the bone tissues which were used in this experiment, *ex vivo* μ CT imaging showed the development of callus in the presence of Mg-Implant within 14 days after implantation [45]; however, it was just started in the control group (S-Implant) at the same time point. Moreover, the fracture was completely healed in both groups on day 21; while callus formation was stronger in the Mg₂Ag group. In their study, fractured bone tissue in the presence of Mg₂Ag, in 14 and 21 days after implantation was stabilized compared to control group. Finally, Mg-implant was fully adsorbed by 133 days after implantation [45].

Here, the impact of Mg₂Ag-nail on the protein composition of mice fractured bone tissue with steel implant as a control group was compared.

Bone tissue sections of mice which were implanted with Mg/S-Implants were cut in 7days, 14 days, 21days, and 133days after implantation, fixed in formalin, embedded in MMA, and sectioned in 5 μ m thicknesses (All the bone sections were prepared in the group of Prof. Hesse at Universitätsklinikum Hamburg-Eppendorf (UKE), and all were fractured bones). De-plastification and protein digestion were performed according to our new method (4.2) and desalted. Then, samples were measured by LC-MS/MS for the purpose of LFQ-analysis (label-free quantification).

The bone sections with steel implants in each time point were set as a control at the same time point due to 1) usage of steel as a permanent implant, and 2) having the same situation (fractured) for both experimental conditions. A total of 378,000 spectra were recorded, yielding ~1400 identified proteins with >9500 peptides.

4.3.1 Clustering of identified proteins from mice bone tissue in the presence of Mg/S-Implant

The first investigation was performed on Gene Ontology (GO) annotation downloaded from UniProt for all identified proteins in various time points. All the identified proteins from implanted fractured mice bone sections in the presence of Mg- & S-Implants were clustered in relation to the cellular component (Fig. 10). The number of extracellular (either extracellular matrix (ECM) or not) & membrane proteins from bone cells *in vitro* and bone tissue *in vivo* were higher than the proteins in the other parts of cells. Also, the profile of the cellular components for the identified proteins in both tests was almost comparable (Fig. 6 from 4.1.1).

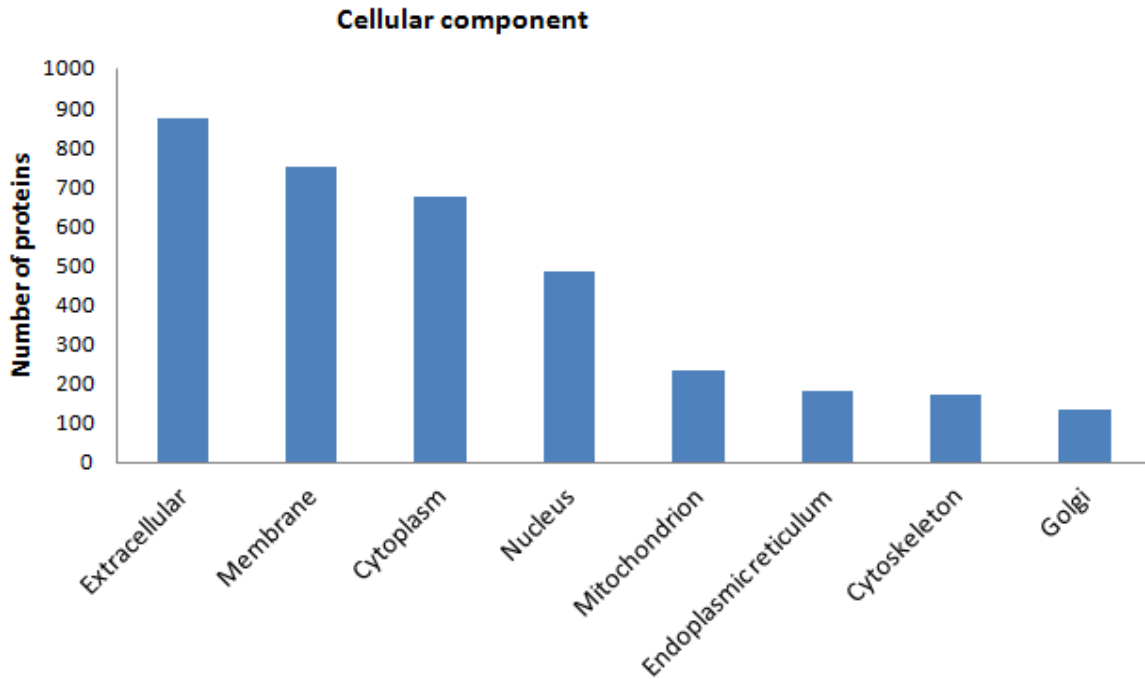


Fig. 10 The number of identified proteins in the presence of Mg/S-Implant sorted due to their location in the cells.

4.3.2 Clustering of the regulated proteins from mice bone tissue in the presence of Mg/St-Implant

For the further analysis, proteins with ≥ 2 unique peptide and two or more than two-fold changes in the amount of proteins in treated bone with Mg-implant Vs S-implant, as well as their presence in at least 5 out of 6 replicates were accepted as regulated ones. The list of regulated proteins in the presence of Mg-implant compared to S-implant in each incubation time is shown in Table 11, Table 12, Table 13, and Table 14.

From the mean value of regulated proteins which were normalized to control (steel) at each time point (7days, 14 days, and 133 days after implantation), considerably regulated proteins in the presence of biodegradable (Mg)-implant compared to S-implant, were created and clustered in “heat map” figures (Fig. 11, Fig. 12, and Fig. 13). In these figures, all of the considerably regulated proteins (controlled by student T-two test) in each time point with two or more than two-fold changes were clustered. Moreover, to get a better insight of the significantly regulated proteins in each time point, fold changes of those proteins in the other incubation times are shown in the

heat map figures as well (Fig. 11, Fig. 12, and Fig. 13). However, their regulation in the other time points was not essentially two-fold.

In the first time point (7days after implantation), 36 of identified proteins were regulated. 14 of these proteins were up- and 22 proteins were down-regulated (Fig. 11, Table 11).

In the second time point (14days), the level of 34 of proteins was increased by more than two-fold. The amount of 16 proteins was significantly increased and the level of 18 proteins was considerably decreased under the influence of Mg-Implant (Fig. 12, Table 12).

The only one significantly regulated proteins in the third time point (21) days was up-regulated (Table 13).

In the last time point (133days), all 6 regulated proteins were considerably up-regulated. (Fig. 13,Table 14).

Table 11 Significantly regulated proteins in mice bone in the presence of Mg-Implant compared to S-Implant in 7days after implantation.

Protein name	Fold changes in Mg7 Vs S7
Periostin (Postn)	↑2.01
14-3-3 protein gamma (Ywhag)	↑2.02
V-type proton ATPase catalytic subunit A (Atp6v1a)	↑2.04
Keratocan (Kera)	↑2.04
Tenascin (Tnc)	↑2.15
Tropomyosin alpha-4 chain (Tpm4)	↑2.16
Creatine kinase B-type(Ckb)	↑2.22
Nuclease-sensitive element-binding protein 1 (Ybx1)	↑2.42
14-3-3 protein theta (Ywhaq)	↑2.74
Selenium-binding protein (Selenbp)	↑3.13
Low-density lipoprotein receptor-related protein 1 (Lrp1)	↑3.13
Cartilage oligomeric matrix protein (Comp)	↑3.45
40S ribosomal protein S11 (Rps11)	↑3.75
Fibrillin-1 (Fbn1)	↑3.82
Olfactomedin-like protein 3 (Olfml3)	↓5.94
Sarcoplasmic/endoplasmic reticulum calcium ATPase	↓4.75
Coagulation factor X (F10)	↓3.33
Myoglobin (Mb)	↓3.00
Protein S100-A9 (S100a9)	↓2.97
Long chain 3-hydroxyacyl-CoA dehydrogenase (Hadha)	↓2.90
40S ribosomal protein S23 (Rps23)	↓2.44
10 kDa heat shock protein (Hspe1)	↓2.39
3-ketoacyl-CoA thiolase (Hadhb)	↓2.35
Prothrombin (F2)	↓2.33
Calmodulin (Calm1)	↓2.30
NADH dehydrogenase [ubiquinone] 1 alpha subcomplex	↓2.27
Alpha-2-HS-glycoprotein (Ahsg)	↓2.24
Histone H1.1 (Hist1h1a)	↓2.16
ATP synthase subunit O (Atp5o)	↓2.16
Glutathione S-transferase P (Gstp)	↓2.15
Osteopontin(Spp1)	↓2.12
Ankyrin-1(Ank1)	↓2.10
F-actin-capping protein subunit alpha-2 (Capza2)	↓2.10
26S proteasome non-ATPase regulatory subunit 6	↓2.10
Histone H1.5 (Hist1h1b)	↓2.06
3-hydroxyacyl-CoA dehydrogenase type-2 (Hsd17b10)	↓2.03

Table 12 Significantly regulated proteins in mice bone in the presence of Mg-Implant compared to S-Implant in 14 days after implantation

Protein name	Fold changes in Mg14 Vs S14
Tenascin (Tnc)	↑2.00
Alkaline phosphatase (Alpl)	↑2.03
Alcohol dehydrogenase [NADP(+)](Akr1a1)	↑2.10
Collagen alpha1(IX) chain (Col9a1)	↑2.12
Basement membranespecific heparan sulfate	↑2.23
40S ribosomal protein S11 (Rps11)	↑2.27
Epidermal growth factor receptor (Egfr)	↑2.37
Hemopexin (Hpx)	↑2.38
Fibrillin1 (Fbn1)	↑2.41
Lactadherin (Mfge8)	↑2.60
Collagen alpha1(XI) chain (Col11a1)	↑2.60
Aggrecan core protein (Acan)	↑2.98
Vtype proton ATPase subunit B (Atp6v1b2)	↑3.20
Hyaluronan and proteoglycan link protein 1 (Hapln1)	↑3.31
Cartilage oligomeric matrix protein (Comp)	↑3.42
Matrilin3 (Matn3)	↑5.31
Protein S100-A9 (S100a9)	↓4.80
DNA (cytosine-5)-methyltransferase 1 (Dnmt1)	↓3.34
RNA 3-terminal phosphate cyclase (RtcA)	↓3.09
Ankyrin-1 (Ank1)	↓3.07
Carbonic anhydrase 2 (Ca2)	↓2.93
Neutrophil elastase (Elane)	↓2.89
Band 3 anion transport protein (Slc4a1)	↓2.80
DNA replication licensing factor MCM7 (Mcm7)	↓2.70
Calmodulin (Calm1)	↓2.67
Chitinase-like protein 3 (Chil3)	↓2.34
DNA replication licensing factor MCM2 (Mcm2)	↓2.26
Neutrophilic granule protein (Ngp)	↓2.25
Olfactomedin-like protein 3 (Olfml3)	↓2.24
Coagulation factor X (F10)	↓2.18
Methylenetetrahydrofolate dehydrogenase (Mthfd1)	↓2.18
Lactotransferrin (Ltf)	↓2.15
Histone H1.5 (Hist1h1b)	↓2.14
Cytochrome c oxidase subunit 6B1 (Cox6b1)	↓2.04

Table 13 Significantly regulated protein in mice bone in the presence of Mg-Implant compared to S-Implant in 21days after implantation

Protein name	Fold changes in Mg21 Vs S21
Olfactomedin-like protein 3 (Olfml3)	↓2.313307

Table 14 Significantly regulated proteins in mice bone in the presence of Mg-Implant compared to S-Implant in 133days after implantation

Protein name	Fold changes in Mg133 Vs S133
Alkaline phosphatase, tissue-nonspecific isozyme (Alpl)	↑2.75
Tenascin(Tnc)	↑2.81
Plastin-3(Pls3)	↑2.83
Clusterin (Clu)	↑2.87
Serpin H1(Serpinh1)	↑3.27
Creatine kinase B-type(Ckb)	↑4.72

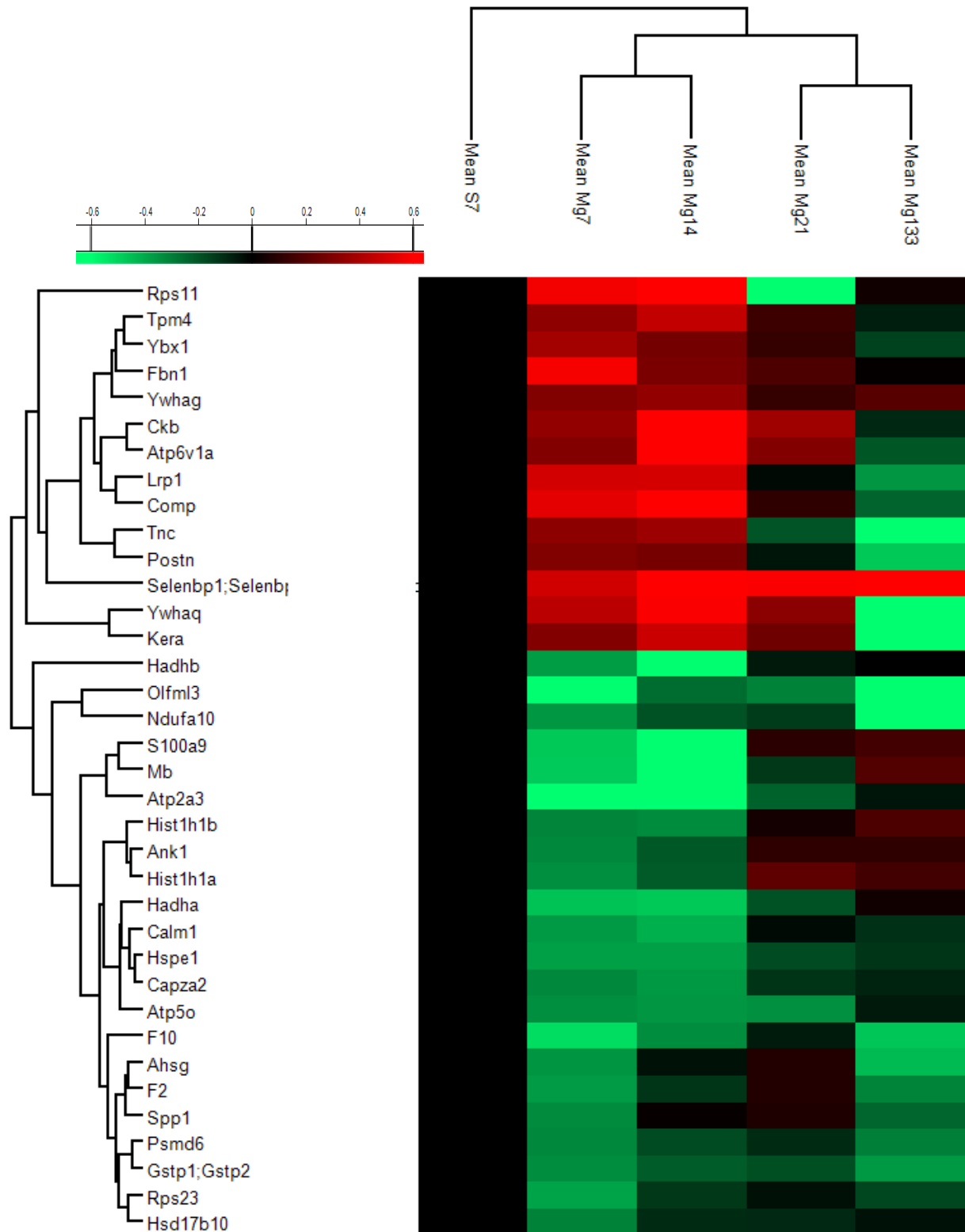


Fig. 11 Heat-map and hierarchical clustering of the significantly up- and down-regulated proteins (P-value= 0.05; min. fold-change of 2) in 7 days in mice bone tissue in the presence of Mg-Implant compared to S-Implant (as control) based on the mean values of the biological replicates (normalized on S7). Fold changes of these proteins in the other incubation times are shown in the heat map figure as well.

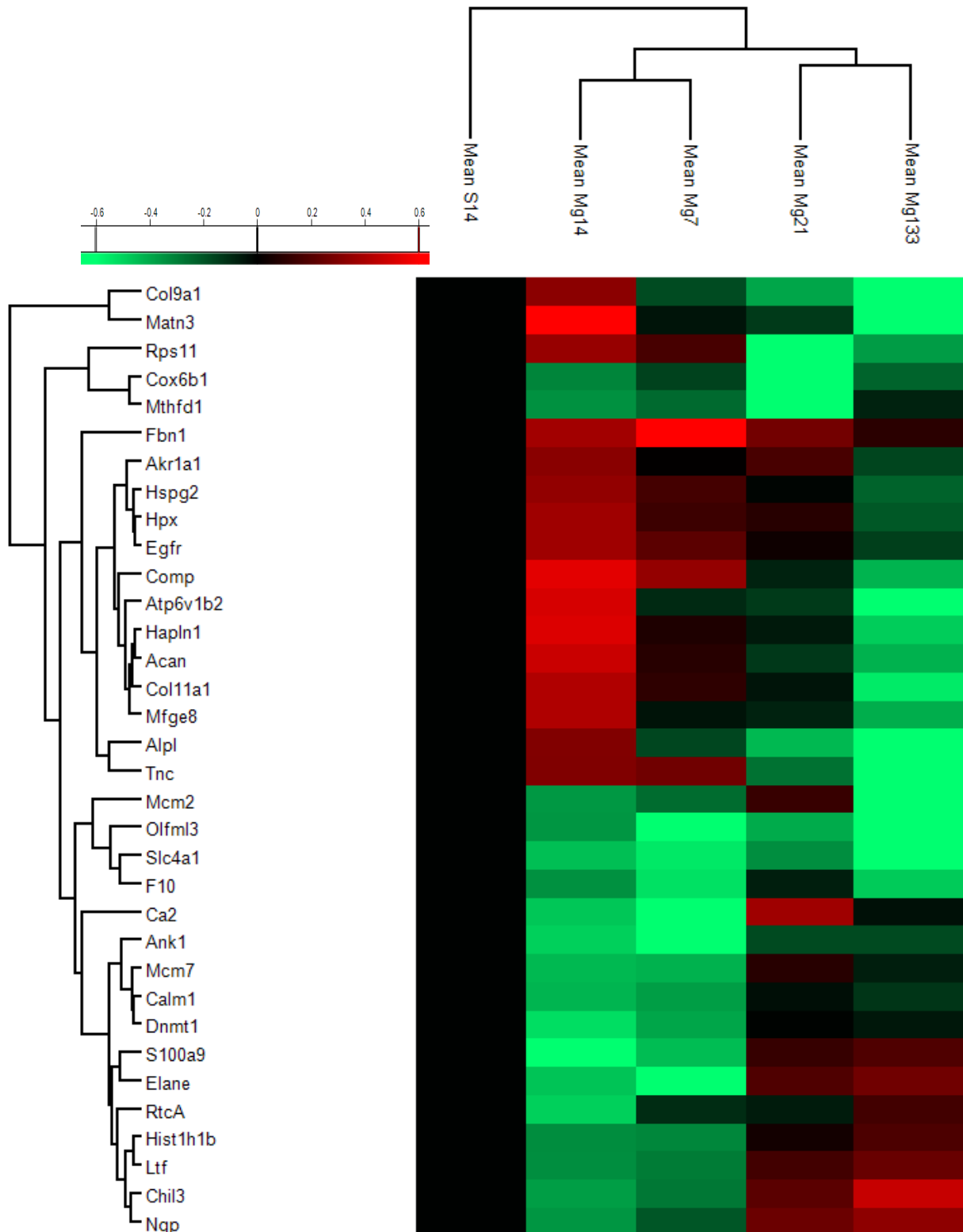


Fig. 12 Heat-map and hierarchical clustering of the up- and down-regulated proteins (P-value= 0.05; min. fold-change of 2) in 14 days in mice bone tissue in the presence of Mg-Implant compared to S-Implant (as control) based on the mean values of the biological replicates (normalized on S14). Fold changes of these proteins in the other incubation times are shown in the heat map figure as well.

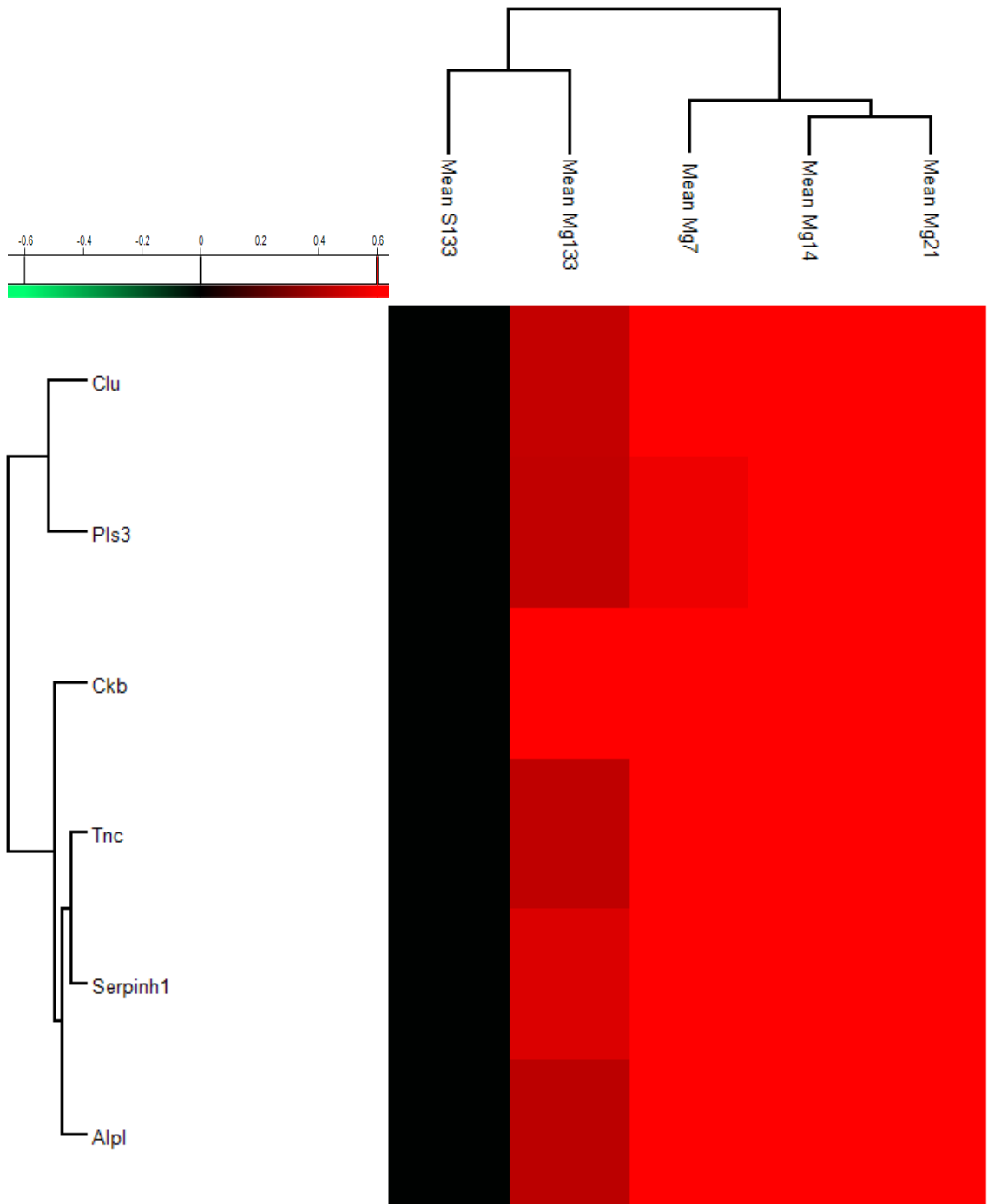


Fig. 13 Heat-map and hierarchical clustering of the up- and down-regulated proteins (P-value= 0.05; min. fold-change of 2) in 133 days in mice bone tissue in the presence of Mg-Implant compared to S-Implant (as control) based on the mean values of the biological replicates (normalized on S133). Fold changes of these proteins in the other incubation times are shown in the heat map figure as well.

4.3.3 Regulated proteins in bone cells and bone tissues (*in vivo*) under the influence of bio-adsorbable and conventional implants

Regarding the direct contact of bone-implant with the tissue, series of biological reactions occurs at the peri-implant site after implantation, which includes; protein adsorption, blood coagulation, inflammatory reaction, and new tissue formation [170, 171].

Checking the molecular function and involvement in various biological processes of the regulated proteins in UniProt gave a general overview about proteins. In many cases, this information does not provide a deep insight about the importance of a special protein in diverse biological pathways.

Thus, all the regulated proteins were searched one after each in 'PubMed' and 'Web of Science'. By searching for the function of the regulated proteins in PubMed search, the number of proteins which are involved in diverse biological processes was higher than the GO-annotation downloaded from UniProt. This was thus more reliable than the UniProt search. For the final data interpretation, regulated proteins were clustered based on their involvement in bone development, inflammation, and coagulation.

4.3.3.1 Regulated proteins involved in bone remodeling

Bone remodeling (bone formation and resorption by bone cells), is a dynamic life-time process in bone tissue [35, 36]. Since the proteins which are involved in bone remodeling have a crucial role throughout bone morphogenesis, up/down-regulated bone remodeling-related proteins in the presence of Mg-Implants in different time points compared to S-implant (*in vivo*) will be discussed in this chapter.

4.3.3.1.1 Regulated proteins which are involved in bone development

Fibrillin-1 (Fbn1)

The amount of fibrillin-1 (Fbn1), an extracellular matrix protein [172, 173], was significantly increased in the presence of Mg-implant compared to S-Implant during the incubation time (Fig. 14). The proteins of fibrillin family (Fibrillin-1 &2) regulate

TGF β family signaling [173-175] and mesenchymal stem cells (MSC) activity [174]. These proteins have diverse impacts on the differentiation of marrow mesenchymal stem cells [176]. In a fibrillin-1-mutant, enhancement of bone length and reduction of bone mineralization was observed [177]. In another study, Arteaga-Solis *et al.* showed the lack of fibrillin-1 and fibrillin-2, affect mechanical properties of bone and bone materials [173]. They showed fibrillin-2 has a positive effect on mechanical properties of bone; however, the role of fibrillin-1 in the material properties of bone is higher than fibrillin-2 [173]. Regarding the importance of this protein in the mechanical properties of bone [173], its up-regulation in the presence of Mg-Implant seems beneficial for bone health.

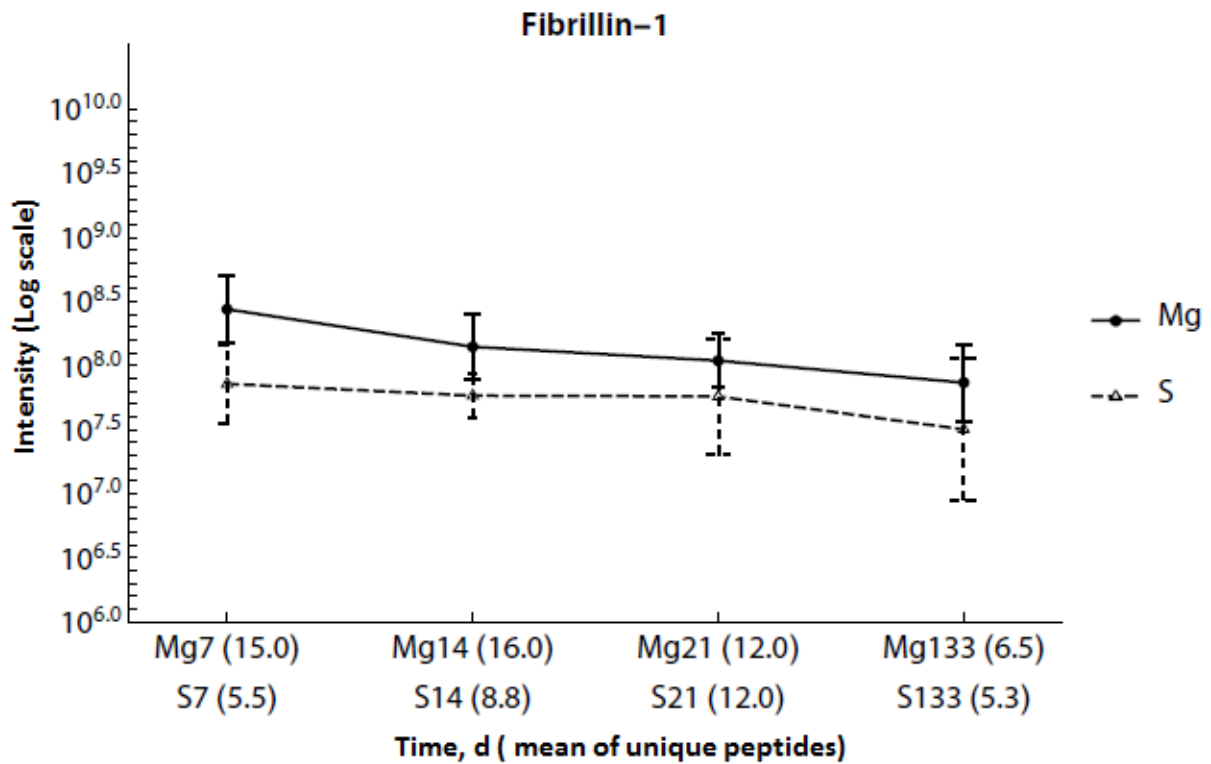


Fig. 14 Regulation of fibrillin-1 (Fbn1) during the incubation of mice bone with Mg-implant Vs S-Implant during the time.

Cartilage oligomeric matrix protein (Comp)

Cartilage oligomeric matrix protein (Comp) was up-regulated in the mouse bone tissues within 7 and 14 days after Mg-implantation (Fig. 15). In mesenchymal stem cells, Comp gene activates chondrogenic differentiation and suppresses osteogenic

differentiation [178]. In a study by Guo *et al.*, they found suppression effects of Comp on osteogenic differentiation and activation effects on chondrogenic differentiation [179]. On the other hand, Lim *et al.* found the acceleration of bone formation, angiogenesis, and chemoattraction in the presence of recombinant COMP-angiopoietin 1 in rat calvarial defects [180]. Moreover, Ishida *et al.* observed that comp increases bone formation activity of BMP-2 *in vitro* and *in vivo* [181]. Thus, it can be concluded that Mg-implant might be supportive for bone regeneration *in vivo* in the first two weeks of implantation.

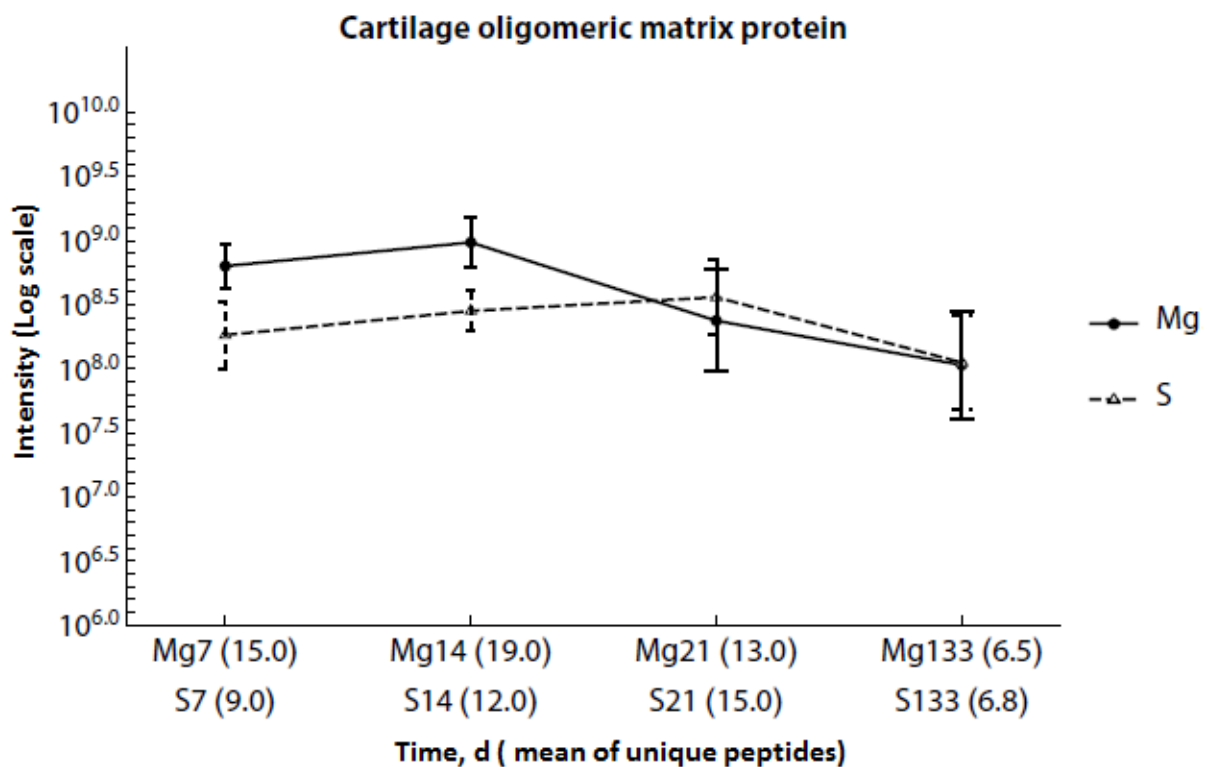


Fig. 15 Regulation of cartilage oligomeric matrix protein (Comp) during the incubation of mice bone with Mg-implant Vs S-Implant during the time.

Tenascin (Tnc)

Tenascin (Tnc) was another up-regulated protein after Mg- implantation in mice bone tissue until complete absorption (Fig. 16). Tenascins family including tenascin C and W, are extracellular matrix proteins in different connective tissue cells [182]. Tenascin has roles in bone formation and osteoblasts adhesion [94, 183]. In tenascin-C-knockout (KO) mouse, osteoblast differentiation is suppressed, and

osteoporosis is stimulated [184]. Chatakun *et al.* Found that tenascin does not affect early stage of bone formation; however, it has a role in bone mineralization and induces bone formation in a multicellular environment [182]. Furthermore, Morgan *et al.* mentioned cell interaction with the surrounding pericellular matrix is modulated by tenascin C & W. Moreover, they found tenascin c is up-regulated during osteoblast differentiation; however, tenascin w is down-regulated [183]. In summary, Mg-implant seems to be beneficial for new bone formation and fracture healing by increasing the amount of tenascin.

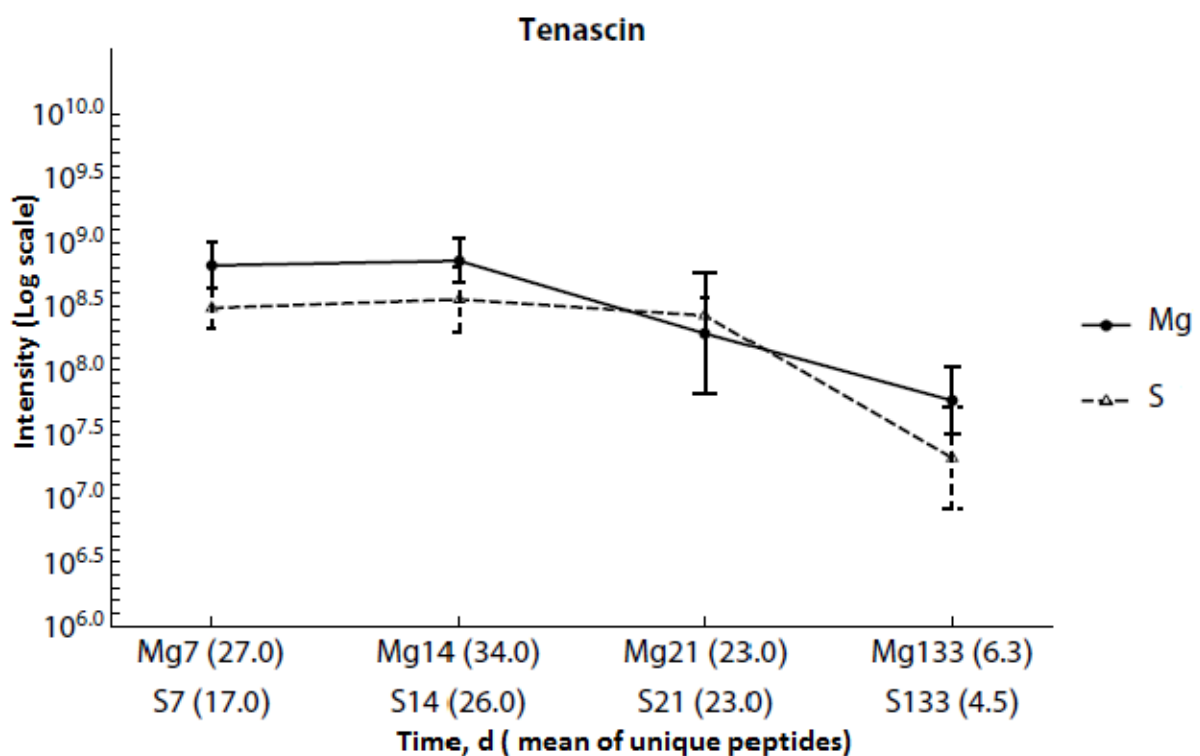


Fig. 16 Regulation of tenascin (Tnc) during the incubation of mice bone with Mg-implant Vs S-Implant during the time.

Low-density lipoprotein receptor-related protein 1 (Lrp1)

Another significantly up-regulated protein in mouse bone tissue in the presence of magnesium implant after 7 days incubation was a multifunctional protein [185], low-density lipoprotein receptor-related protein 1 (Lrp1) (Fig. 17). It aids in postprandial lipoproteins and vitamin K1 metabolism in human osteoblasts [185]. Lrp1 is strongly

synthesized in human osteoblasts and marrow stromal cells [185]. Additionally, galectin-8, which has a role in osteoclastogenesis, is negatively regulated by Lrp-1 [186]. Hence, an increase of this protein in the presence of magnesium implant gives a positive impact on bone tissue.

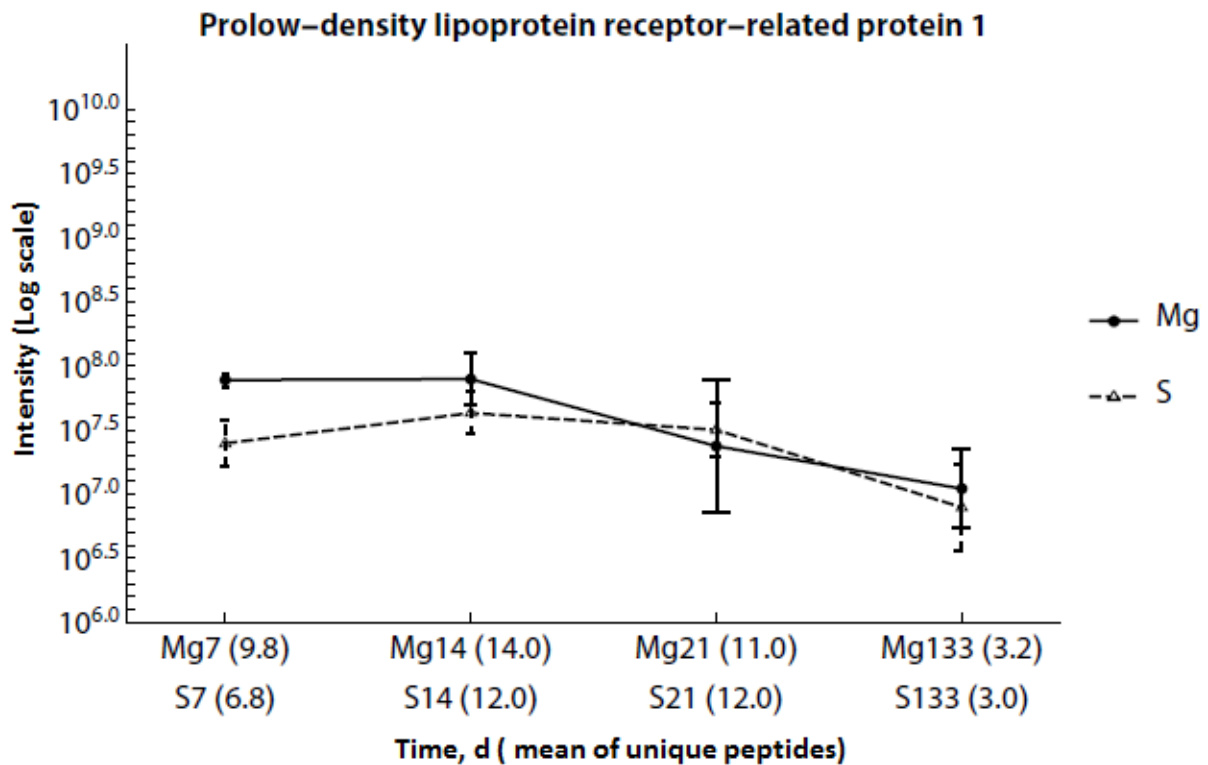


Fig. 17 Regulation of low-density lipoprotein receptor-related protein 1 (Lrp1) during the incubation of mice bone with Mg-implant Vs S-Implant during the time.

Nuclease-sensitive element-binding protein 1 or Y-box binding protein-1 (Ybx1)

Nuclease-sensitive element-binding protein 1 or Y-box binding protein-1 (Ybx1), a multifunctional protein with a potential to be a biomarker for osteosarcoma [187, 188], was significantly up-regulated in 7 days after implantation with Mg-implant (Fig. 18). A higher amount of YB-1 was observed in a patient with osteosarcoma with a higher rate of metastasis [187]. Fujiwara-Okada *et al.* mentioned YB-1 regulates the development of cell cycle in osteosarcoma [188]. Also, YB-1 is the target protein for miR-382 which is a tumor suppressor [189]. Therefore,

increasing the amount of this protein under the influence of Mg-implant might be harmful to the health of bone; nevertheless this significantly up-regulation was not continued in the subsequent incubation times and the amount of this protein reduced to reach the amount in control (S-implant).

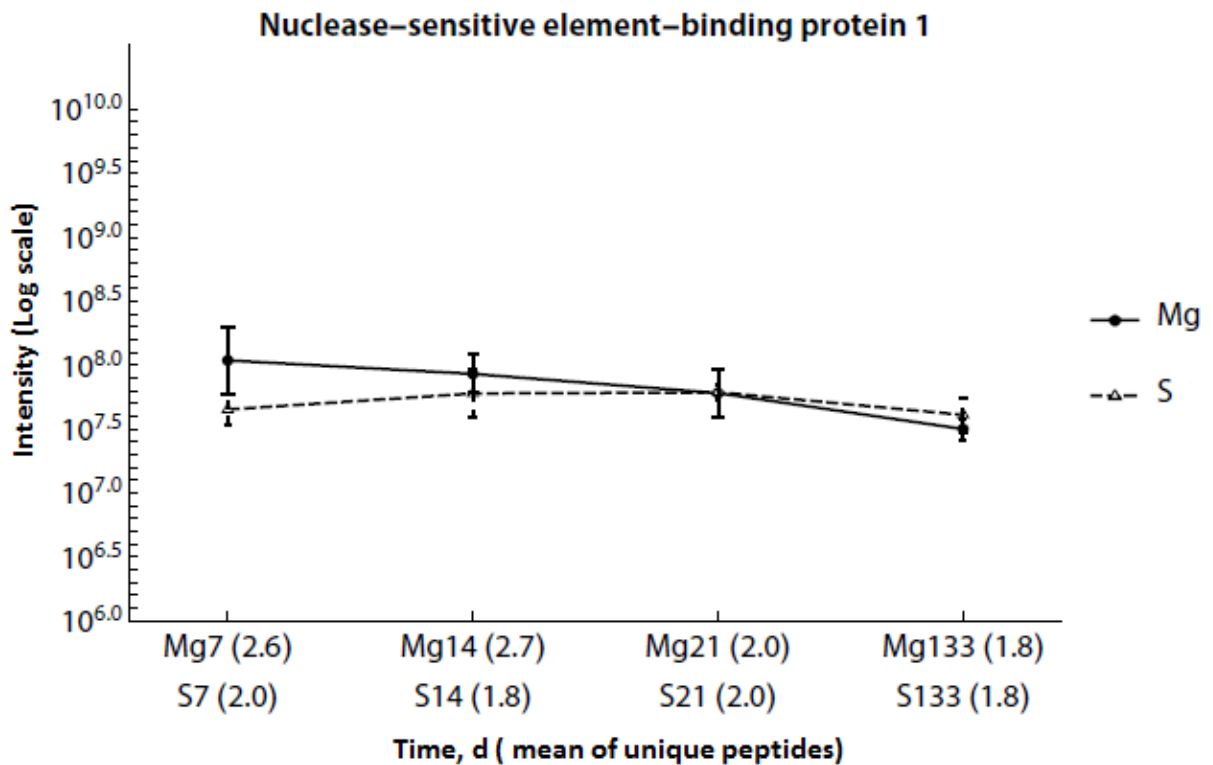


Fig. 18 Regulation of nuclease-sensitive element-binding protein 1 or Y-box binding protein-1 (Ybx1) during the incubation of mice bone with Mg-implant Vs S-Implant during the time.

Tropomyosin alpha-4 chain (Tpm4)

Tropomyosin alpha-4 chain (Tpm4) was significantly up-regulated in the Mg-implanted bone tissue within 7 days (Fig. 19). It belongs to the family of tropomyosins (Tms) which stabilizes actin microfilaments, includes four genes with more than 40 kinds of tropomyosins [190]. It is synthesized [191] and up-regulated in osteoclasts, regulating their adhesion structures [190, 191]. Thus, up-regulation of this protein is disadvantageous for bone formation.

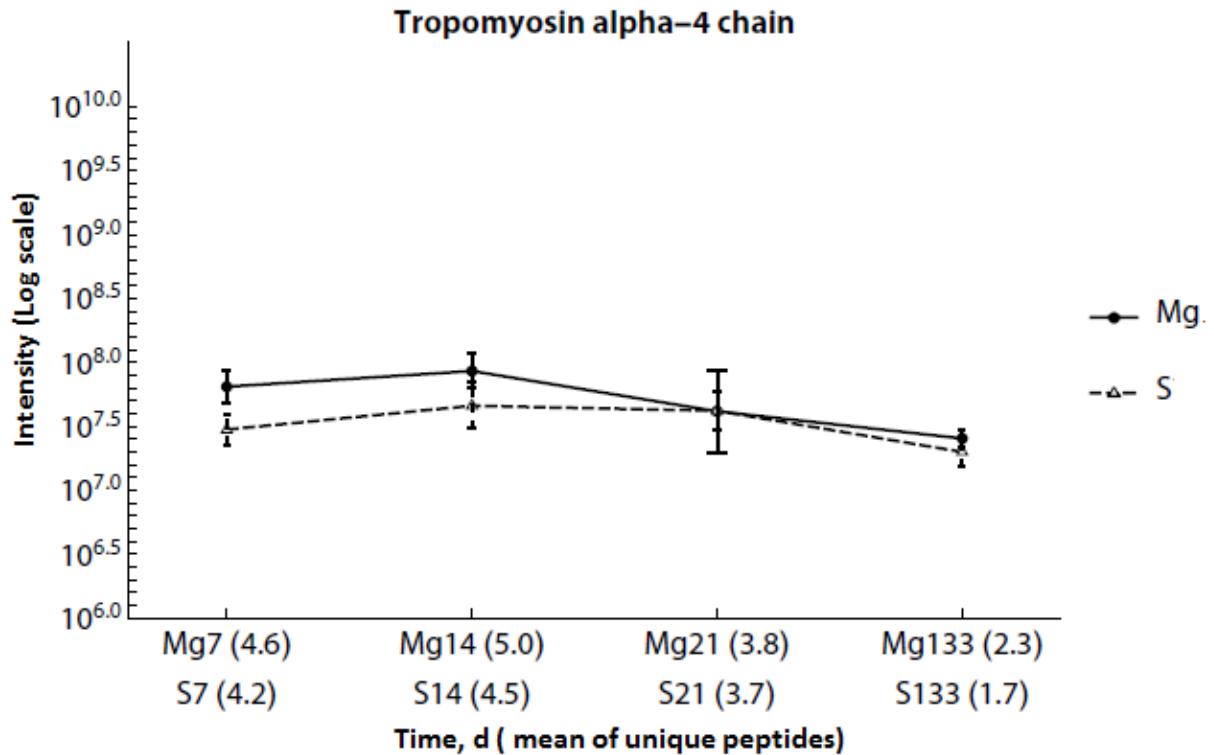


Fig. 19 Regulation of tropomyosin alpha-4 chain (Tpm4) during the incubation of mice bone with Mg-implant Vs S-Implant during the time.

Keratocan (Kera)

Another up-regulated protein in the presence of Mg-implant in mouse bone tissue after 7 days implantation is keratocan (Kera) (Fig. 20). This protein is one of the extracellular matrix proteins from the small leucine-rich proteoglycan family [192, 193]. It is highly synthesized by osteoblasts in day 14, poorly in days 7&21; and not by osteocytes (or in a small amount)[194], and it is one of the essential proteins for osteoblast maturation [194]. The rate of bone formation and mineral deposition are significantly decreased in keratocan-KO mouse [194]. Therefore, Mg-implant might have a positive effect on bone formation and fracture healing mainly in the first two weeks by up-regulating this protein.

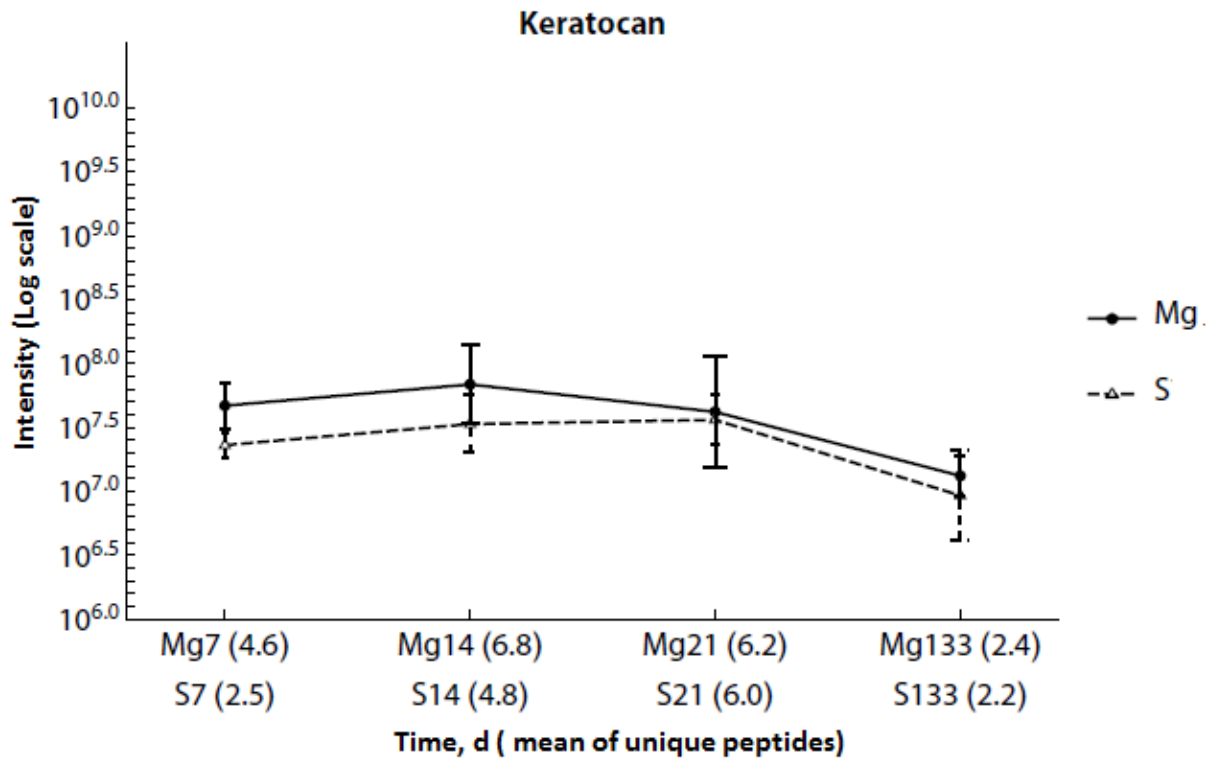


Fig. 20 Regulation of keratocan (Kera) during the incubation of mice bone with Mg-implant Vs S-Implant during the time.

Periostin (Postn)

Periostin (Postn), an extracellular matrix protein [195-197] and an osteoblast-specific-factor [198], was also up-regulated in the presence of Mg within seven days (Fig. 21). Diverse tissues synthesize periostin during ontogenesis [195]. It is synthesized in bone, especially in periodontal ligaments and periosteum, and plays a crucial role in bone formation and bone metabolism [196]. Also, it has been mentioned by Gerbaix *et al.* that periostin increases bone healing process by "inducing proliferation of transplanted hASCs and angiogenesis in calvarial defects" [197]. Furthermore, periostin positively regulates bone size as well as TGF-beta [199]. Hence, up-regulation of this protein under the influence of Mg-Implant is beneficial for bone formation and bone healing; however, it occurs particularly in the first two weeks of implantation.

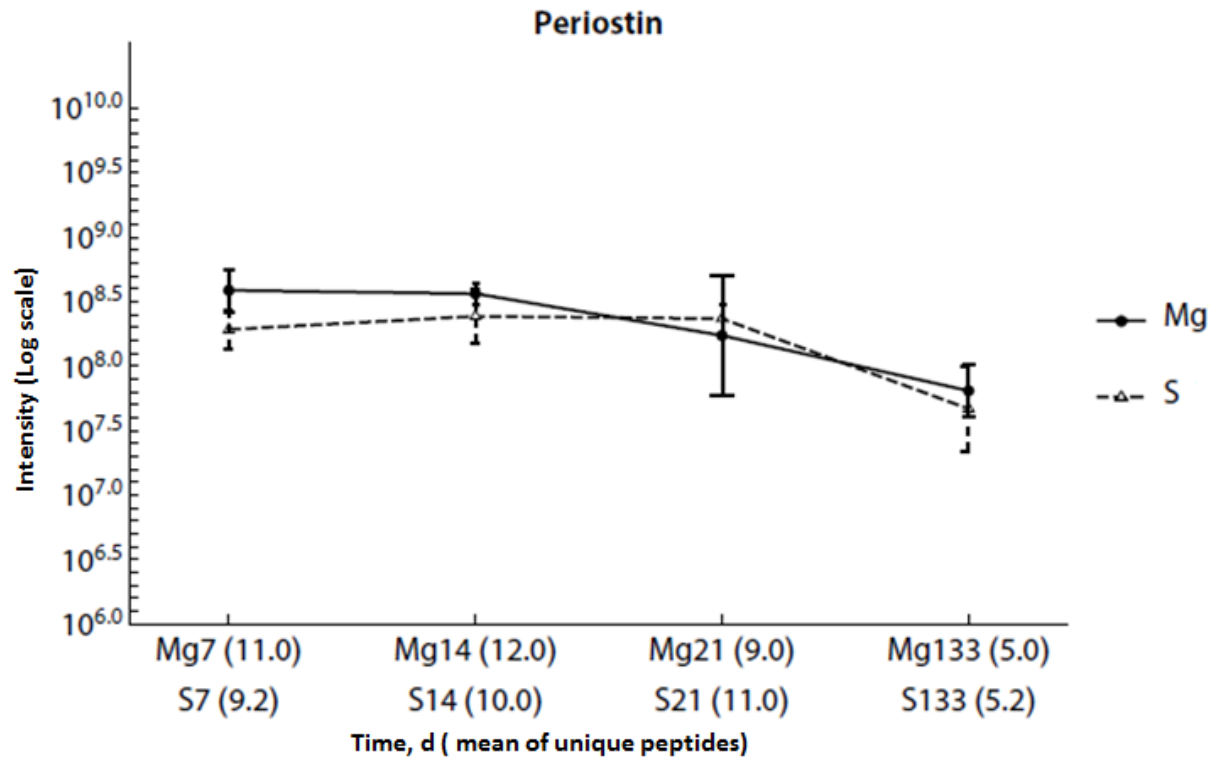


Fig. 21 Regulation of periostin (Postn) during the incubation of mice bone with Mg-implant Vs S-Implant during the time.

Aggrecan core protein (Acan)

Aggrecan core protein (Acan), which is an extracellular matrix component with a critical role in the development of (growing plate) cartilage [200, 201], was another meaningfully up-regulated protein in the presence of Mg-implant in 14 days (Fig. 22). Aggrecan is a proteoglycan [200], and a typical chondrogenic protein [202]. The synthesis of aggrecan is positively modulated by Runx3 [201]. Lee *et al.* demonstrated that aggrecanases are active during cartilage resorption [203]. Therefore, Mg-induced enhancement of aggrecan *in vivo* has a positive effect on fracture healing process.

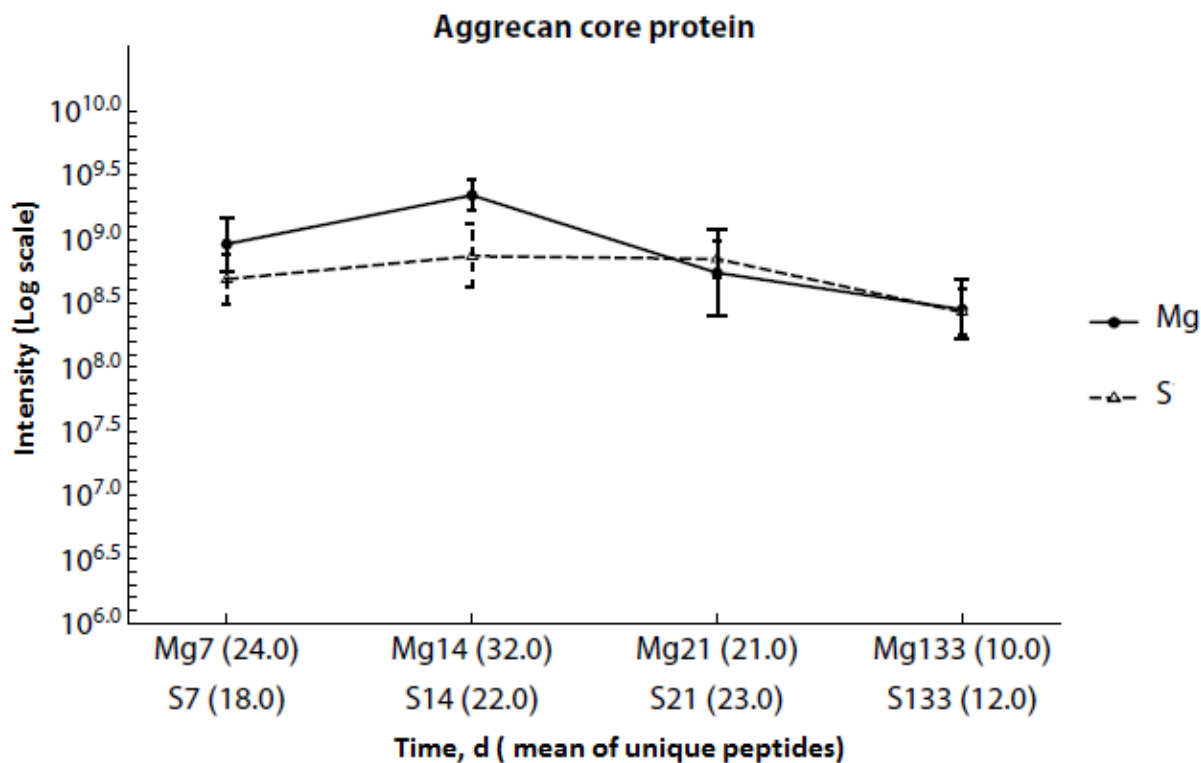


Fig. 22 Regulation of aggrecan core protein (Acan) during the incubation of mice bone with Mg-implant Vs S-Implant during the time.

3-hydroxyacyl-CoA dehydrogenase type-2 (Hsd17b10)

The amount of 3-hydroxyacyl-CoA dehydrogenase type-2 (Hsd17b10) was decreased in mice bone who received Mg-Implant in 7days (Fig. 23). This protein belongs to the short-chain dehydrogenase/reductase superfamily [204]. Man *et al.* mentioned Hsd17b10 gene in the list of 45 genes which they discriminate amongst good or poor responders to chemotherapy in osteosarcoma [205]. Furthermore, Salas *et al.* found up-regulation of Hsd17b10 in patients who were not responding well to chemotherapy [204]. Later in 2013, a higher level of HSD17B10 mRNA in prostate cancer bone metastases was reported by Jenberg *et al.* [206]. Since down-regulation of this protein in the presence of Mg-Implant was observed in the first incubation time (7days) and it was not continued throughout the subsequent incubations, this reduction might not be disadvantageous for bone health.

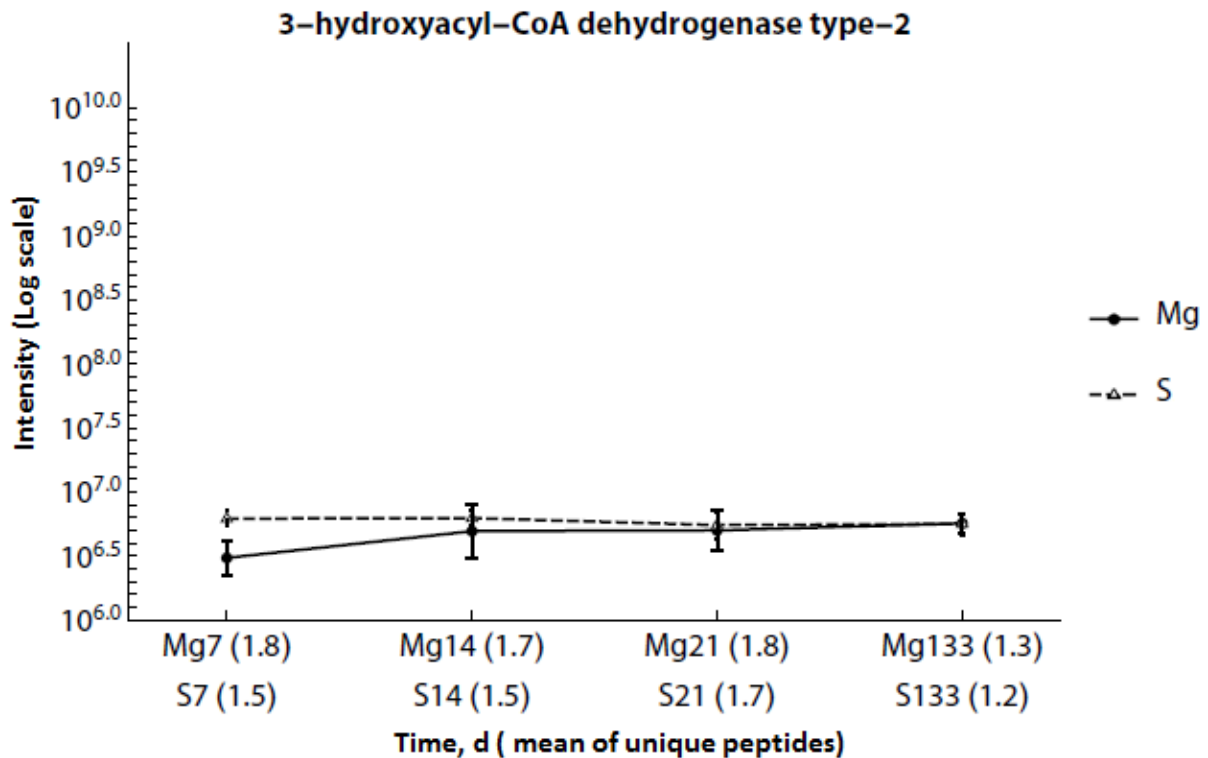


Fig. 23 Regulation of 3-hydroxyacyl-CoA dehydrogenase type-2 (Hsd17b10) during the incubation of mice bone with Mg-implant Vs S-Implant during the time.

V-type proton ATPase subunit B (ATP6V1B2)

The amount of V-type proton ATPase subunit B(ATP6V1B2), the multi-subunit complex protein [103] which has a crucial role in amelogenesis during the development of enamel [103, 104] was meaningfully increased in 7&14 days in mice bone with Mg-implant (Fig. 24). No changes were observed in the amount of this protein at last time point (133). This protein is among four up-regulated V-type ATPases through maturation phase of amelogenesis in a study by Sarkar *et al.* [103]. In conclusion, increasing the amount of this protein could be helpful for bone maturation and bone development during fracture healing process.

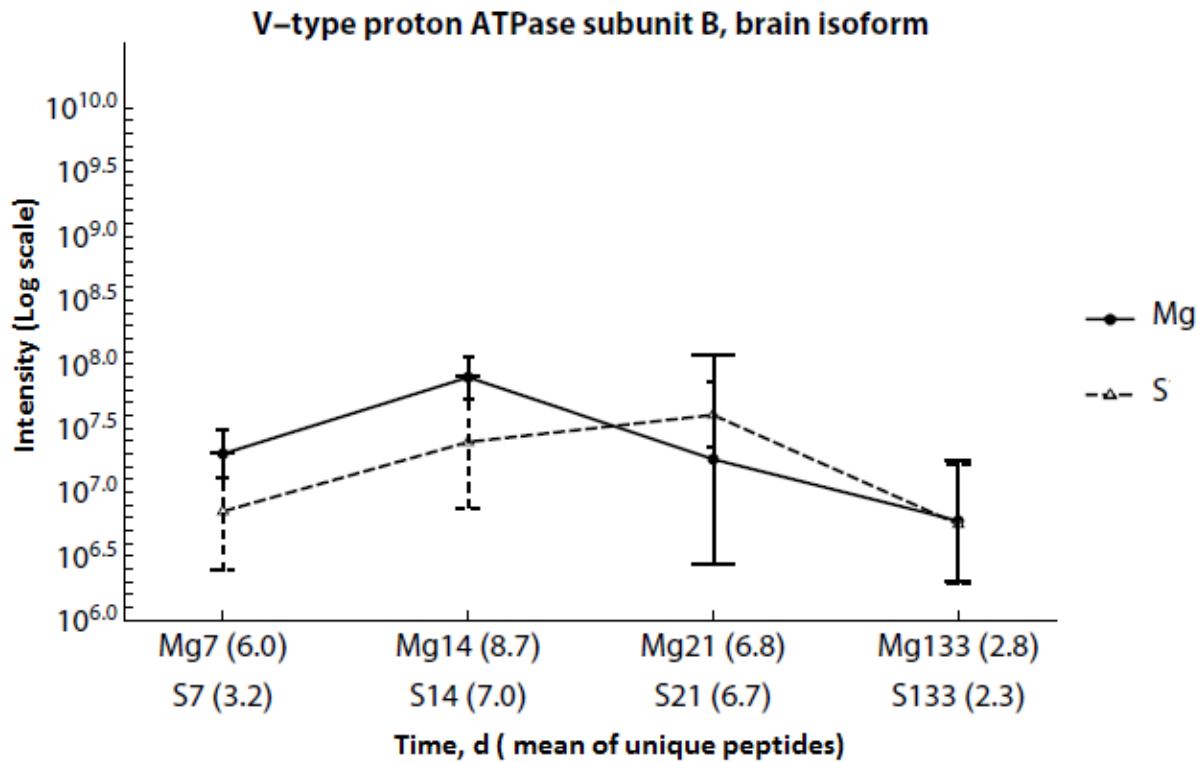


Fig. 24 Regulation of V-type proton ATPase subunit B (ATP6V1B2) during the incubation of mice bone with Mg-implant Vs S-Implant during the time.

Matrilin-3 (Matn3)

Enhancement of matrilin-3 (Matn3), an ECM component [207-209], which is specially synthesized in cartilage tissue [209], was observed in the presence of Mg-implants in 14 days (Fig. 25). Matrilin-3 functions in the development of cartilage and ossification [208]. Also, it is involved in osteoarthritis pathomechanisms [208]. In a study by Yilmaz *et al.* in Temporomandibular joint internal derangement (TMJ ID), polymorphism in matrilin-3 was observed [207]. Furthermore, this protein has a role in inflammation, matrix formation and degradation in cartilage and osteoarthritis [208]. In another study which was done by Kung *et al.* in multiple epiphyseal dysplasia (MED) and pseudoachondroplasia (PSACH), mutations in genes encoding cartilage oligomeric matrix protein and matrilin-3 was observed [210]. Moreover, matrilin-3 and Cyclin-I also have roles in chondrocyte differentiation “during impairment and recovery of the growth plate in TD” [211]. Taken together, the effect of Mg-implants in the first two weeks of implantation on up-regulation of this protein seems beneficial for bone development.

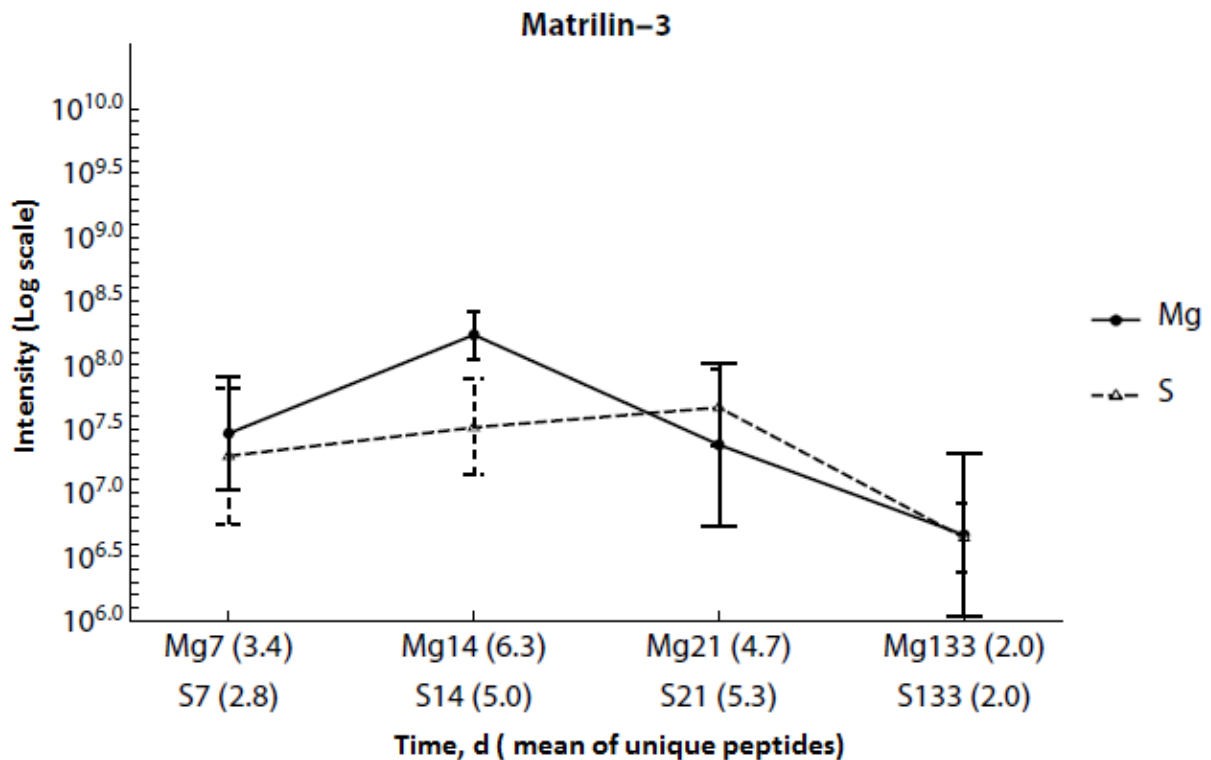


Fig. 25 Regulation of matrilin-3 (Matn3) during the incubation of mice bone with Mg-implant Vs S-Implant during the time.

Lactadherin (Mfge8)

Lactadherin (Mfge8), a glycoprotein [212, 213], which aids in bone homeostasis [212-214], was meaningfully up-regulated in 14 days after implantation of mouse bone tissue with Mg-implant (Fig. 26). Increase in osteoclastogenesis in MFG-E8-KO mice was observed in various studies [212-214]. Abe *et al.* found chronic periodontal bone loss in Mfge8^{-/-} mice compared to wild-type mice [212]. They reported that Mfge8 is synthesized and regulates osteoclast differentiation and function in the osteoclasts of mouse and human [212]. Furthermore, this protein has a role as an anti-inflammatory molecule [214]. Also, Ait-Oufella *et al.* found a deficiency of Mfge8 in bone marrow-derived cells increases apoptosis [215]. Therefore, Mg-Implant can help bone formation and prevent bone resorption by up-regulating this protein. Moreover, the anti-inflammatory effect of this protein prevents further inflammatory reactions in bone.

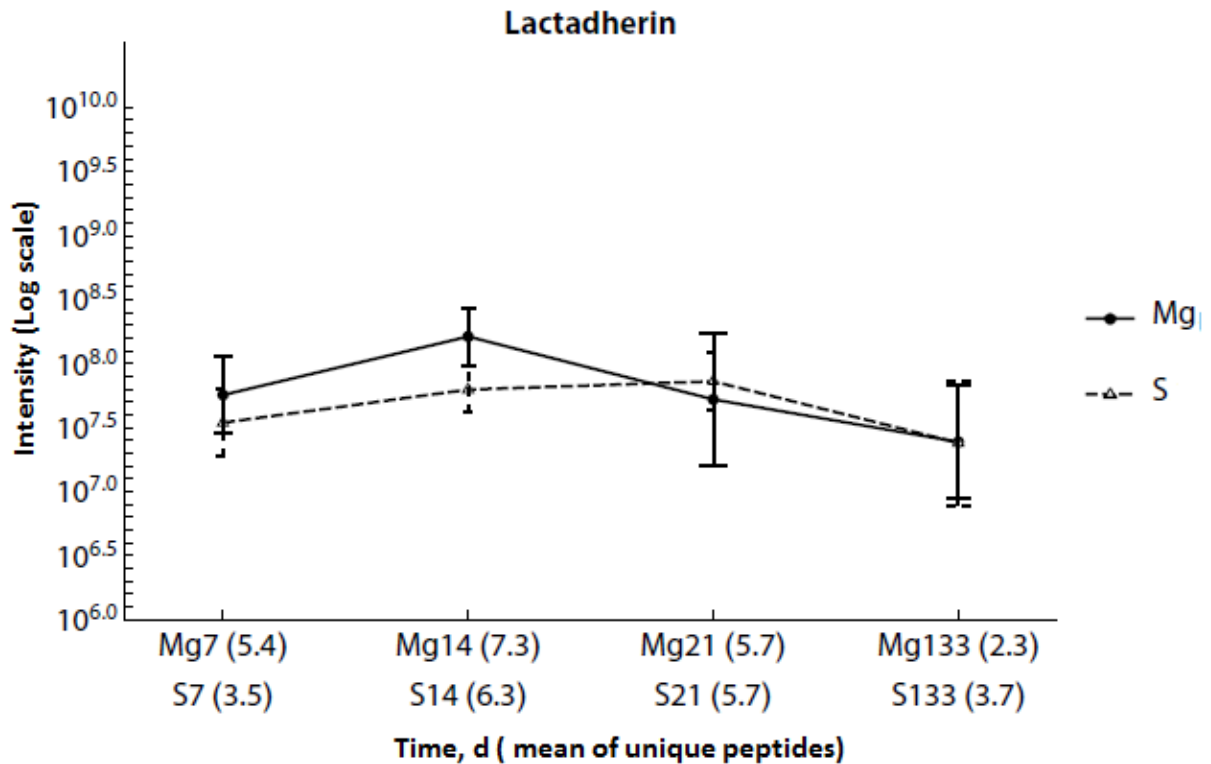


Fig. 26 Regulation of lactadherin (Mfge8) during the incubation of mice bone with Mg-implant Vs S-Implant during the time.

Alkaline phosphatase, tissue-nonspecific isozyme (Alpl)

The level of alkaline phosphatase, tissue-nonspecific isozyme (Alpl) was significantly increased in the presence of mg-implants in 7, 14, and 133 days after implantation (Fig. 27). Alkaline phosphatase is an osteoblastic marker [216, 217] with pyrophosphatase activity which dissolves calcium pyrophosphate dihydrate crystals [218]. Since this enzyme is used to check the osteoblast differentiation in various studies [216-218], its up-regulation in the presence of Mg-implants demonstrates osteoblast differentiation *in vivo* via fracture healing.

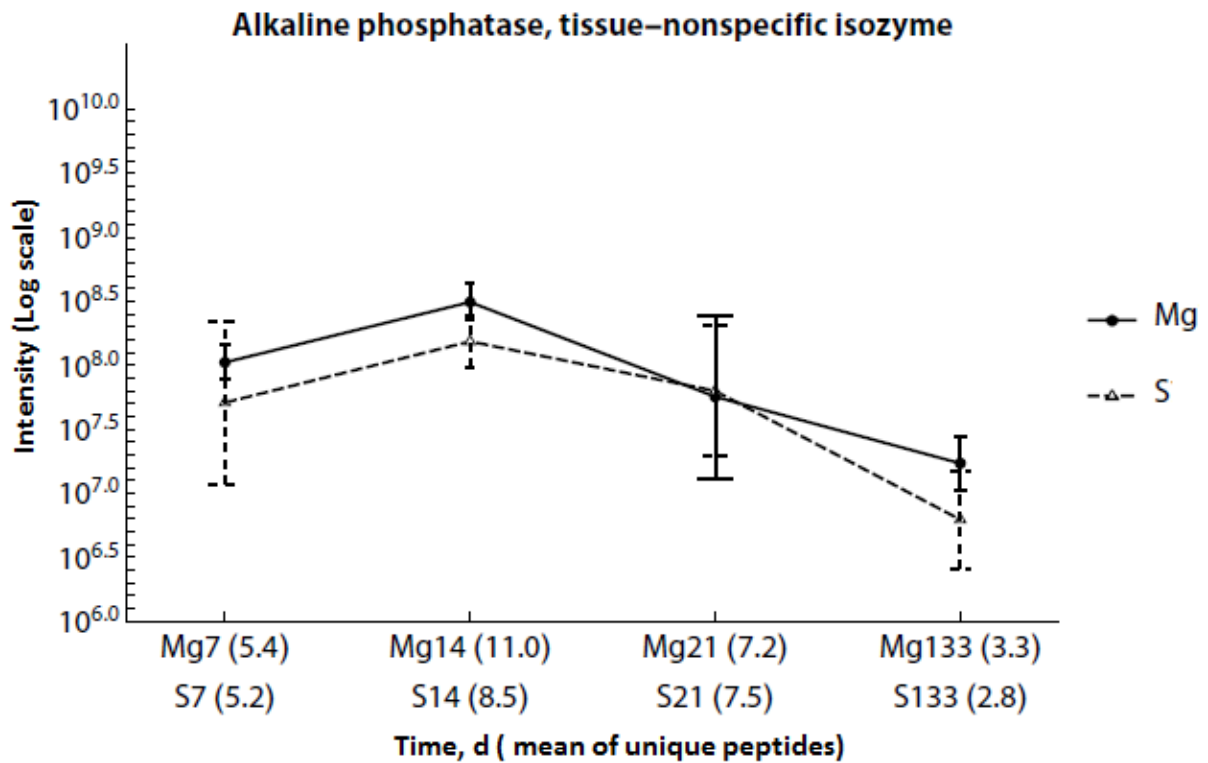


Fig. 27 Regulation of alkaline phosphatase, tissue-nonspecific isozyme (AlpI) during the incubation of mice bone with Mg-implant Vs S-Implant during the time.

Chitinase-like protein 3 (Chil3)

The level of chitinase-like protein 3 (Chil3) was reduced in 14 days after Mg implantation (Fig. 28). Chitinase-like proteins have roles in differentiation, inflammation, and tissue remodeling [219]. Chitinase-like protein, Chi3L1, is synthesized in chondrocytes and is associated with the native (innate) response of immune system [220]. The amount of Chil3 is down-regulated in preterminal acute exacerbations of IPF, whereas apoptosis is increased in this condition [221]. Also, the level of this protein is reduced during injury [221]. Thus, it can be concluded that down-regulation of this protein in the presence of Mg-Implant might not be ideal for bone healing.

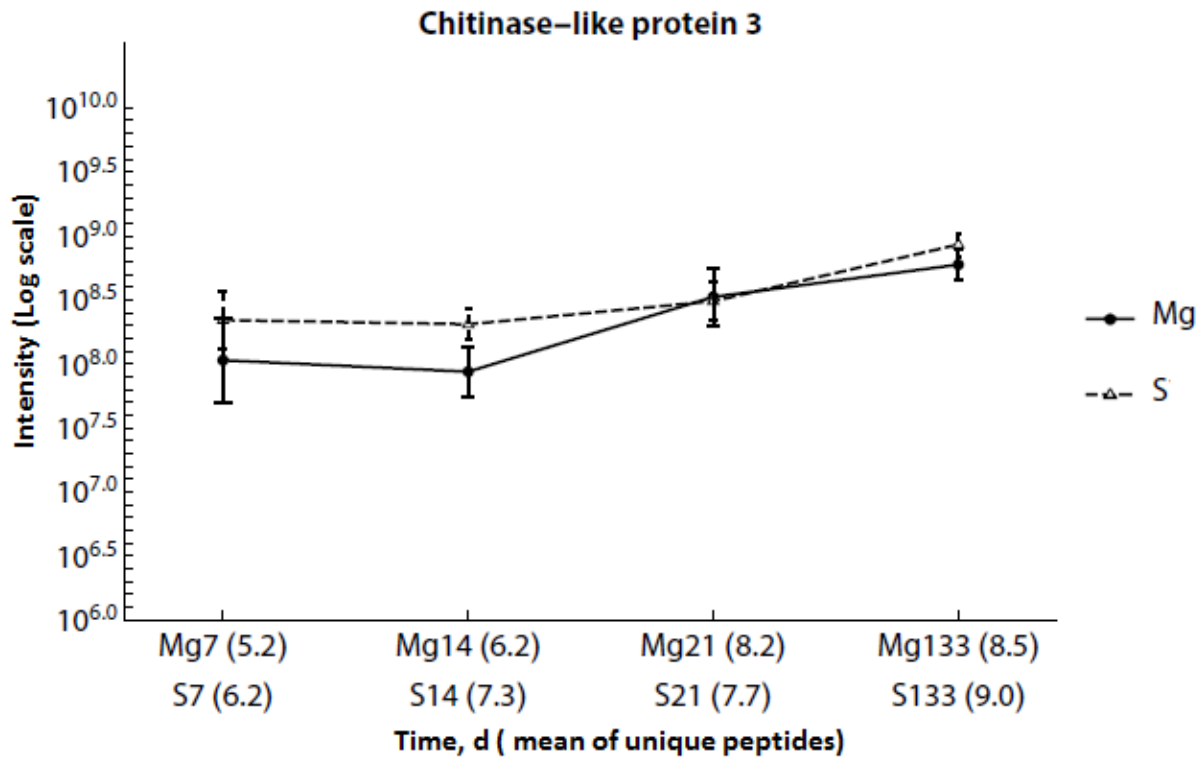


Fig. 28 Regulation of chitinase-like protein 3 (Chil3) during the incubation of mice bone with Mg-implant Vs S-Implant during the time.

Plastin-3 (Pls3)

Another significantly up-regulated protein after 133 days was plastin-3 (Pls3) (Fig. 29). Plastin3 aids in actin bundle formation [222-224]. Mutation in PLS3 causes early onset osteoporosis [222, 223]. Van Dijk *et al.* found that PLS3 is a new factor for multi-factorial osteoporosis [224]. On the other hand, plastin 3 was up-regulated in the differentiation of dental follicle precursor cells (DFPCs) [225]. Therefore, up-regulation of this protein in the presence of Mg-implant seems helpful for cell differentiation and fracture healing.

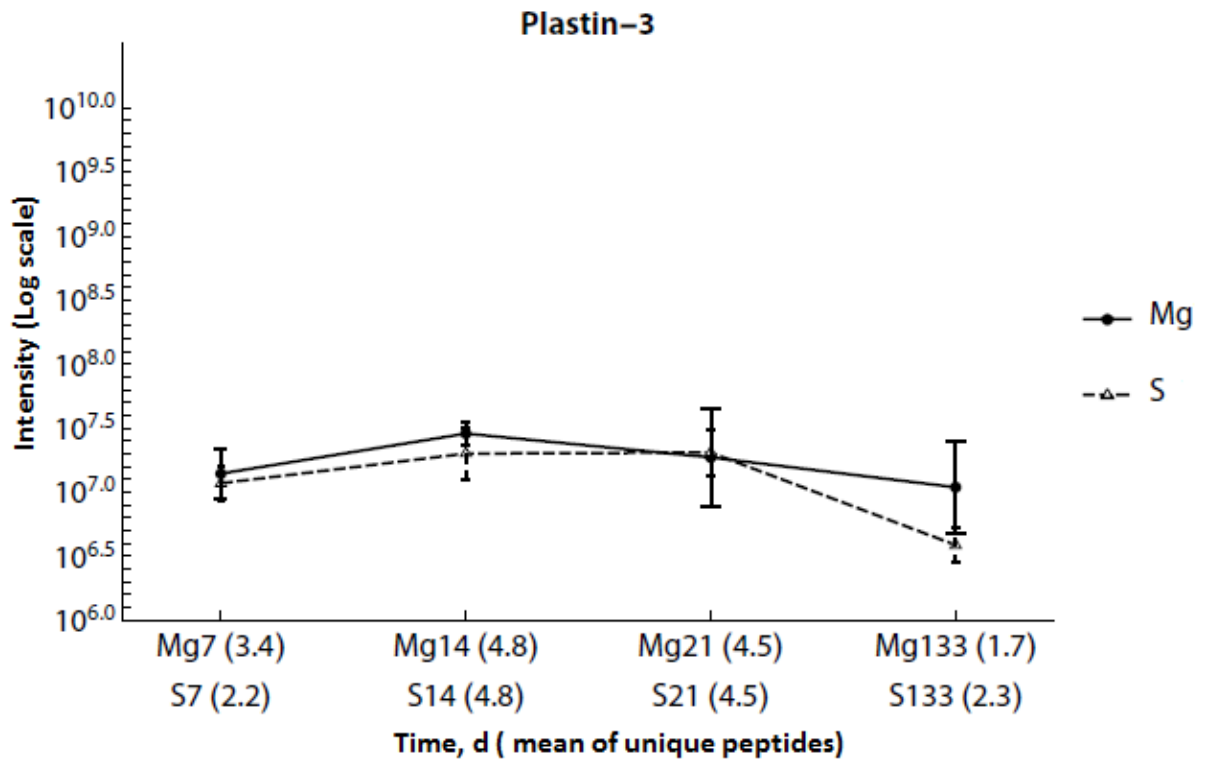


Fig. 29 Regulation of plastin-3 (Pls3) during the incubation of mice bone with Mg-implant Vs S-Implant during the time.

HSP47 or serpin-H1 (Serpinh1)

HSP47 or serpin-H1 (Serpinh1) is a procollagen-specific chaperone molecule [226], which was significantly up-regulated in the presence of Mg-implant particularly in 133days after implantation (Fig. 30). Mutation of serpin-H1 was found in osteogenic imperfecta (OI), a bone disorder with less bone mass, high risk of fragility and fracture [226-230]. Therefore, Mg-implants can be advantageous for bone health by up-regulating this protein.

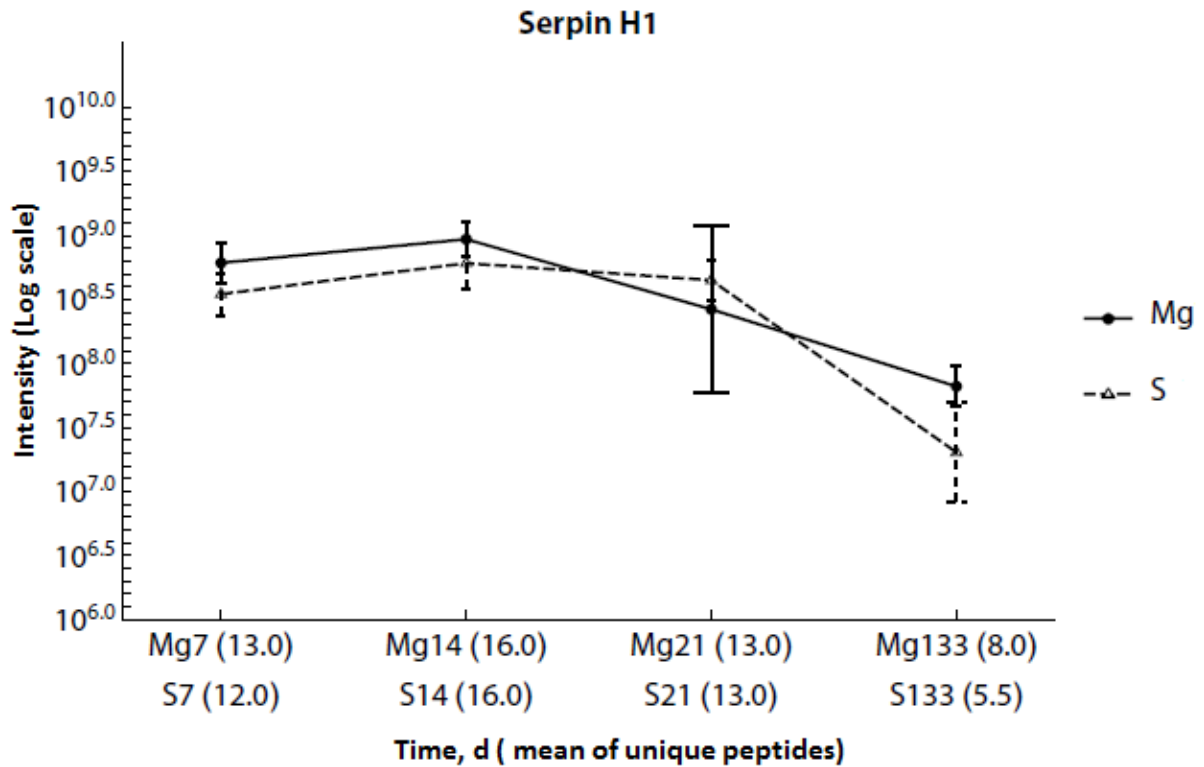


Fig. 30 Regulation of HSP47 or serpin-H1 (Serpinh1) during the incubation of mice bone with Mg-implant Vs S-Implant during the time.

Hyaluronan and proteoglycan link protein 1 (Hapln1)

Another up-regulated protein in the mouse bone tissue after implantation with Mg-implant was hyaluronan and proteoglycan link protein 1 (Hapln1) (Fig. 31). The regulation of this protein was significant in 14 days, and there was no change in its amount in 133 days. Hapln1 is a central extracellular matrix component of cartilage [231]. Polymorphism of the gene of HAPLN-1 might be associated with spinal degeneration [231]. Therefore, the influence of Mg-implant on the amount of this protein is suitable for bone health.

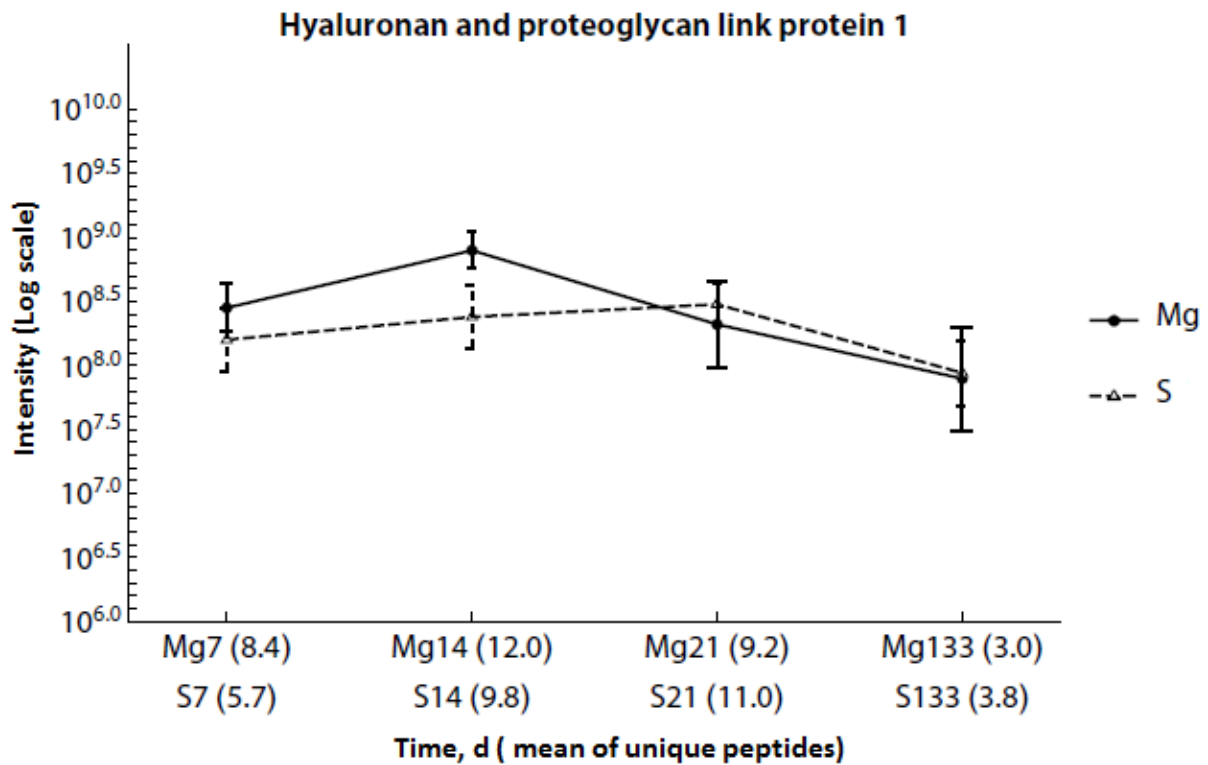


Fig. 31 Regulation of hyaluronan and proteoglycan link protein 1 (Hapln1) during the incubation of mice bone with Mg-implant Vs S-Implant during the time.

Epidermal growth factor receptor (Egfr)

Epidermal growth factor receptor (Egfr) was another significantly up-regulated protein after 14 days of Mg-implantation *in vivo* (Fig. 32). This protein has a significant role in the development of cartilage tissue in regulating the degradation of cartilage matrix throughout secondary ossification center (SOC) formation [232]. Morita *et al.* reported that the amount of EGFR was enhanced in temporal bone squamous cell carcinoma (TBSCC) [233]. Moreover, a significant decrease in tibial trabecular bone mass with abnormalities in trabecular number and thickness was observed by complete deletion of EGFR in a study by Zhang *et al.* [234]. Also, in EGFR-KO the number of osteoblasts was reduced as well as mineralization activity, whereas the number of osteoclasts was increasing [234]. Hence, it can be concluded that Mg-implant could be advantageous for bone formation by inducing the up-regulation of this protein in mice bone which could possibly improve osteoblast number and bone mineralization.

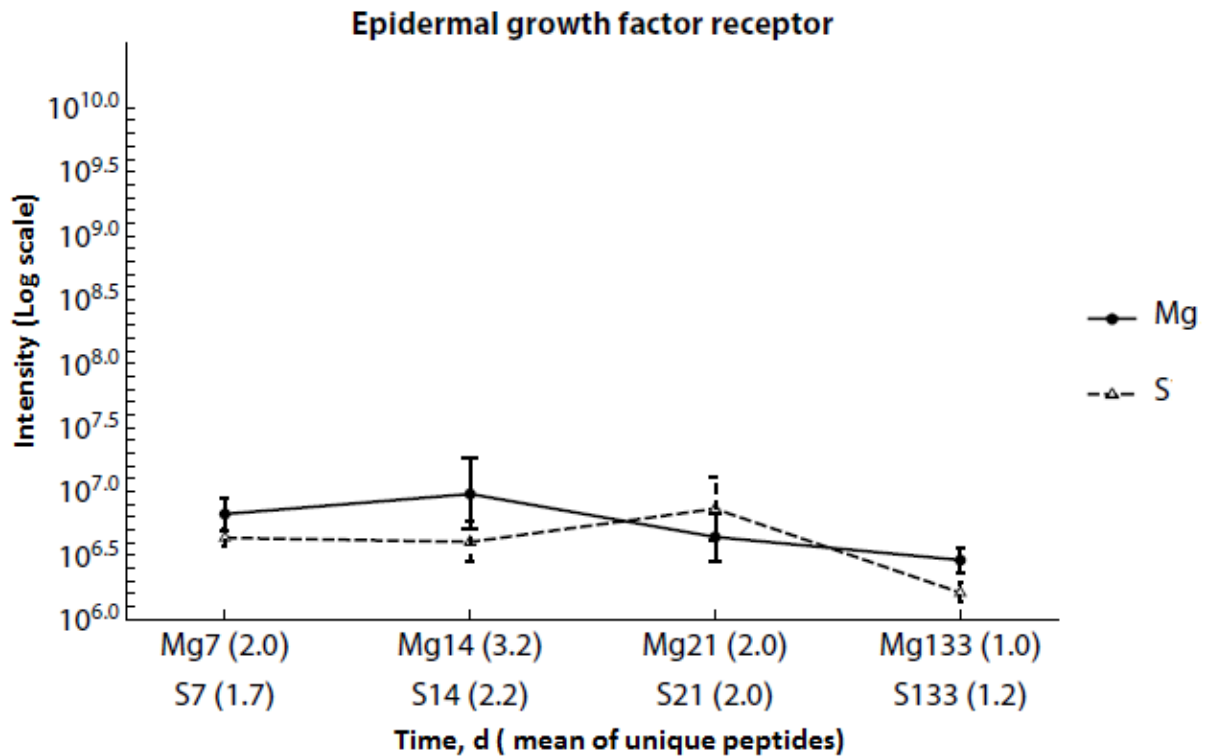


Fig. 32 Regulation of epidermal growth factor receptor (Egfr) during the incubation of mice bone with Mg-implant Vs S-Implant during the time.

Collagen alpha-1(XI) chain (Col11a1)

Another type of collagen which was considerably up-regulated after 14 days in the presence of Mg-Implant was collagen alpha-1(XI) chain (Col11a1) (Fig. 33). Type XI collagen is present in the extracellular matrix of cartilage [235, 236]. Li *et al.* found that collagen XI has a crucial role in the formation of cartilage collagen fibrils [235]. The amount of Col11A1 which is synthesized in the intervertebral disc is lower in the intervertebral disc of the patients who have lumbar disc herniation (LDH) [236]. Furthermore, Hufnagel *et al.* found that mutation in Col11a1 causes severe skeletal dysplasia, and the interaction of col11a1 and collagen II& V is affected by Col11a1 mutation which defects cartilage and ocular vitreous [237]. Thus, up-regulation of Col11A1 is beneficial for bone health. Also, it must be mentioned; there was no regulation of this protein at the last time point, which might indicate that the bone tissue acts normal (normal remodeling process) after completely absorbing the Mg-implants.

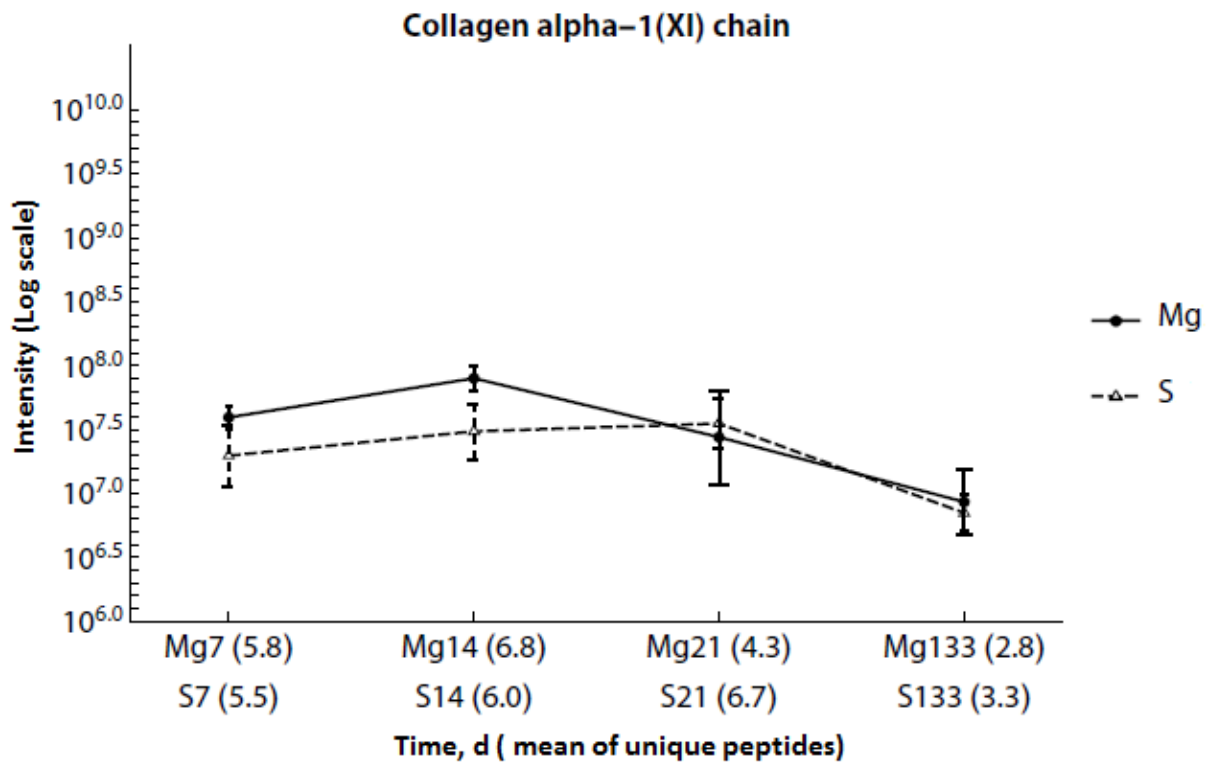


Fig. 33 Regulation of collagen alpha-1(XI) chain (Col11a1) during the incubation of mice bone with Mg-implant Vs S-Implant during the time.

Collagen alpha-1(IX) chain (Col9a1)

In the mice bone with Mg-Implant, the level of collagen alpha-1(IX) chain (Col9a1) was significantly enhanced in 14 days and down-regulated to the same amount as controls in 133 days (Fig. 34). Type IX collagen is an extracellular matrix protein in cartilage [238-240]. Nakata *et al.* mentioned that a mutation in type IX collagen in humans might cause special types of chondrodysplasia and osteoarthritis [239]. In another study, COL9A1 was down-regulated in the patients with peri-implantitis, which occurs in around 30% of patients who use dental implants [240]. Therefore, it can be assumed that Mg-implant induces up-regulation of this ECM component which is beneficial for bone health.

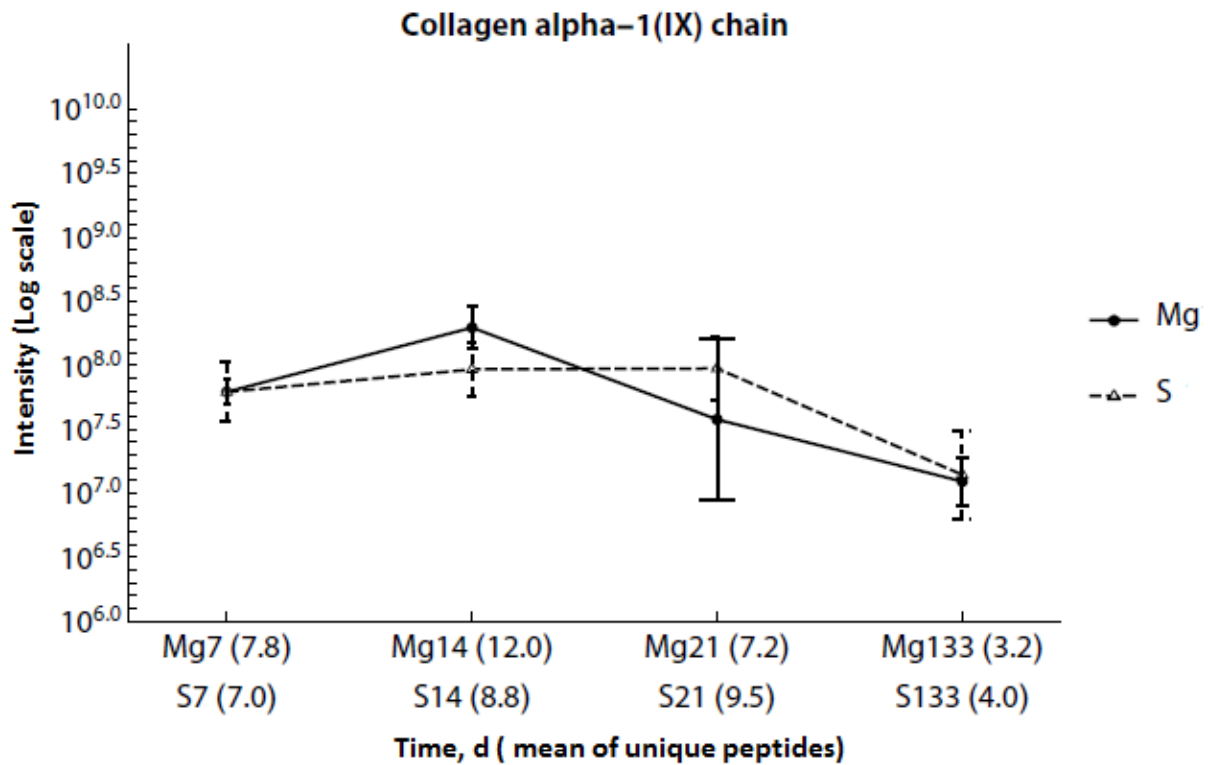


Fig. 34 Regulation of collagen alpha-1(IX) chain (Col9a1) during the incubation of mice bone with Mg-implant Vs S-Implant during the time.

V-type proton ATPase catalytic subunit A (Atp6v1a)

V-type proton ATPase catalytic subunit A (Atp6v1a), a subunit of the vacuolar H⁺-ATPase gene [241, 242], was significantly up-regulated in the first two weeks of implantation with Mg (Fig. 35). Garcia-Gomez *et al.* found that this protein was down-regulated in osteoclasts [242]. Therefore, enhancement of this protein in the presence of Mg-implant might be advantageous regarding bone formation and more activity of osteoblasts.

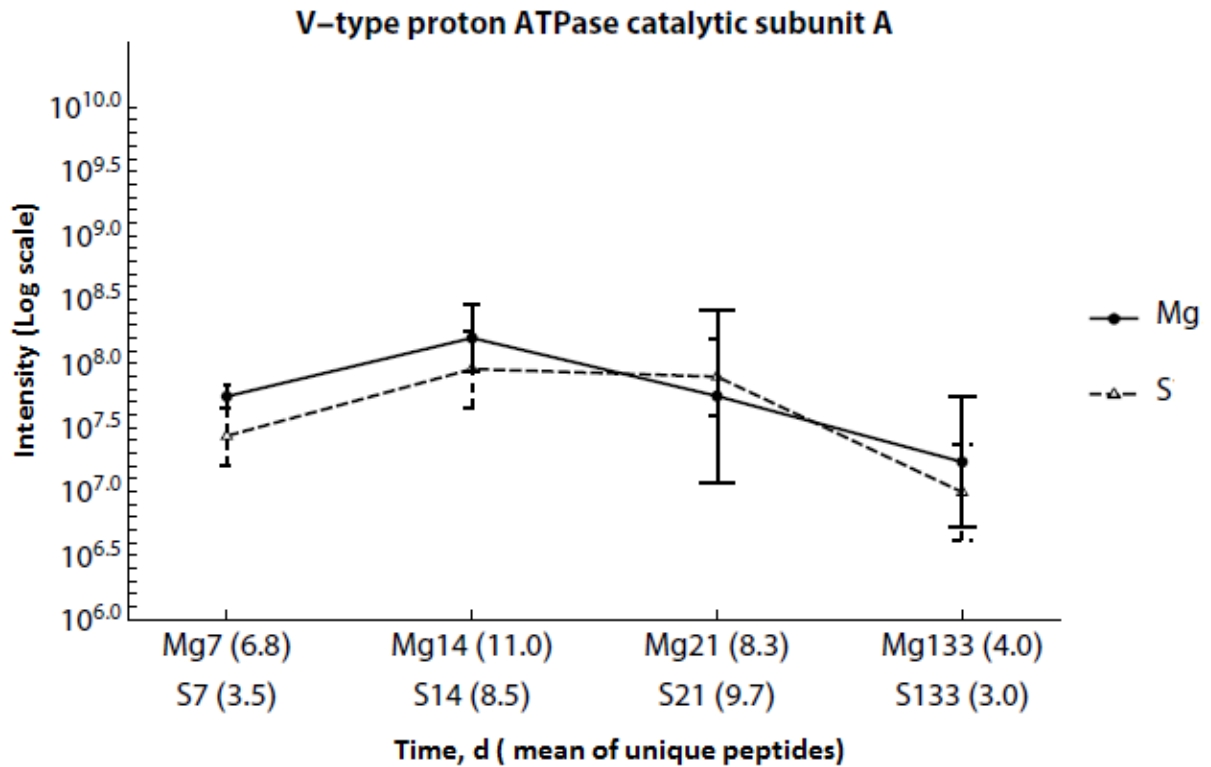


Fig. 35 Regulation of V-type proton ATPase catalytic subunit A (Atp6v1a) during the incubation of mice bone with Mg-implant Vs S-Implant during the time.

Creatine kinase B-type (Ckb)

Creatine kinase B-type (Ckb) was also significantly up-regulated during the corrosion of Mg-implant in 7, 14 & 133days (Fig. 36). This protein is from creatine kinase isoenzymes which have a role in the modulation of ATP homeostasis [243]. Creatine kinase B-type is the major proteoform of creatine kinases throughout osteoclastogenesis. In RANKL-induced osteoclastogenesis, the amount of creatine kinase B-type is increased [244]. Therefore, Mg-induced up-regulation of this protein during this time seems disadvantageous for fracture healing.

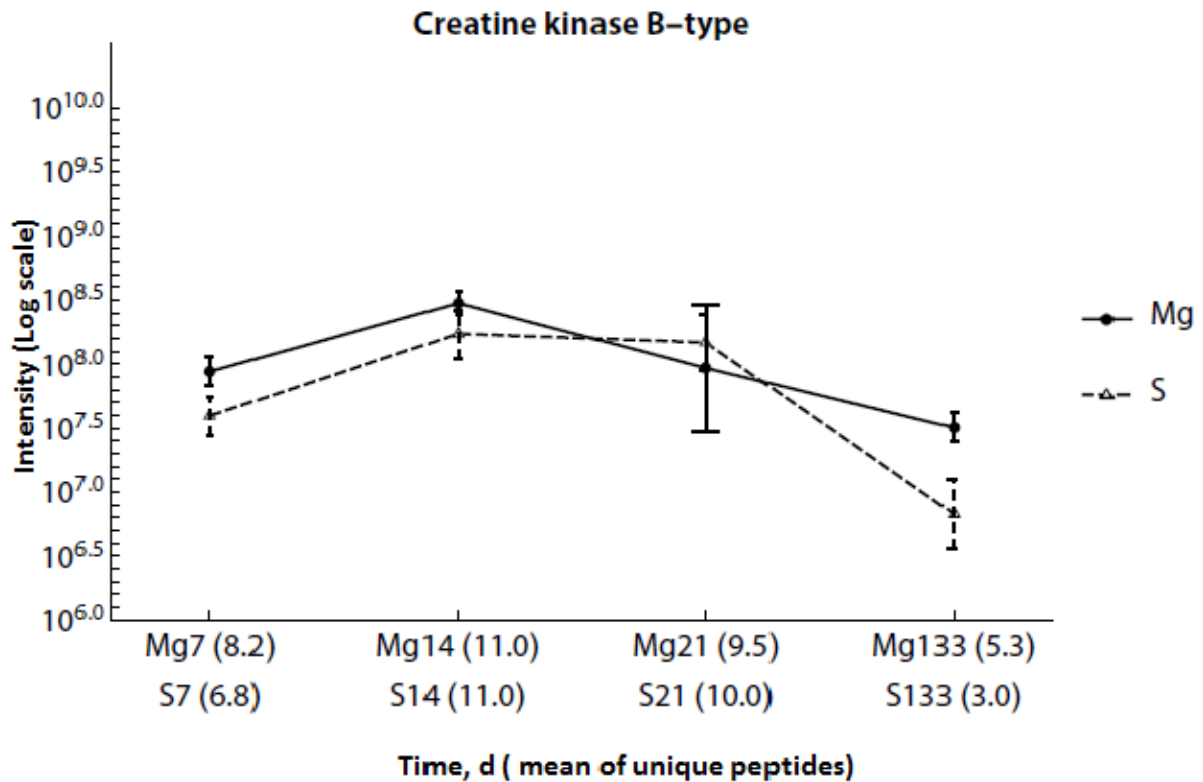


Fig. 36 Regulation of creatine kinase B-type (Ckb) during the incubation of mice bone with Mg-implant Vs S-Implant during the time.

Clusterin (Clu)

Clusterin (Clu), a glycoprotein which is secreted in diverse type of tissues [245, 246], was considerably up-regulated in mice with Mg₂Ag-nail in day 133 (Fig. 37). This protein suppresses the function of macrophage colony-stimulating factor (M-CSF), which is one of the regulators for osteoclast differentiation [247], resulting in reduced osteoclast formation [248]. In conclusion, enhancement of the amount of this protein is beneficial for bone formation; although a significant increase of this protein in the samples which were incubated with Mg-implants occurred when the implant was fully adsorbed. However, bone tissue is a dynamic tissue and bone remodeling is an on-going process. So, this up-regulation could suggest a regular cycle of bone remodeling in the mouse tissue was triggered after 133 days.

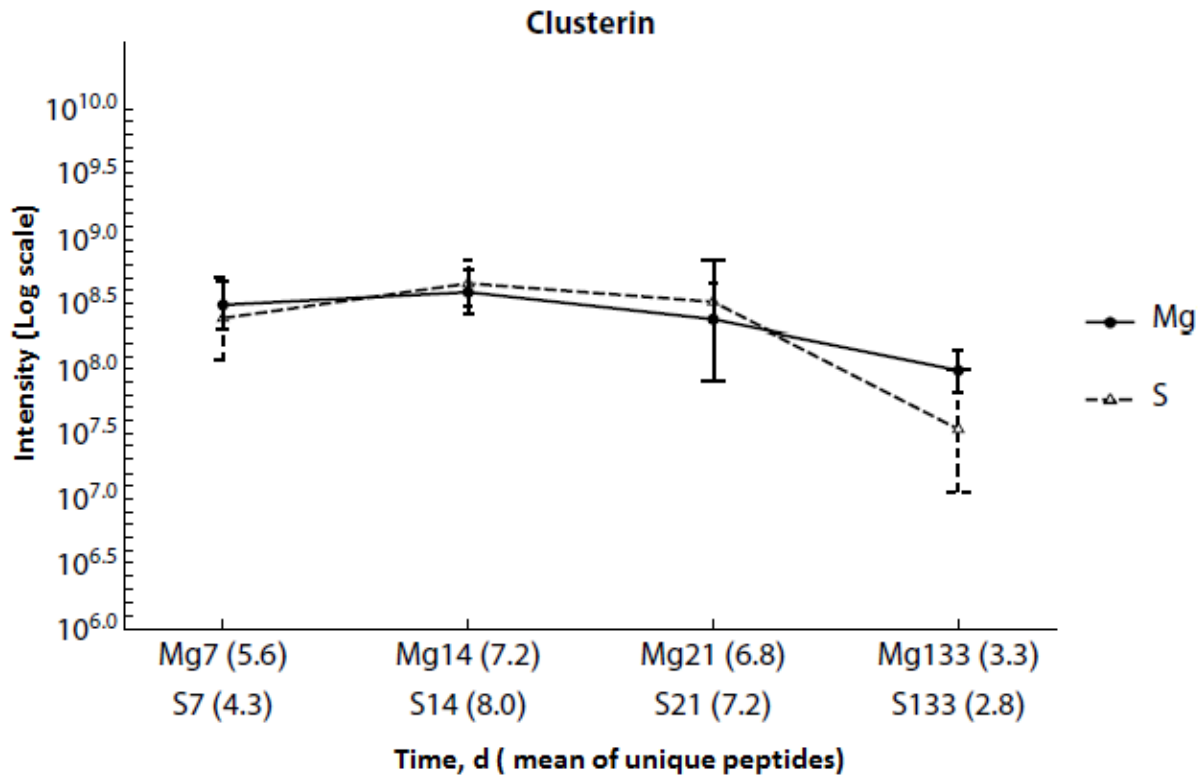


Fig. 37 Regulation of clusterin (Clu) during the incubation of mice bone with Mg-implant Vs S-Implant during the time.

Carbonic anhydrase 2 (CA2)

Up to 14 days after Mg implantation, the amount of carbonic anhydrase 2 (CA2) was significantly decreased (Fig. 38). An inborn absence of CAII, which is involved in acid production [249] causes osteoporosis [250]. Shah *et al.* observed a deficiency of CAII in most of the patients with osteoporosis with renal tubular acidosis and brain calcification. The mutation occurred in the gene of the CAII in these patients [251]. Since deficiency of CA II causes osteoporosis [250, 251], its down-regulation in the presence of Mg-implant is probably unprofitable for bone tissue.

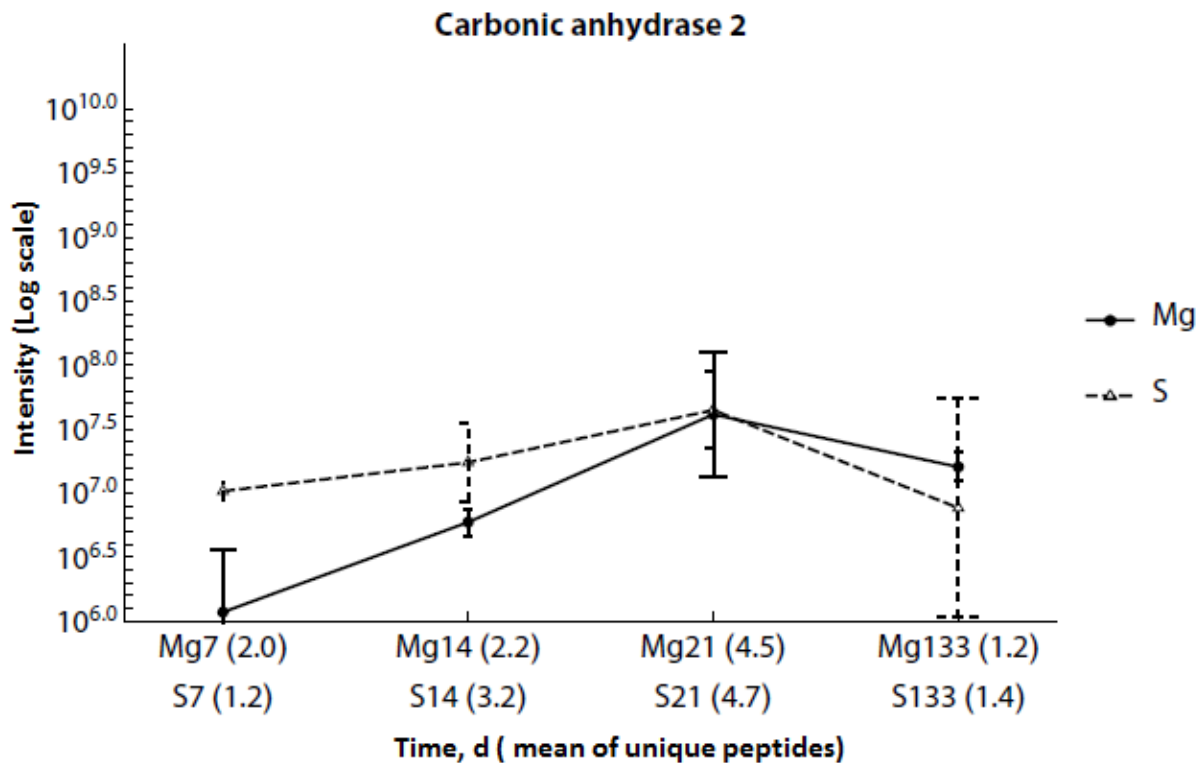


Fig. 38 Regulation of carbonic anhydrase 2 (CA2) during the incubation of mice bone with Mg-implant Vs S-Implant during the time.

Osteopontin (Spp1) or OPN

Osteopontin (spp1) or OPN, which is known as an osteogenic marker [252-255], was significantly down-regulated with Mg-implant compared to S-implant after seven days (Fig. 39). Osteopontin is a pro-inflammatory protein which protects bone destruction in a mouse from endodontic infection [256]. Moreover, the amount of osteopontin is increased in osteogenic adipose-derived MSCs and osteogenic Ad-MSC sheets [257]. Li *et al.* reported that the amounts of osteopontin and bone sialoproteinase, as well as collagen, are up-regulated in the presence of Mg-1Ca.2.0Sr alloy [258]. Thus, down-regulation of this protein in the presence of Mg-implant seems disadvantageous for bone tissues. However, reduction of the amount of this protein was not significant in further incubation time points.

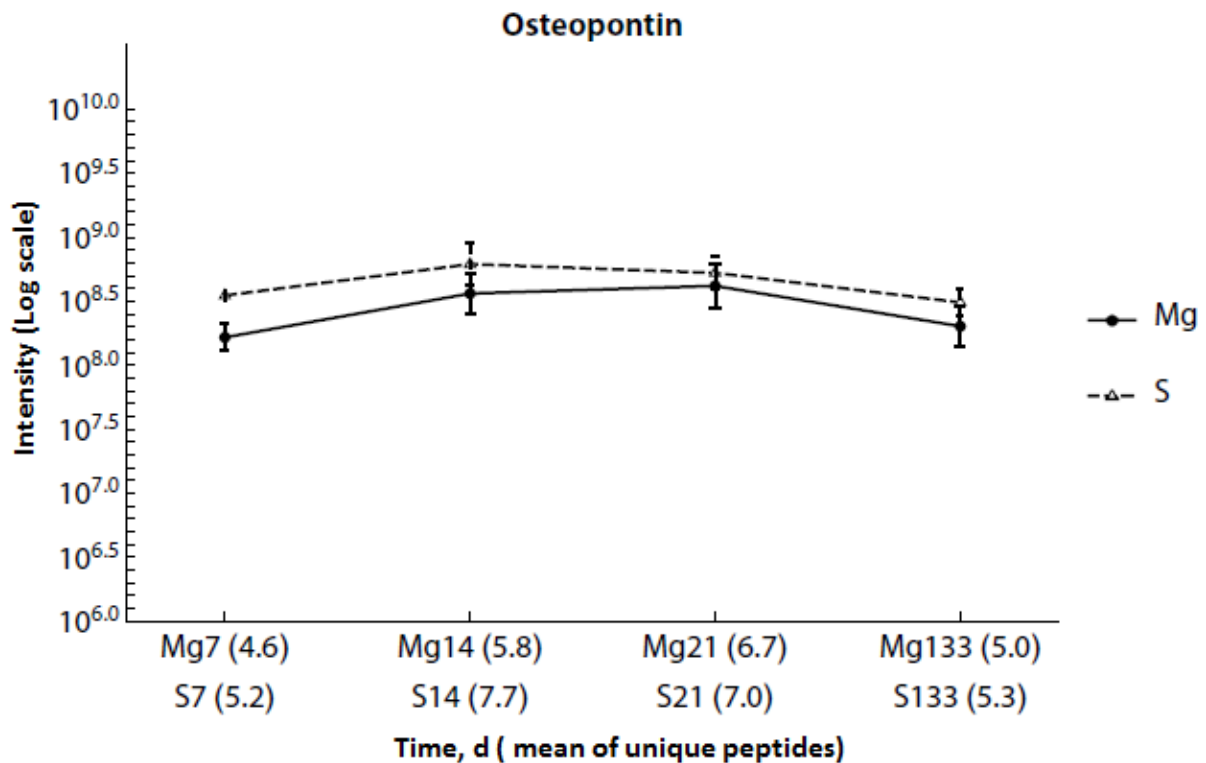


Fig. 39 Regulation of osteopontin (Spp1) or OPN during the incubation of mice bone with Mg-implant Vs S-Implant during the time.

Alpha-2-HS-glycoprotein (Ahsg)

Alpha-2-HS-glycoprotein (Ahsg), also known as fetuin-A is a multifunctional plasma protein [259-261]. It was down-regulated in the mouse bone tissues after seven days incubation with Mg-implant compared to steel implant (Fig. 40). Fetuin-A is synthesized in bone cells especially osteocytes [259, 262] and it accumulates in bone matrix [261]. This protein has a role in the early stage bone formation and bone remodeling [259, 263] and the metabolism of calcium [259]. It is also synthesized by hepatocytes with a drastic increase during liver dysfunctions [259]. Fetuin-A suppresses insulin receptor tyrosine kinase too [259]. Fink *et al.* did not see any proof which shows a significant association of fetuin-A and the risk of hip or composite fracture [264]. In another study, Brylka *et al.* mentioned fetuin-A regulates synthesis of the calciprotein particles (CPPs), as well as the role of this protein in lipid binding, which might affect calcification, apoptosis, and inflammation [260]. In

Ahsg-KO mice, femoral bones were stunted, and cortical thickness of femoral bones was increased as well as mechanical stability [261].

Since fetuin-A is down-regulated in bone tissues 7days after implantation, regarding its role in bone mineralization and calcification, its down-regulation is not advantageous for bone stability. However, our results did not show any significant change (more than two-fold) of this protein in mice bone, 14, 21, and 133 days after implantation. On the other hand, in an experiment by Jähn *et al.* on the same bone tissues [45], they observed an enhancement of cortical thickness in the Mg-implanted bone compared to S-implanted bone in 21 days. It might be concluded that down-regulation of fetuin-7 changes the phenotype of bone, and it is observable after 21 days.

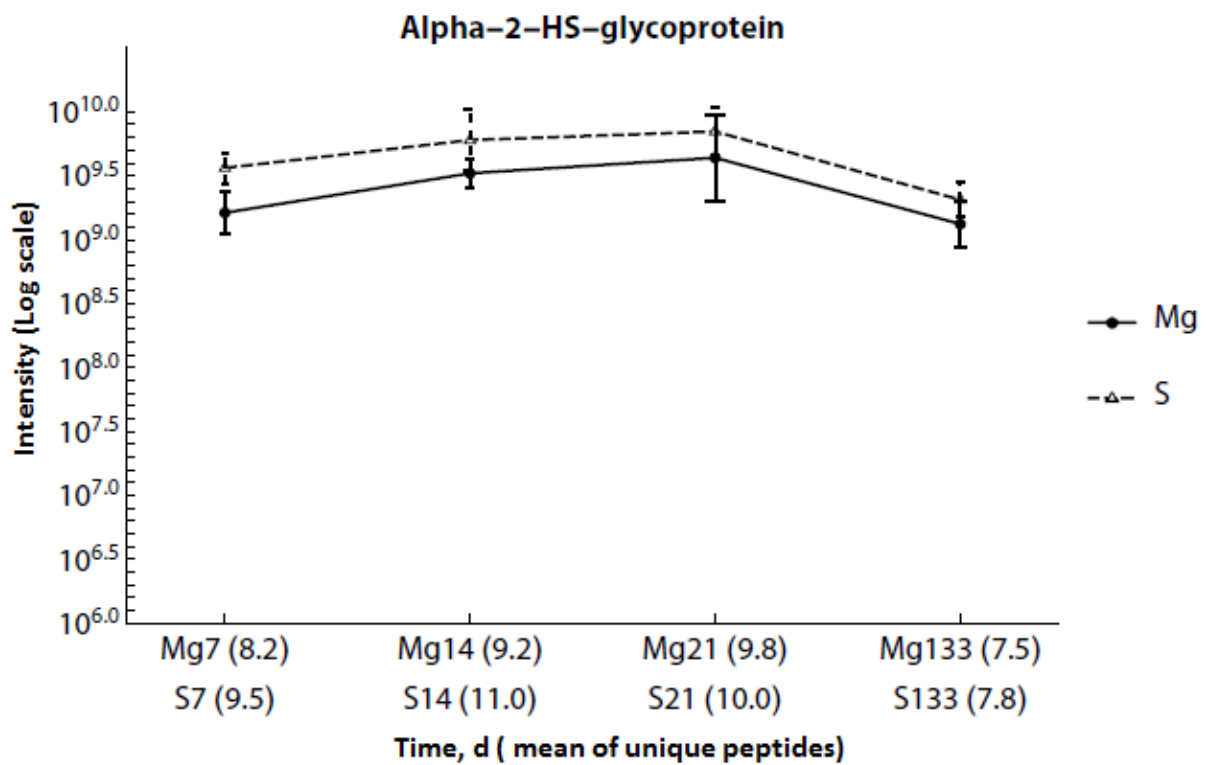


Fig. 40 Regulation of alpha-2-HS-glycoprotein (Ahsg) during the incubation of mice bone with Mg-implant Vs S-Implant during the time.

Calmodulin (Calm1)

Another down-regulated protein after 7 days *in vivo* incubation of bone tissue with magnesium implant is calmodulin (Calm1) (Fig. 41). Calmodulin from CaM family (includes CALM1, CALM2, and CALM3), is a calcium binding protein [265, 266]. It modulates a variety of cellular functions such as signal transduction, cell differentiation, and cell division by binding to calcium [267]. Rajasekaran *et al.* found the gene of Cam1 among the five genes associated with severe lumbar disc degeneration [265]. Furthermore, polymorphisms in the gene of calmodulin1 have been found to cause osteoarthritis within the Japanese population [268]. This protein is synthesized in cultured chondrocytes and cartilage and up-regulated during osteoarthritis [265]. In chondrocytes, the suppression of CaM has been found to cause a deficiency in the genes of Col2a1 and Agc1 which are the major cartilage matrix genes. [268]. Calmodulin1 in chondrocytes regulates signaling pathway, and it can be used for the treatment of osteoarthritis [268]. In conclusion, down-regulation of calmodulin1 in the presence of Mg-implant does not seem beneficial for bone healing. However, a reduction in the amount of this protein was observed only in the first two weeks of Mg-implantation.

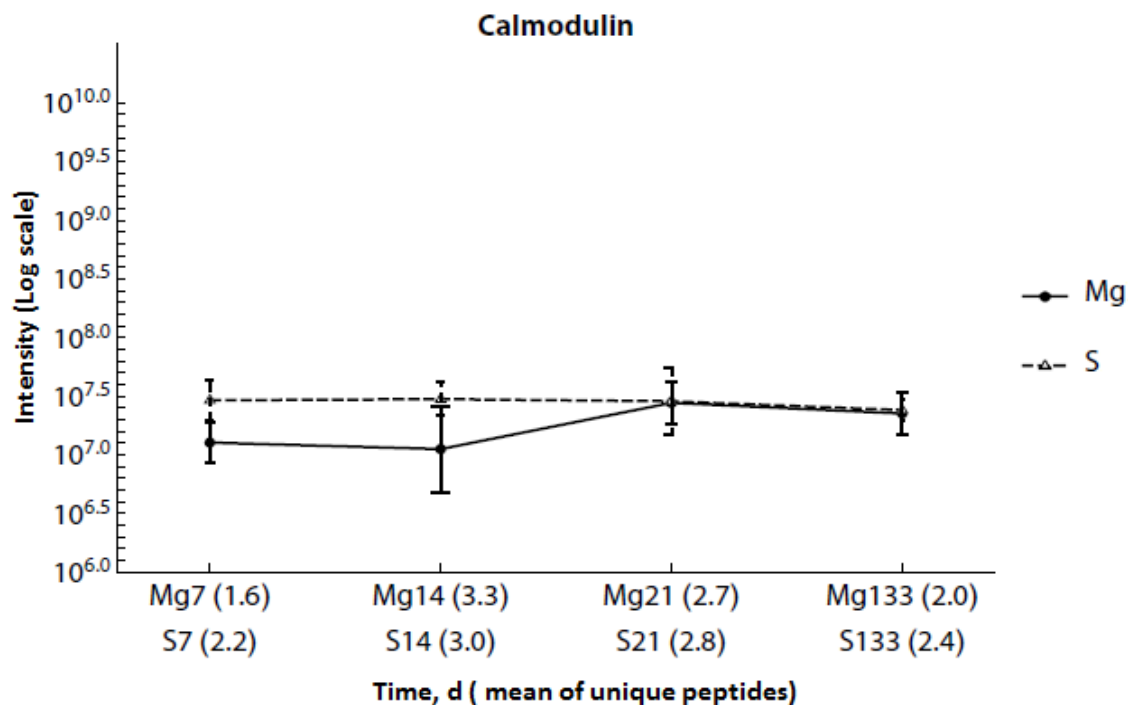


Fig. 41 Regulation of calmodulin (Calm1) during the incubation of mice bone with Mg-implant Vs S-Implant during the time.

40S ribosomal protein S23 (Rps23)

Another down-regulated protein in mice bone in the presence of Mg-implant within seven days of implantation was 40S ribosomal protein S23 (Rps23) (Fig. 42). Yang *et al.* observed that a dysfunction of the RPS23 gene occurs in disc degeneration (DD) which is one of the leading causes of low back pain [269]. Therefore, reduction of the amount of this protein under the influence of Mg-implant might be dangerous for bone tissue; nonetheless, this decrease was not continuous.

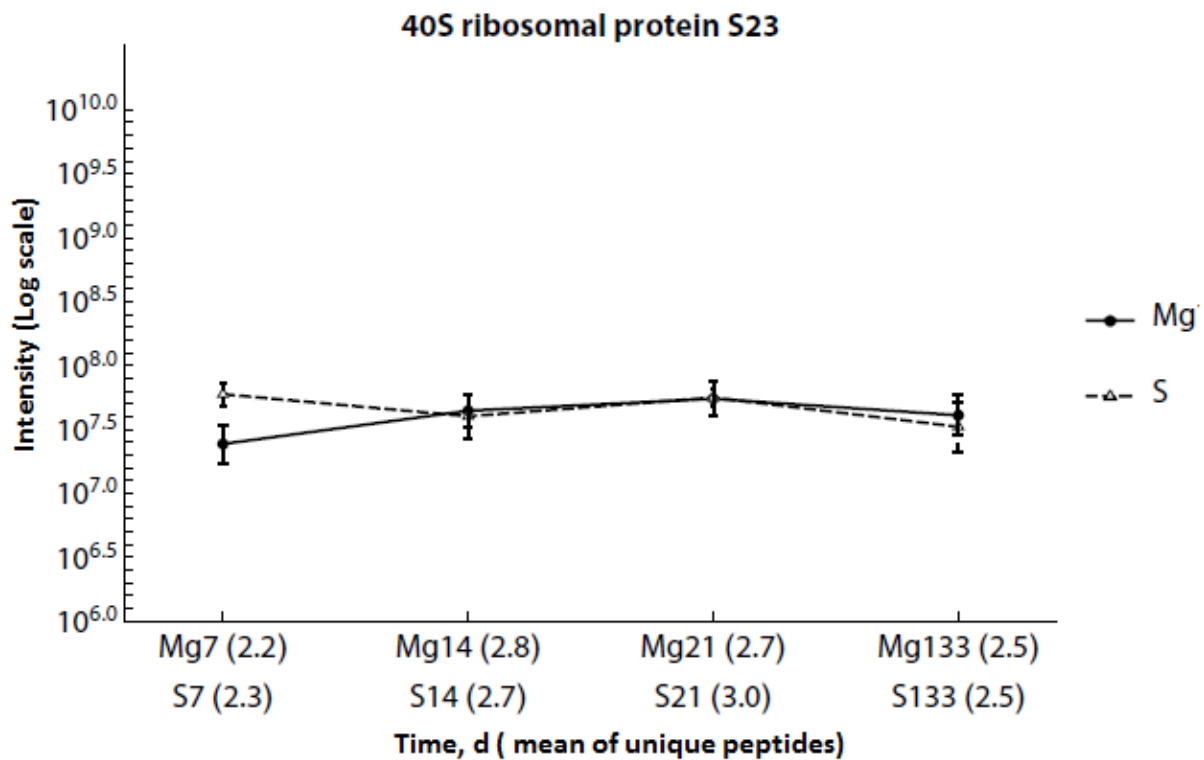


Fig. 42 Regulation of 40S ribosomal protein S23 (Rps23) during the incubation of mice bone with Mg-implant Vs S-Implant during the time.

Selenium-binding protein 2

The antioxidant protein [270] selenium-binding protein (Selenbp), was significantly up-regulated in the presence of Mg-implant within 7 days after implantation (Fig. 43). Zhang *et al.* showed selenoproteins are necessary for bone mineralization. Also, it protects bone from bone loss [270]. Regarding their study and our results, it can be

concluded that the effect of Mg-implant on these proteins is advantageous for bone mineralization in the first two weeks of implantation.

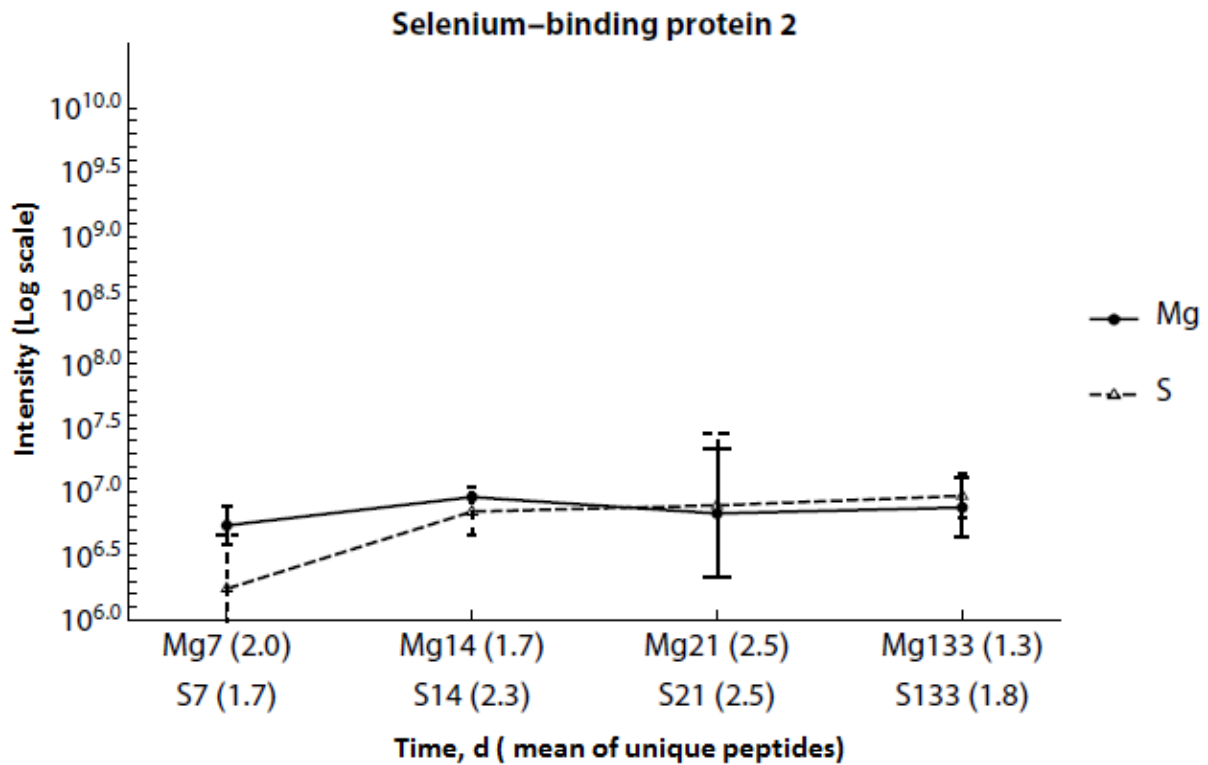


Fig. 43 Regulation of selenium-binding protein (Selenbp) during the incubation of mice bone with Mg-implant Vs S-Implant during the time.

DNA (cytosine-5)-methyltransferase 1 (Dnmt1)

DNA (cytosine-5)-methyltransferase 1 (Dnmt1), was also down-regulated in 14 days after implantation with Mg-Implant (Fig. 44). In a study by Thaler *et al.* DNA methylation and Fas methylation was increased in collagen coated dishes. Fas induces apoptosis, and its activity is suppressed by hypermethylation. In their study, the amounts of Runx2, OCN, and Dnmt1 were increased; and the amount of Fas was decreased in the mouse MC3T3-E1 pre-osteoblastic cells which were cultured on collagen coated dishes [271]. Thus, down-regulation of Dnmt1 in the presence of Mg-implant might not be helpful. Nonetheless, no significant change was observed in the amount of this protein in 21 & 133 days after implantation.

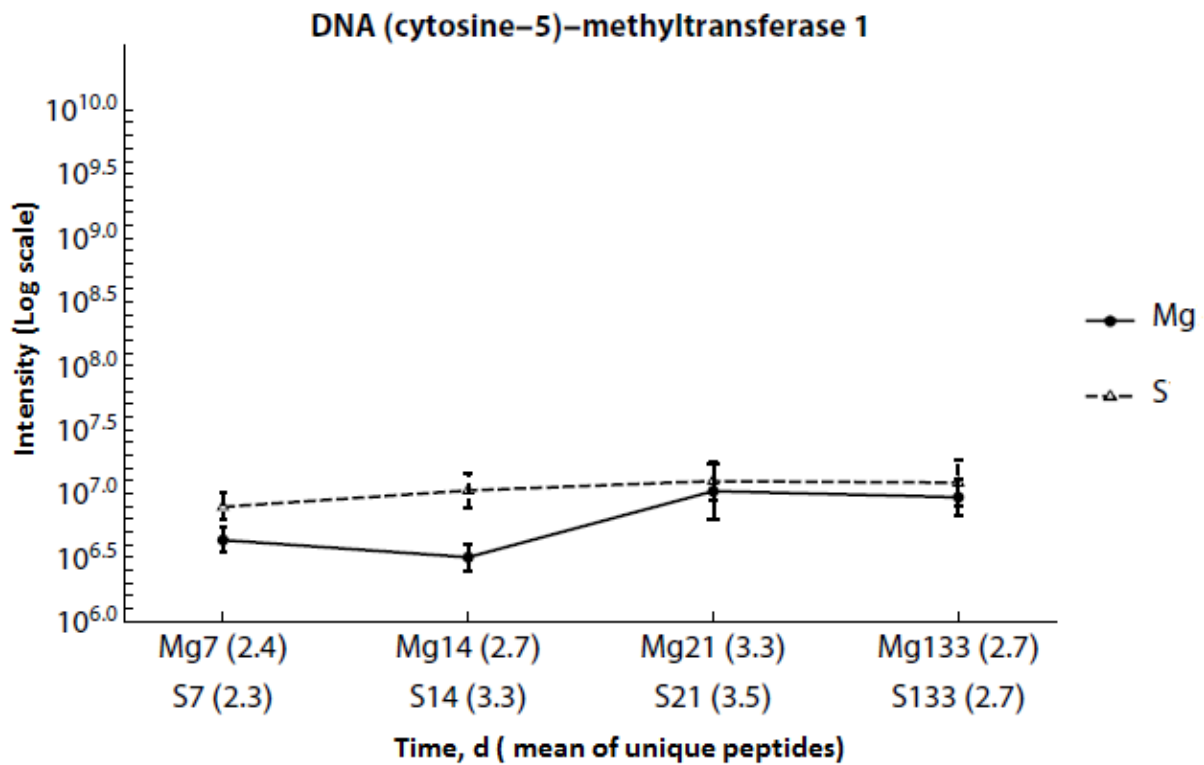


Fig. 44 Regulation of DNA (cytosine-5)-methyltransferase 1 (Dnmt1) during the incubation of mice bone with Mg-implant Vs S-Implant during the time.

Neutrophil elastase (Elane)

The amount of neutrophil elastase (Elane) was significantly reduced in the presence of Mg-implant after 14 days of implantation (Fig. 45). A genetically heterogeneous disorder of bone marrow failure known as severe congenital neutropenia (SCN), is caused by a mutation in ELANE in more than a half of the patients [272-281]. SCN is commonly diagnosed in early childhood and characterized by a chronic and severe shortage of neutrophils [272]. Touw *et al.* suggested that the mutation of ELANE in Severe congenital neutropenia (SCN) should be checked as this happens in more than 50% of the patients [273]. Furthermore, mutation of ELANE causes cyclic neutropenia (CN) [274]. Therefore, down-regulation of this protein *in vivo* under the influence of Mg-implant might cause severe problems for young patients; however, this down-regulation lasted only 14 days.

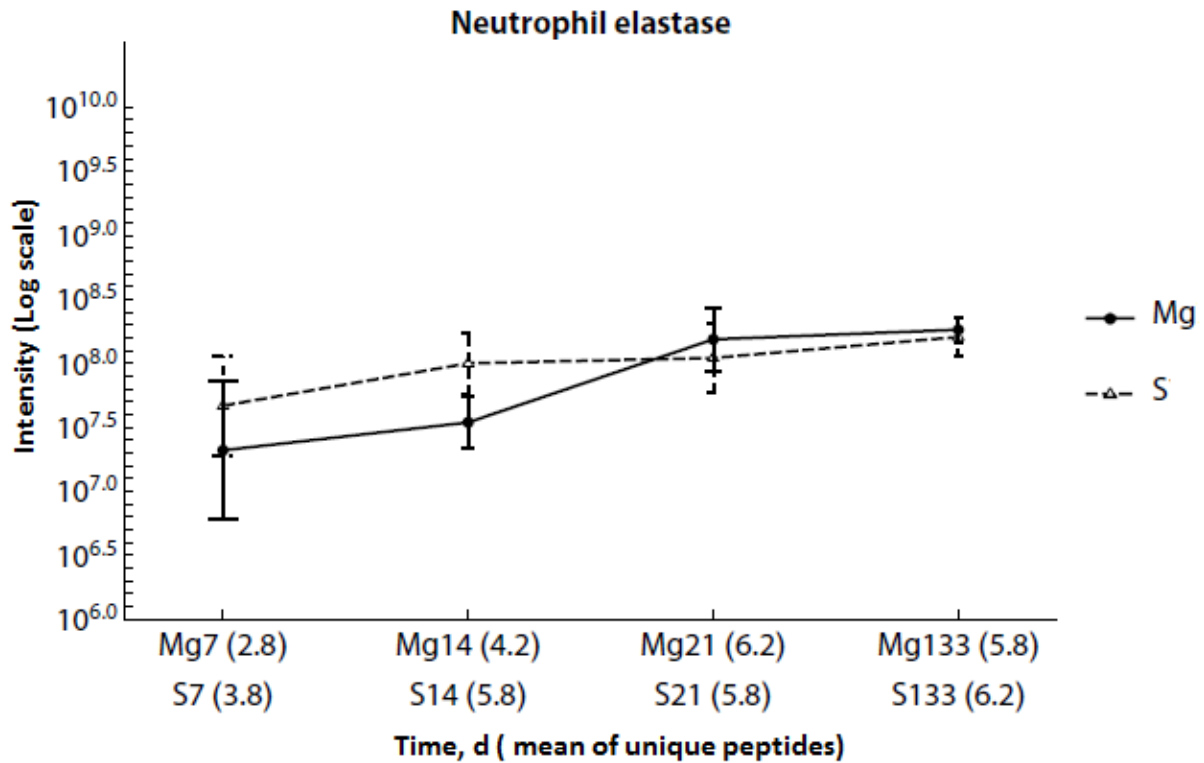


Fig. 45 Regulation of neutrophil elastase (Elane) during the incubation of mice bone with Mg-implant Vs S-Implant during the time.

10 kDa heat shock protein, mitochondrial (Hspe1)

The amount of 10 kDa heat shock protein (Hspe1) was decreased significantly within seven days implantation of mice bone tissues with Mg-Implant (Fig. 46). It belongs to the heat shock proteins family also known as chaperons. It is an intracellular protein which serves as a catalytic enzyme in protein folding [282]. A class of bacterial chaperone, chaperonine, stimulates bone resorption [282]. So, down-regulation of chaperon 10 in the presence of Mg-implant seems beneficial for bone health regarding its role in bone resorption.

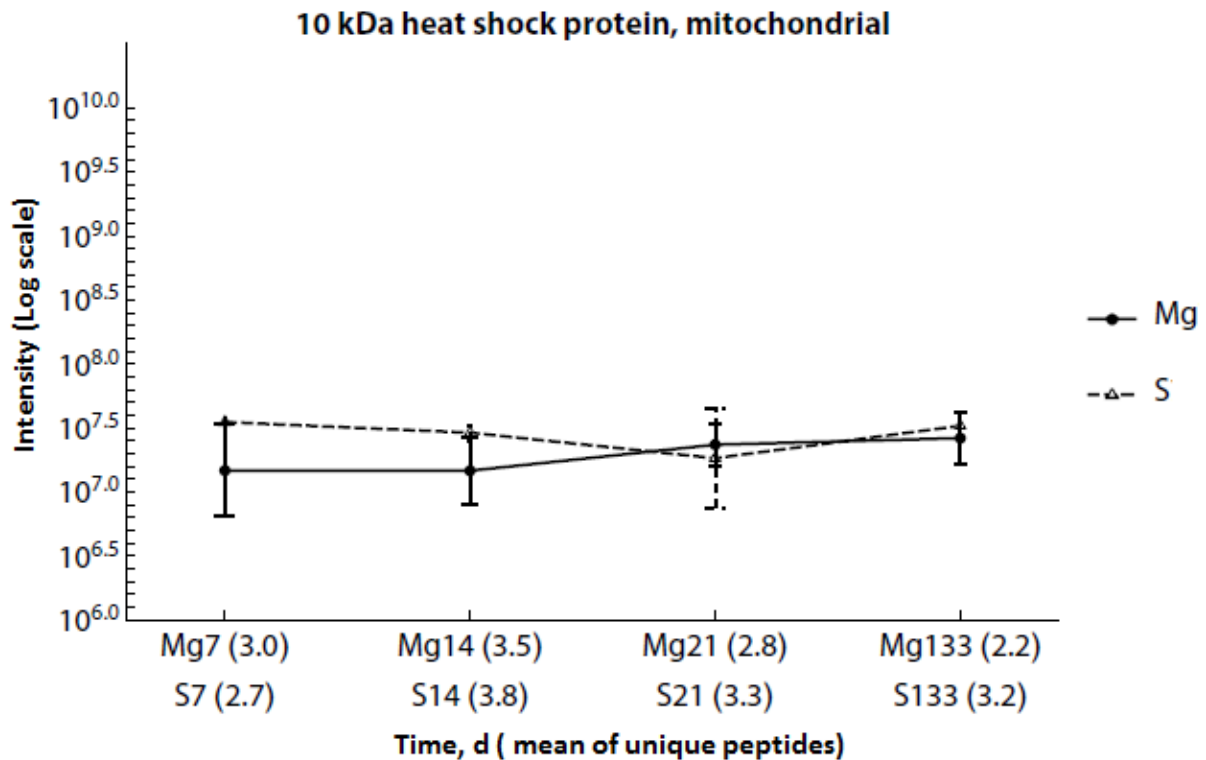


Fig. 46 Regulation of 10 kDa heat shock protein, mitochondrial (Hspe1) during the incubation of mice bone with Mg-implant Vs S-Implant during the time.

DNA replication licensing factor MCM2 (Mcm2) and MCM7 (Mcm7)

The amounts of DNA replication licensing factor MCM2 & MCM7 were decreased in 14 days in the presence of Mg-implant (Fig. 47, Fig. 48). They play vital roles in cell proliferation [283-285]. Up-regulation of MCM2 has also been observed in many tumor cells and therefore the Mcm2 gene has been suggested to be used as markers in diseases like diffuse large B-cell lymphoma (DLBCL) [283]. Its up-regulation has also been associated with cases of apoptosis in Myelodysplastic syndromes (MDS) [286]. MCM7, which is contributed in tumor formation in diverse types of cancer [287], was also up-regulated in neurons, astrocytes, and microglia after spinal cord injury in the study of Chen *et al.* They suggested that MCM7 might be associated with neuronal apoptosis in caspase-3-dependent apoptotic pathway [287]. Taken together, down-regulation of these proteins in the presence of Mg-implant seems beneficial for differentiation of the bone cells during fracture healing.

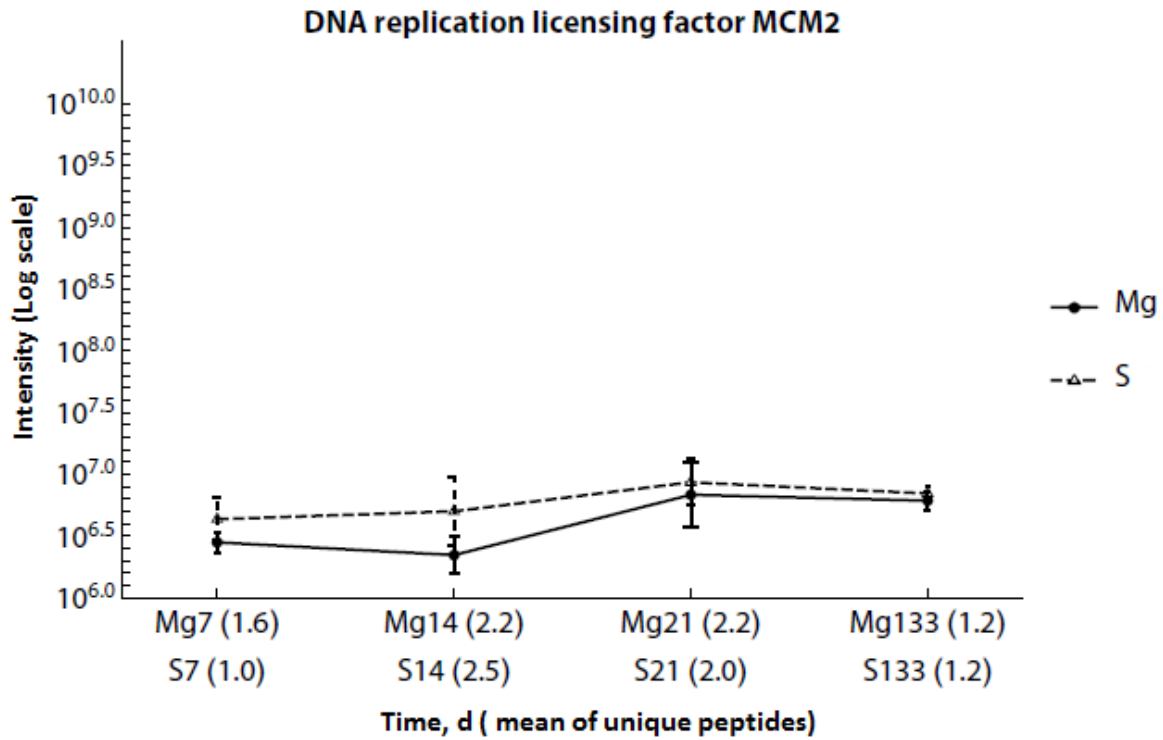


Fig. 47 Regulation of DNA replication licensing factor MCM2 during the incubation of mice bone with Mg-implant Vs S-Implant during the time.

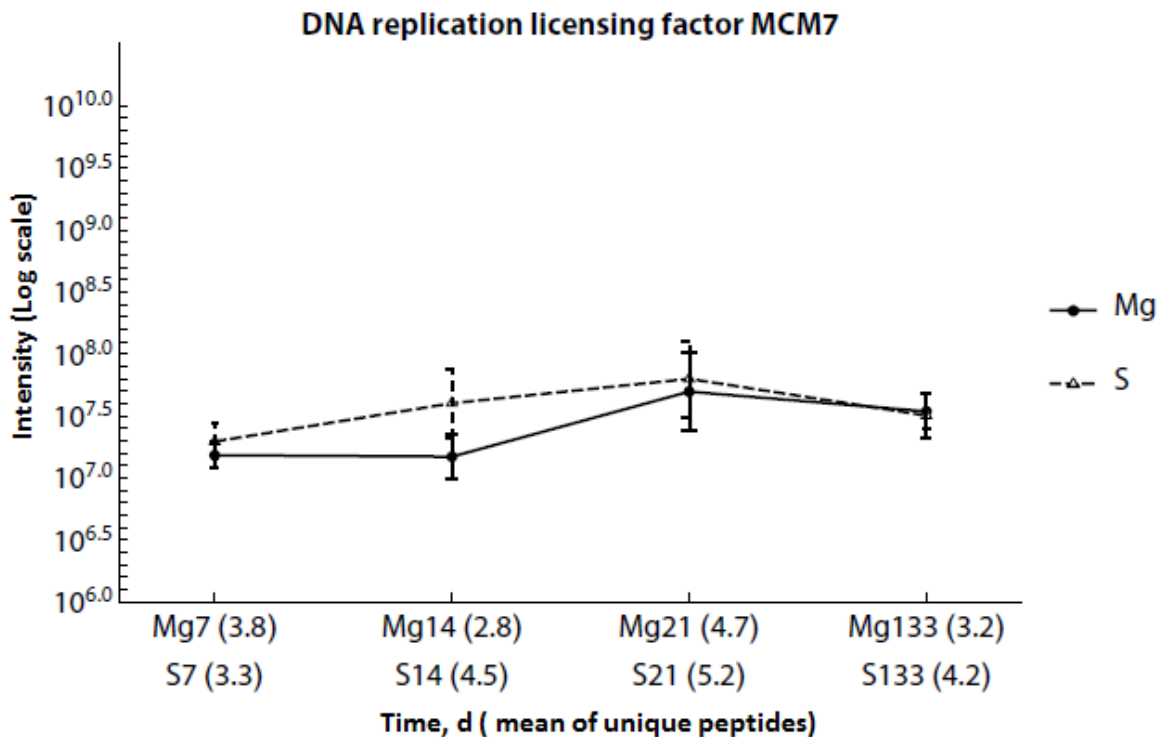


Fig. 48 Regulation of DNA replication licensing factor MCM7 during the incubation of mice bone with Mg-implant Vs S-Implant during the time.

4.3.3.2 Regulated blood proteins in the mouse bone tissue

Blood proteins

Concerning the direct contact of bone-implant with the tissue, the first step after implantation is protein adsorption [170] which is closely associated with biological processes such as cell adhesion, thrombosis, inflammatory reactions, and infections [171].

Instantly, a layer of proteins will be adsorbed to the surface of biomaterial (even faster than cells) which depends on the polarity (hydrophobicity/hydrophilicity) of the surface, the properties of hydrogen binding, and so on [288-291]. Albumin, the most abundant serum protein, fibrinogen, and immunoglobulin G (IgG) are the first adsorbed proteins to the surface of the implant [290, 292-295].

Blood is in contact and interacts with the implanted materials in the first stage of implantation [48]. This interaction leads to the adsorption of blood proteins on the surface of implant and formation of provisional matrix on it [48].

Coagulation system

Blood coagulation is affected by two types of substances: procoagulants coagulation stimulators which are activated in damaged vessel and anticoagulants coagulation suppressors which are dominant in the circulating blood stream. The balance between procoagulant and anticoagulants is decisive of the coagulation process [296]. During coagulation, all the steps are guided by a series of enzymes. An inactivated enzyme is converted to an activated enzyme using the activated product of the previous step. Coagulation occurs in three main steps. Firstly, prothrombin activator is formed by the activation of a cascade of coagulation factors. Secondly, prothrombin is converted to its active form “thrombin”, and finally a clot is formed via conversion of fibrinogen to fibrin which entangles blood components (cells, plasma, and platelets) [296].

Three pathways are possible for coagulation: Extrinsic pathway, intrinsic pathway, and common pathway.

In the extrinsic pathway, a complex of factors are activated and released into the blood in about 15 seconds after tissue damage. Upon the release of tissue factor, the compound of lipoprotein activates Factor VII (FVII) to FVIIa [296]. Then, TF:FVIIa

complex activates factor IX . Also, FVIIa can directly activate FX. FX can be also be activated by FIXa in the presence of F VIII. Deficiency in either FVIII or FIX causes hemophilia A or B respectively [297]. Via the interaction of FXa (the activated form of FX), phospholipids of tissue factor and FVa, prothrombin activator will be formed [296, 298].

The intrinsic pathway is slower (1-6minutes) than the extrinsic pathway [296]. This pathway is initiated after blood comes in contact with the surface of damaged vessel. Platelets are activated followed by the release of phospholipids, resulting in a negatively charged membrane. Then, FXII is activated (to FXIIa) and it gets in contact with the negatively charged membrane of the activated platelets. FXIIa activates FXI to FXIa and FXIa activates FX to FXa, and FXa combines with FVa and platelet phospholipids to form prothrombin activator [296, 298].

The common pathway is initiated by catalyzing the conversion of prothrombin activator to thrombin which was formed either in extrinsic or intrinsic pathways. In this step, prothrombins bind to platelets which are attached to damaged tissues and converted to thrombin. Thrombin has a positive effect on platelets to make a plug and it also converts fibrinogen to fibrin [296].. Fibrin fibers are formed by a linkage between fibrin monomers. Finally, blood cells, platelets, and plasma components are enmeshed in fibrin fibers which are bound to blood vessels. Ultimately, this blood clot can stick to open vascular and prevent blood loss [296].

Prothrombin (F2)

A reduction of prothrombin (F2) was observed in the presence of Mg-Implant in the time period after incubation (Fig. 49). Prothrombin is a vitamin K-dependent single chain glycoprotein [299]. Its deficiency can happen genetically or acquired from conditions such as liver disease, vitamin k deficiency [300]. A deficiency in prothrombin has also been observed in Antiphospholipid syndrome (APS) which is an autoimmune disease [301]. Hypoprothrombinemia causes bleeding [302]. In mice, prothrombin deficiency causes partial embryonic lethality due to a failure in blood coagulation. These mice died before birth or after the birth because of bleeding [303]. Therefore, hypoprothrombinemia which occurred in the presence of Mg-Implant might cause a severe problem for mice regarding blood coagulation; however, this significant reduction was no longer observed at 21 days and beyond.

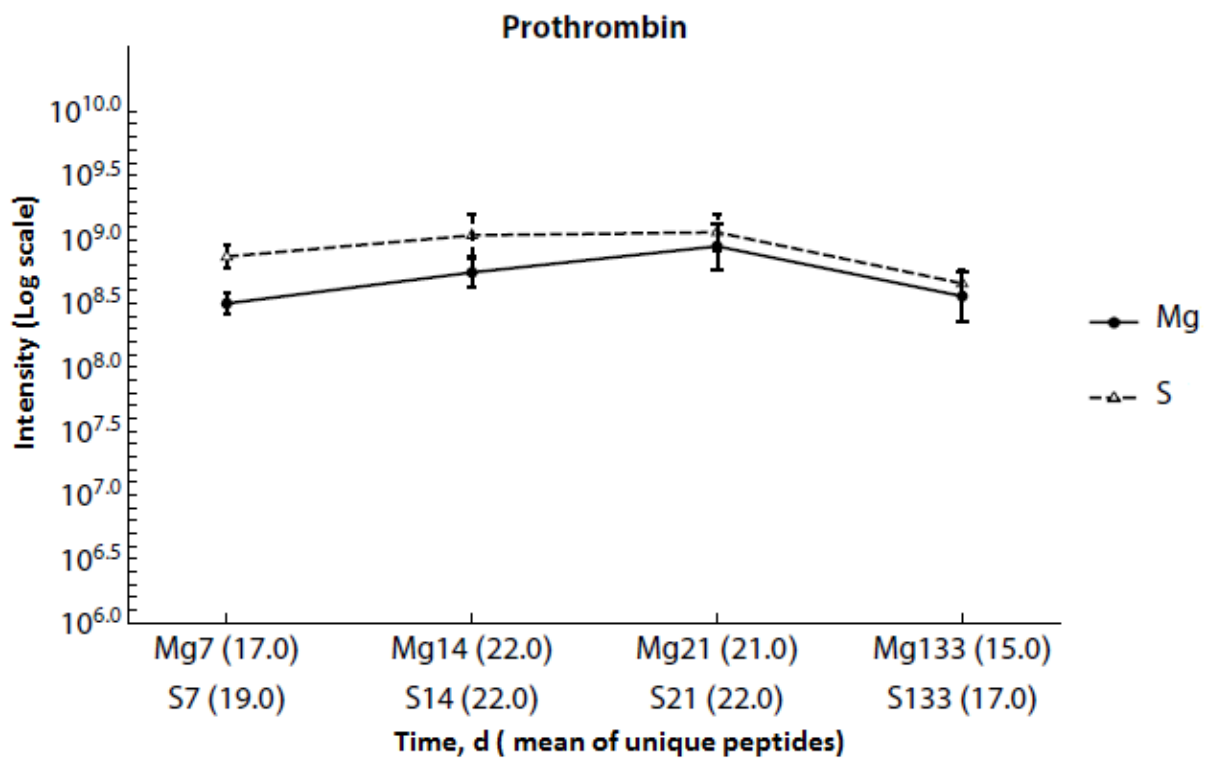


Fig. 49 Regulation of prothrombin (F2) during the incubation of mice bone with Mg-implant Vs S-Implant during the time.

Coagulation factor X (F10)

The blood coagulation factor, coagulation factor X (F10), was considerably down-regulated in the presence of Mg-Implant during the incubation time (Fig. 50). Factor X-deficiency is a rare disorder [304-307] and is associated with major bleeding. Enjeti *et al.* mentioned that FX-deficiency has been seen in a third of the amyloidosis patients [308]. Thus, down-regulation of this blood factor might cause severe bleeding complications. Since bleeding was not been seen in these mice which got the Mg-Implants, the question whether the deficiencies in blood factors FII & FX are local (only in the site of implants), or systematical (in the blood system) is raised.

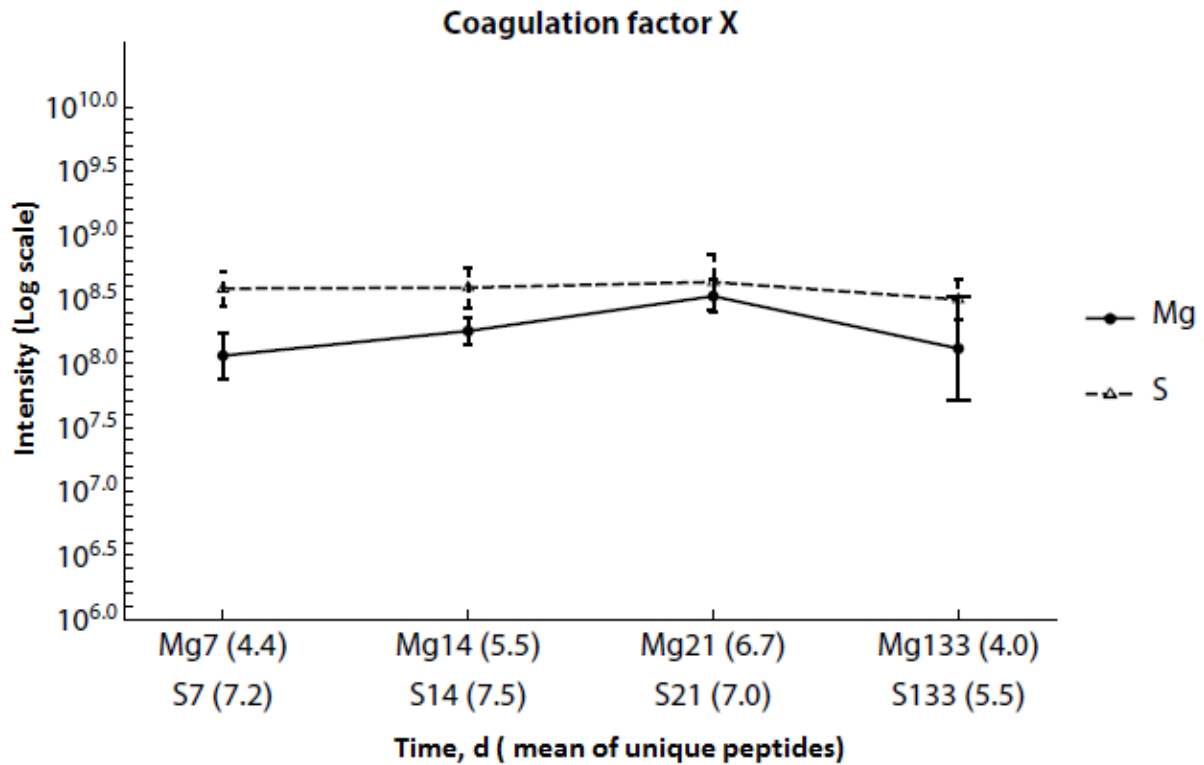


Fig. 50 Regulation of coagulation factor X (F10) during the incubation of mice bone with Mg-implant Vs S-Implant during the time.

4.3.3.3 Regulated proteins in the mouse bone tissues which are involved in inflammatory reaction

The body's response to damage and inflammation which occurs after biomaterial implantation is known as body foreign reaction (FBR) [48]. The 'provision matrix formation' is the deposition of blood proteins on the surface of biomaterials which is followed by FBR and cell adhesion [48]. In this time, immune system cells (especially fibroblasts) deposit collagen matrix on the surface of the implants and encapsulate materials in a fibrous tissue layer [48]. The inflammation is reduced after a successful implantation. However, in case of improper implantation, inflammation is extended, molecular signals from cells are released which inhibit tissue healing [309]. In the first days after injury, neutrophils are predominant; followed by macrophages in the next step [48].

Upon formation of the provisional matrix, acute and chronic inflammation takes place [48]. The level of this inflammatory reaction depends on the level of injury during the implantation and the implanted organ/tissue, as well as the level of the “provisional matrix formation” [48].

Since immune response is one of the aspects affected by implantation, investigation of the regulated proteins in mouse bone tissue in the presence of Mg-Implant which are involved in immune response will be discussed in this chapter.

Hemopexin (Hpx)

The amount of hemopexin (Hpx), a plasma glycoprotein [310], was increased in 7 days and 14 days after implantation of mice bone with Mg-implant (Fig. 51). Its amount is usually decreased in the serum of patients with Sickle cell disease (SCD) because of the chronic hemolysis [311]. Vercellotti *et al.* found that up-regulation of hemopexin suppresses inflammation and vaso-occlusion in the mice with Sickle Cell Disease [311]. So, the effect of Mg-implant on the amount of this protein seems beneficial for bone health due to its anti-inflammatory functions.

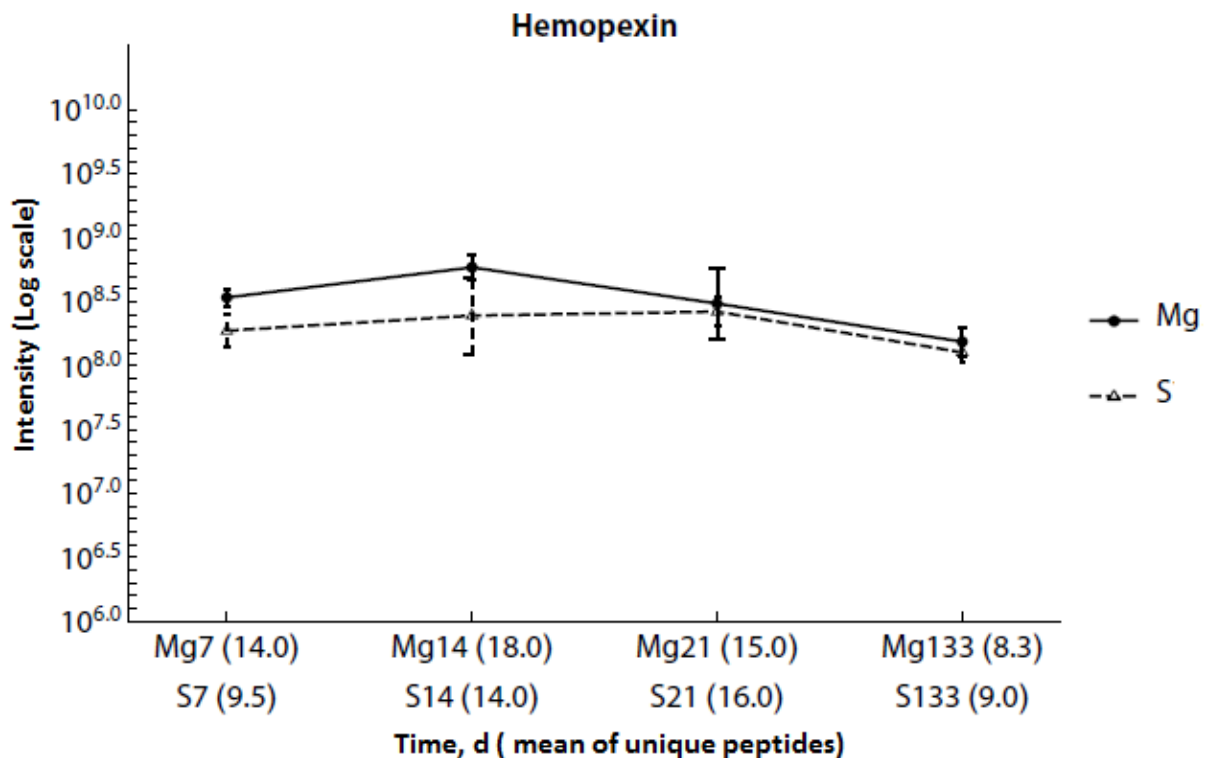


Fig. 51 Regulation of hemopexin (Hpx) during the incubation of mice bone with Mg-implant Vs S-Implant during the time.

Transient receptor potential ankyrin-1 (ANK1) or (TRPA1)

Another significantly down-regulated protein in the first two weeks in the presence of Mg-implant was transient receptor potential ankyrin-1 (ANK1) or (TRPA1 [312]) (Fig. 52) Ankyrin-1 participates in the transmission of chronic neuropathic pain [313]. Rank *et al.* found that Ank-1 mutant mice mostly die perinatally because of severe anemia [312]. However, Ankyrin-1 has a crucial role in the stabilization of the cytoskeleton of red cells [312], Okada *et al.* reported ANK1_KO mice have a reduction in the inflammation of corneal stroma [314]. Therefore, the influence of Mg-implant on this protein seems beneficial to reduce inflammation in bone tissue.

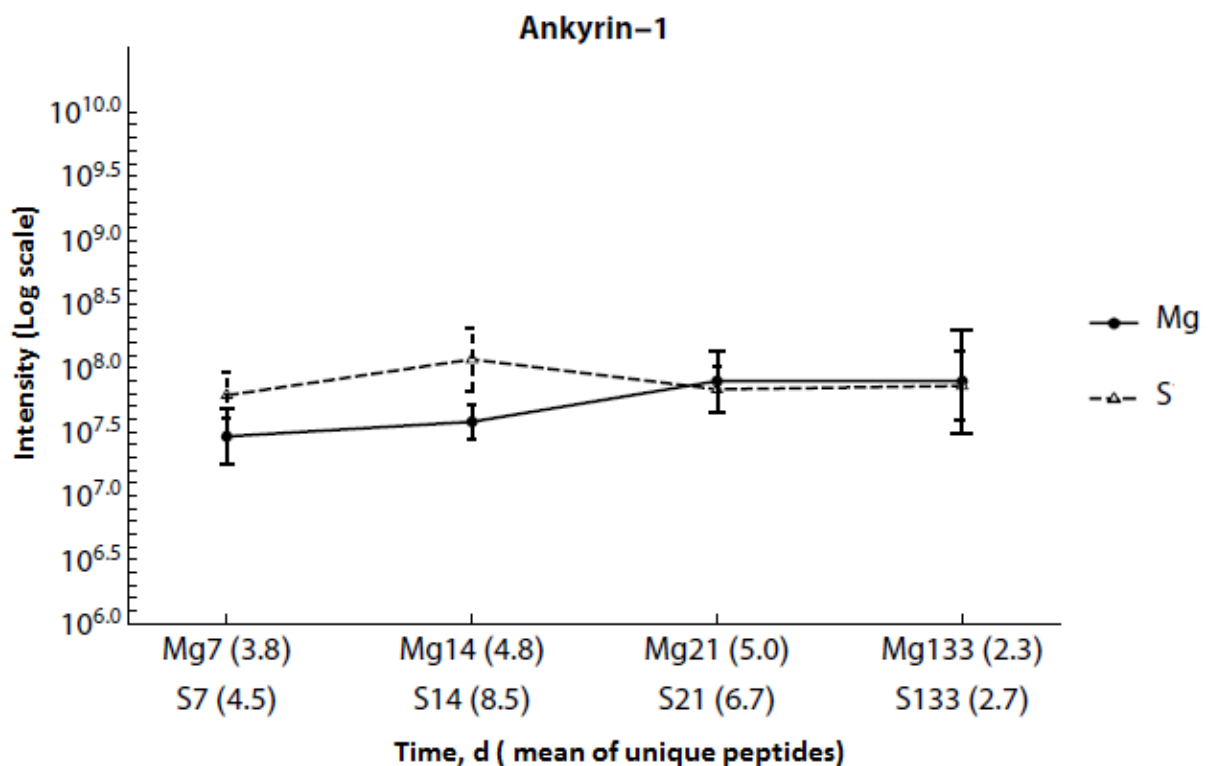


Fig. 52 Regulation of transient receptor potential ankyrin-1 (ANK1) during the incubation of mice bone with Mg-implant Vs S-Implant during the time.

Protein S100-A9

The amount of S100-A9 (s100a9), an inflammatory regulator in neutrophil function [315, 316], was considerably decreased by day 14 of implantation with Mg₂Ag (Fig. 53). S100A9 and S100A8 are present in the intracellular and extracellular spaces

and they have critical roles in heart function [316, 317]. Under inflammatory circumstances in immune cells, the amount of S100A9 and S100 A8 increases [318]. Regulation of S100-A9 was significant in day 14 but not in the other time points. Therefore, it can be assumed that, in the present of Mg-Implant, inflammatory reaction of the host body is less than permanent implant, which can be advantageous for bone health.

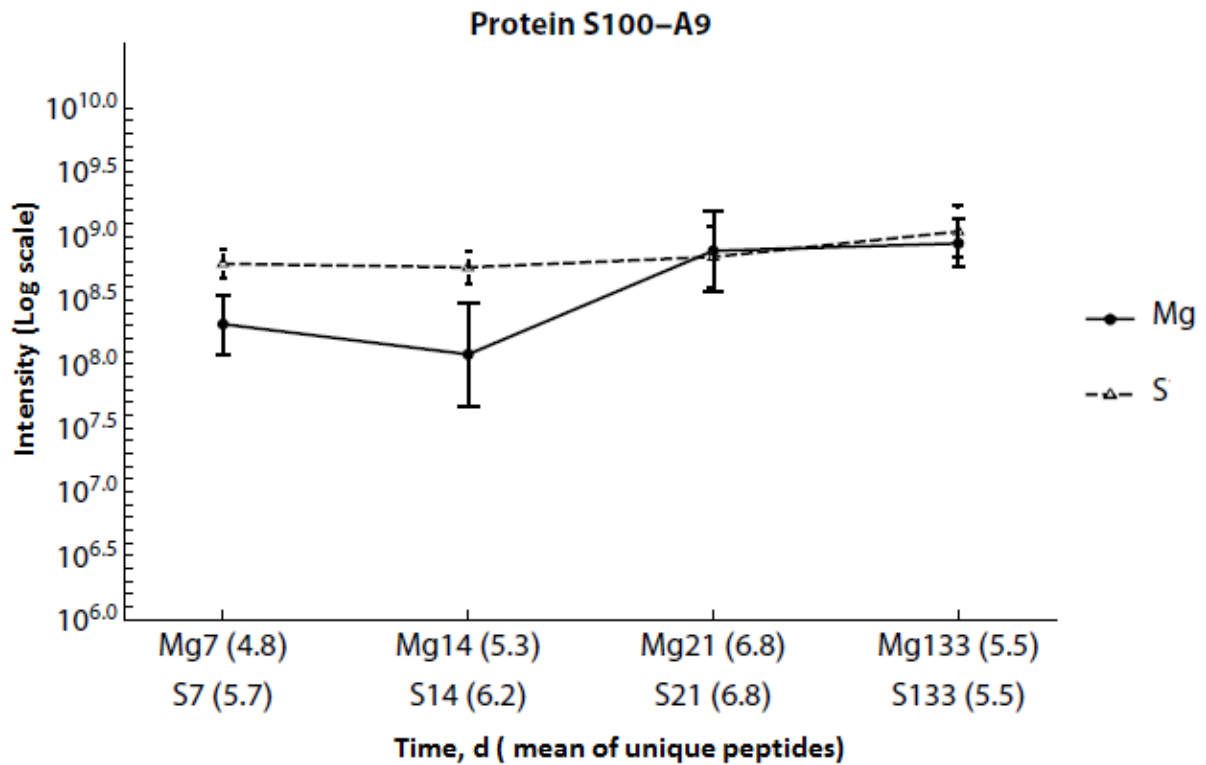


Fig. 53 Regulation of S100-A9 (s100a9) during the incubation of mice bone with Mg-implant Vs S-Implant during the time.

5 Conclusion and outlook

Using proteomics in this study, the impact of metal discs/implants on the bone cells and bone tissue was investigated based on changes in the proteome of bone cells and bone tissue.

The results show that the proteome of osteoblasts changed with response towards both metals (Mg&Ti); however, these changes were more significant in the response of cells toward Mg-discs. Particularly, the regulation of bone-formation related proteins in the presence of Mg-discs was more significant than Ti-discs. Furthermore, regulation of a few proteins in osteoblasts in the presence of Mg-discs was beneficial for cell viability. On the other hand, there was one significantly regulated protein in osteoblasts in response to Mg-disc and its corrosion products related to toxicity.

Concerning the second study on bone tissue, many of the regulated proteins in the presence of Mg-implant compared to S-implant were effectively involved in the bone development. While a few of bone formation-related proteins either have adverse roles in bone formation or positive role in bone resorption. This could be due to the lifetime on-going bone remodeling process. Most of the changes in the proteome of bone tissue in the presence of Mg-implant compared to S-implant were significant in 7 days, and 14 days after implantation (during fracture healing). “A significant increase in callus size due to an augmented bone formation rate and a reduced bone resorption in fractures“ was observed by Jähn *et al.* [45] from the same samples.

There were also a few regulated proteins by the time the Mg-implant was fully absorbed in day 133 which could be due to the dynamic lifetime bone remodeling. Furthermore, many other proteins in this field were regulated either less than two-fold or their presentation was not repeated in all the replicates such as diverse types of collagens.

Additionally, regulation of inflammatory-reaction-related proteins was significant especially in the first and second week after Mg-implantation compared to steel. However, their regulation was not significant after 14 days. No significant regulation of these proteins was observed at the last time point. This could be due to the fact

that the Mg-implant has been fully absorbed and the bone tissue was back to a normal state.

On the other hand, the amount of coagulation factor X which was significantly down-regulated in the first two weeks after Mg-implantation was still lower than in S-implant at the last time point (133 days). To find out if this down-regulation occurred systematically or only at the site of implant, it is highly recommendable to check the blood proteins besides bone proteins in further experiments. This should be done throughout all healing stages (from implantation till complete absorption of the implant).

6 References

1. Elin, R.J., *Magnesium: the fifth but forgotten electrolyte*. Am J Clin Pathol, 1994. **102**(5): p. 616-22.
2. Bohl, C.H. and S.L. Volpe, *Magnesium and exercise*. Crit Rev Food Sci Nutr, 2002. **42**(6): p. 533-63.
3. Rubin, H., *The paradox of the contrasting roles of chronic magnesium deficiency in metabolic disorders and field cancerization*. Magnes Res, 2014. **27**(3): p. 94-102.
4. Elin, R.J., *ASSESSMENT OF MAGNESIUM STATUS*. Clinical Chemistry, 1987. **33**(11): p. 1965-1970.
5. Moe, S.M., *Disorders involving calcium, phosphorus, and magnesium*. Primary Care, 2008. **35**(2): p. 215-+.
6. Martindale, L. and F.W. Heaton, *Magnesium deficiency in the adult rat*. Biochemical Journal, 1964. **92**(1): p. 119-126.
7. Castiglioni, S., et al., *Magnesium and Osteoporosis: Current State of Knowledge and Future Research Directions*. Nutrients, 2013. **5**(8): p. 3022-3033.
8. Rude, R.K., et al., *Magnesium deficiency: Effect on bone and mineral metabolism in the mouse*. Calcified Tissue International, 2003. **72**(1): p. 32-41.
9. Rude, R.K., et al., *Immunolocalization of RANKL is Increased and OPG Decreased During Dietary Magnesium Deficiency in the Rat*. Nutrition & Metabolism, 2005. **2**: p. 24-24.
10. Sojka, J.E. and C.M. Weaver, *Magnesium supplementation and osteoporosis*. Nutr Rev, 1995. **53**(3): p. 71-4.
11. Clark, I. and L. Bélanger, *The effects of alterations in dietary magnesium on calcium, phosphate and skeletal metabolism*. Calcified Tissue Research, 1967. **1**(1): p. 204-218.
12. Schwartz, R. and A.H. Reddi, *Influence of magnesium depletion on matrix-induced endochondral bone formation*. Calcif Tissue Int, 1979. **29**(1): p. 15-20.
13. Zofkova, I. and R.L. Kancheva, *The relationship between magnesium and calciotropic hormones*. Magnes Res, 1995. **8**(1): p. 77-84.
14. Carpenter, T.O., *Disturbances of vitamin D metabolism and action during clinical and experimental magnesium deficiency*. Magnes Res, 1988. **1**(3-4): p. 131-9.
15. Rude, R.K., et al., *Magnesium deficiency-induced osteoporosis in the rat: uncoupling of bone formation and bone resorption*. Magnes Res, 1999. **12**(4): p. 257-67.
16. Rude, R.K., F.R. Singer, and H.E. Gruber, *Skeletal and hormonal effects of magnesium deficiency*. J Am Coll Nutr, 2009. **28**(2): p. 131-41.
17. Seo, J.W. and T.J. Park, *Magnesium Metabolism*. Electrolytes & Blood Pressure : E & BP, 2008. **6**(2): p. 86-95.
18. Saris, N.E., et al., *Magnesium. An update on physiological, clinical and analytical aspects*. Clin Chim Acta, 2000. **294**(1-2): p. 1-26.

19. Vormann, J., *Magnesium: nutrition and metabolism*. Mol Aspects Med, 2003. **24**(1-3): p. 27-37.
20. Saggese, G., et al., *BONE DEMINERALIZATION AND IMPAIRED MINERAL METABOLISM IN INSULIN-DEPENDENT DIABETES-MELLITUS - A POSSIBLE ROLE OF MAGNESIUM-DEFICIENCY*. Helvetica Paediatrica Acta, 1989. **43**(5-6): p. 405-414.
21. Wallach, S., *Effects of magnesium on skeletal metabolism*. Magnes Trace Elem, 1990. **9**(1): p. 1-14.
22. Jones, G., *Early Life Nutrition and Bone Development in Children*, in *Early Nutrition: Impact on Short- and Long-Term Health*, H. VanGoudoever, S. Guandalini, and R.E. Kleinman, Editors. 2011, Karger: Basel. p. 227-236.
23. Luthringer, B.J.C., F. Feyerabend, and R. Willumeit-Romer, *Magnesium-based implants: a mini-review*. Magnesium Research, 2014. **27**(4): p. 142-154.
24. Mittal, R., et al., *Use of bio-resorbable implants for stabilisation of distal radius fractures: the United Kingdom patients' perspective*. Injury-International Journal of the Care of the Injured, 2005. **36**(2): p. 333-338.
25. Hermawan, H. and D. Mantovani, *Degradable metallic biomaterials: the concept, current developments and future directions*. Minerva Biotechnologica, 2009. **21**(4): p. 207-216.
26. Claes, L.E., *Mechanical characterization of biodegradable implants*. Clinical Materials, 1992. **10**(1): p. 41-46.
27. Gonzalo, N. and C. Macaya, *Absorbable stent: focus on clinical applications and benefits*. Vascular Health and Risk Management, 2012. **8**: p. 125-132.
28. Castellani, C., et al., *Bone-implant interface strength and osseointegration: Biodegradable magnesium alloy versus standard titanium control*. Acta Biomater, 2011. **7**(1): p. 432-40.
29. Bressan, E., et al., *Nanostructured Surfaces of Dental Implants*. International Journal of Molecular Sciences, 2013. **14**(1): p. 1918-1931.
30. Biggs, M.J.P., et al., *Interactions with nanoscale topography: Adhesion quantification and signal transduction in cells of osteogenic and multipotent lineage*. Journal of Biomedical Materials Research Part A, 2009. **91A**(1): p. 195-208.
31. Lambotte, A.L., *Utilisation du magnésium comme matériel perdu dans l'ostéosynthèse*. Bulletins et Mémoires de la Société de Chirurgie de Paris, 1932. **28**: p. 1325–1359.
32. Witte, F., et al., *In vivo corrosion of four magnesium alloys and the associated bone response*. Biomaterials, 2005. **26**(17): p. 3557-63.
33. Witte, F., et al., *Degradable biomaterials based on magnesium corrosion*. Current Opinion in Solid State & Materials Science, 2008. **12**(5-6): p. 63-72.
34. Clarke, B., *Normal bone anatomy and physiology*. Clin J Am Soc Nephrol, 2008. **3 Suppl 3**: p. S131-9.
35. Lee, J.H. and J.Y. Cho, *Proteomics approaches for the studies of bone metabolism*. BMB Rep, 2014. **47**(3): p. 141-8.
36. Hadjidakis, D.J. and Androulakis, II, *Bone remodeling*. Ann N Y Acad Sci, 2006. **1092**: p. 385-96.
37. Phan, T.C., J. Xu, and M.H. Zheng, *Interaction between osteoblast and osteoclast: impact in bone disease*. Histol Histopathol, 2004. **19**(4): p. 1325-44.

38. Franks, C.M., *HANDBOOK OF CLINICAL BEHAVIOR-THERAPY WITH THE ELDERLY CLIENT - WISOCKI,PA.* Journal of Behavior Therapy and Experimental Psychiatry, 1993. **24**(3): p. 269-269.
39. Cooper, C., G. Campion, and L.J. Melton, 3rd, *Hip fractures in the elderly: a world-wide projection.* Osteoporos Int, 1992. **2**(6): p. 285-9.
40. Reginster, J.Y. and N. Burlet, *Osteoporosis: a still increasing prevalence.* Bone, 2006. **38**(2 Suppl 1): p. S4-9.
41. Marie, P.J., *Transcription factors controlling osteoblastogenesis.* Arch Biochem Biophys, 2008. **473**(2): p. 98-105.
42. Fantner, G.E., et al., *Influence of the degradation of the organic matrix on the microscopic fracture behavior of trabecular bone.* Bone, 2004. **35**(5): p. 1013-22.
43. Tiaden, A.N., et al., *Human serine protease HTRA1 positively regulates osteogenesis of human bone marrow-derived mesenchymal stem cells and mineralization of differentiating bone-forming cells through the modulation of extracellular matrix protein.* Stem Cells, 2012. **30**(10): p. 2271-82.
44. Zberg, B., P.J. Uggowitzer, and J.F. Loffler, *MgZnCa glasses without clinically observable hydrogen evolution for biodegradable implants.* Nat Mater, 2009. **8**(11): p. 887-91.
45. Jahn, K., et al., *Intramedullary Mg2Ag nails augment callus formation during fracture healing in mice.* Acta Biomater, 2016. **36**: p. 350-60.
46. Shive, M.S. and J.M. Anderson, *Biodegradation and biocompatibility of PLA and PLGA microspheres.* Adv Drug Deliv Rev, 1997. **28**(1): p. 5-24.
47. Lehr, H.A., et al., *In vitro effects of oxidized low density lipoprotein on CD11b/CD18 and L-selectin presentation on neutrophils and monocytes with relevance for the in vivo situation.* The American Journal of Pathology, 1995. **146**(1): p. 218-227.
48. Anderson, J.M., A. Rodriguez, and D.T. Chang, *Foreign body reaction to biomaterials.* Semin Immunol, 2008. **20**(2): p. 86-100.
49. Wilson, C.J., et al., *Mediation of biomaterial-cell interactions by adsorbed proteins: a review.* Tissue Eng, 2005. **11**(1-2): p. 1-18.
50. McDonald, W.H. and J.R. Yates, 3rd, *Shotgun proteomics and biomarker discovery.* Dis Markers, 2002. **18**(2): p. 99-105.
51. Toyama, B.H. and M.W. Hetzer, *Protein homeostasis: live long, won't prosper.* Nat Rev Mol Cell Biol, 2013. **14**(1): p. 55-61.
52. Berg JM, T.J., Stryer L, *Biochemistry. 5th edition. Protein Structure and Function*, ed. W.H. Freeman. Vol. Chapter 3. 2002, New York.
53. *Proteomics, transcriptomics: what's in a name?* Nature, 1999. **402**(6763): p. 715.
54. Wilkins, M.R., et al., *Progress with proteome projects: why all proteins expressed by a genome should be identified and how to do it.* Biotechnol Genet Eng Rev, 1996. **13**: p. 19-50.
55. Chothia, C., et al., *Evolution of the protein repertoire.* Science, 2003. **300**(5626): p. 1701-3.
56. Fenn, J.B., et al., *Electrospray ionization for mass spectrometry of large biomolecules.* Science, 1989. **246**(4926): p. 64-71.
57. Aebersold, R. and M. Mann, *Mass spectrometry-based proteomics.* Nature, 2003. **422**(6928): p. 198-207.
58. Ong, S.E. and M. Mann, *Mass spectrometry-based proteomics turns quantitative.* Nat Chem Biol, 2005. **1**(5): p. 252-62.

59. Bantscheff, M., et al., *Quantitative mass spectrometry in proteomics: a critical review*. Anal Bioanal Chem, 2007. **389**(4): p. 1017-31.
60. Canas, B., et al., *Mass spectrometry technologies for proteomics*. Brief Funct Genomic Proteomic, 2006. **4**(4): p. 295-320.
61. Chait, B.T., *Chemistry. Mass spectrometry: bottom-up or top-down?* Science, 2006. **314**(5796): p. 65-6.
62. Patel, V.J., et al., *A comparison of labeling and label-free mass spectrometry-based proteomics approaches*. J Proteome Res, 2009. **8**(7): p. 3752-9.
63. Shevchenko, A., et al., *Mass spectrometric sequencing of proteins silver-stained polyacrylamide gels*. Anal Chem, 1996. **68**(5): p. 850-8.
64. Shevchenko, A., et al., *In-gel digestion for mass spectrometric characterization of proteins and proteomes*. Nat Protoc, 2006. **1**(6): p. 2856-60.
65. Switzar, L., M. Giera, and W.M. Niessen, *Protein digestion: an overview of the available techniques and recent developments*. J Proteome Res, 2013. **12**(3): p. 1067-77.
66. Panchaud, A., et al., *Experimental and computational approaches to quantitative proteomics: status quo and outlook*. J Proteomics, 2008. **71**(1): p. 19-33.
67. Dephoure, N. and S.P. Gygi, *Hyperplexing: a method for higher-order multiplexed quantitative proteomics provides a map of the dynamic response to rapamycin in yeast*. Sci Signal, 2012. **5**(217): p. rs2.
68. Latosinska, A., et al., *Comparative Analysis of Label-Free and 8-Plex iTRAQ Approach for Quantitative Tissue Proteomic Analysis*. PLoS One, 2015. **10**(9): p. e0137048.
69. Wang, M., et al., *Label-free mass spectrometry-based protein quantification technologies in proteomic analysis*. Brief Funct Genomic Proteomic, 2008. **7**(5): p. 329-39.
70. Zhang, B., et al., *Detecting differential and correlated protein expression in label-free shotgun proteomics*. J Proteome Res, 2006. **5**(11): p. 2909-18.
71. Washburn, M.P., R.R. Ulaszek, and J.R. Yates, 3rd, *Reproducibility of quantitative proteomic analyses of complex biological mixtures by multidimensional protein identification technology*. Anal Chem, 2003. **75**(19): p. 5054-61.
72. Hawkrige, A.M., *CHAPTER 1 Practical Considerations and Current Limitations in Quantitative Mass Spectrometry-based Proteomics*, in *Quantitative Proteomics*. 2014, The Royal Society of Chemistry. p. 1-25.
73. Wasinger, V.C., M. Zeng, and Y. Yau, *Current status and advances in quantitative proteomic mass spectrometry*. Int J Proteomics, 2013. **2013**: p. 180605.
74. Deracinois, B., et al., *Comparative and Quantitative Global Proteomics Approaches: An Overview*. Proteomes, 2013. **1**(3): p. 180.
75. Fischer, J., et al., *Improved cytotoxicity testing of magnesium materials*. Materials Science and Engineering: B, 2011. **176**(11): p. 830-834.
76. Steurer, S., et al., *MALDI imaging-based identification of prognostically relevant signals in bladder cancer using large-scale tissue microarrays*. Urol Oncol, 2014. **32**(8): p. 1225-33.
77. Lakhkar, N.J., et al., *Bone formation controlled by biologically relevant inorganic ions: role and controlled delivery from phosphate-based glasses*. Adv Drug Deliv Rev, 2013. **65**(4): p. 405-20.

78. Tang, C.H., et al., *Enhancement of fibronectin fibrillogenesis and bone formation by basic fibroblast growth factor via protein kinase C-dependent pathway in rat osteoblasts*. *Mol Pharmacol*, 2004. **66**(3): p. 440-9.
79. Owens, R.J. and F.E. Baralle, *Mapping the collagen-binding site of human fibronectin by expression in Escherichia coli*. *Embo j*, 1986. **5**(11): p. 2825-30.
80. Mosher, J.X.a.D., *The Extracellular Matrix: an Overview, Biology of Extracellular Matrix, Chapter 2: Fibronectin and Other Adhesive Glycoproteins*, in *Springer-Verlag Berlin Heidelberg*. 2011.
81. Kim, S., et al., *The effect of fibronectin-coated implant on canine osseointegration*. *J Periodontal Implant Sci*, 2011. **41**(5): p. 242-7.
82. Zhang, W.B. and L. Wang, *Label-free quantitative proteome analysis of skeletal tissues under mechanical load*. *J Cell Biochem*, 2009. **108**(3): p. 600-11.
83. Lieu, S., et al., *Impaired remodeling phase of fracture repair in the absence of matrix metalloproteinase-2*. *Dis Model Mech*, 2011. **4**(2): p. 203-11.
84. Visse, R. and H. Nagase, *Matrix metalloproteinases and tissue inhibitors of metalloproteinases: structure, function, and biochemistry*. *Circ Res*, 2003. **92**(8): p. 827-39.
85. Egeblad, M. and Z. Werb, *New functions for the matrix metalloproteinases in cancer progression*. *Nat Rev Cancer*, 2002. **2**(3): p. 161-74.
86. Henle, P., G. Zimmermann, and S. Weiss, *Matrix metalloproteinases and failed fracture healing*. *Bone*, 2005. **37**(6): p. 791-8.
87. Martignetti, J.A., et al., *Mutation of the matrix metalloproteinase 2 gene (MMP2) causes a multicentric osteolysis and arthritis syndrome*. *Nat Genet*, 2001. **28**(3): p. 261-5.
88. Nagase, H., R. Visse, and G. Murphy, *Structure and function of matrix metalloproteinases and TIMPs*. *Cardiovasc Res*, 2006. **69**(3): p. 562-73.
89. Hatori, K., et al., *Osteoblasts and osteocytes express MMP2 and -8 and TIMP1, -2, and -3 along with extracellular matrix molecules during appositional bone formation*. *Anat Rec A Discov Mol Cell Evol Biol*, 2004. **277**(2): p. 262-71.
90. Bord, S., et al., *Tissue inhibitor of matrix metalloproteinase-1 (TIMP-1) distribution in normal and pathological human bone*. *Bone*, 1999. **24**(3): p. 229-35.
91. Jensen, E.D., et al., *p68 (Ddx5) interacts with Runx2 and regulates osteoblast differentiation*. *J Cell Biochem*, 2008. **103**(5): p. 1438-51.
92. Kasap, M., et al., *Comparative Proteome Analysis of hAT-MSCs Isolated from Chronic Renal Failure Patients with Differences in Their Bone Turnover Status*. *PLoS One*, 2015. **10**(11): p. e0142934.
93. Honore, B., et al., *Heterogeneous nuclear ribonucleoproteins H, H', and F are members of a ubiquitously expressed subfamily of related but distinct proteins encoded by genes mapping to different chromosomes*. *J Biol Chem*, 1995. **270**(48): p. 28780-9.
94. Foster, L.J., et al., *Differential expression profiling of membrane proteins by quantitative proteomics in a human mesenchymal stem cell line undergoing osteoblast differentiation*. *Stem Cells*, 2005. **23**(9): p. 1367-77.
95. Han, C., et al., *Rat cortex and hippocampus-derived soluble factors for the induction of adipose-derived mesenchymal stem cells into neuron-like cells*. *Cell Biol Int*, 2014. **38**(6): p. 768-76.

96. Li, Y., et al., *Nicotinamide phosphoribosyltransferase (Nampt) affects the lineage fate determination of mesenchymal stem cells: a possible cause for reduced osteogenesis and increased adipogenesis in older individuals.* J Bone Miner Res, 2011. **26**(11): p. 2656-64.
97. Nakalekha, C., et al., *Increased bone mass in adult prostacyclin-deficient mice.* J Endocrinol, 2010. **204**(2): p. 125-33.
98. Ryan, Z.C., et al., *Enhanced prostacyclin formation and Wnt signaling in sclerostin deficient osteocytes and bone.* Biochem Biophys Res Commun, 2014. **448**(1): p. 83-8.
99. Tuncbilek, G., P. Korkusuz, and F. Ozgur, *Effects of iloprost on calvarial sutures.* J Craniofac Surg, 2008. **19**(6): p. 1472-80.
100. Besio, R., et al., *Lack of prolidase causes a bone phenotype both in human and in mouse.* Bone, 2015. **72**: p. 53-64.
101. Hata, K., et al., *Paraspeckle protein p54nrb links Sox9-mediated transcription with RNA processing during chondrogenesis in mice.* J Clin Invest, 2008. **118**(9): p. 3098-108.
102. Vairo, F., et al., *Diagnostic and treatment strategies in mucopolysaccharidosis VI.* Appl Clin Genet, 2015. **8**: p. 245-55.
103. Sarkar, J., et al., *V-type ATPase proton pump expression during enamel formation.* Matrix Biol, 2016. **52-54**: p. 234-45.
104. Lacruz, R.S., et al., *Adaptor protein complex 2-mediated, clathrin-dependent endocytosis, and related gene activities, are a prominent feature during maturation stage amelogenesis.* J Bone Miner Res, 2013. **28**(3): p. 672-87.
105. Barton, N.W., et al., *Replacement therapy for inherited enzyme deficiency--macrophage-targeted glucocerebrosidase for Gaucher's disease.* N Engl J Med, 1991. **324**(21): p. 1464-70.
106. Rosenthal, D.I., et al., *Enzyme replacement therapy for Gaucher disease: skeletal responses to macrophage-targeted glucocerebrosidase.* Pediatrics, 1995. **96**(4 Pt 1): p. 629-37.
107. Niu, X., et al., *mRNA and protein expression of the angiogenesis-related genes EDIL3, AMOT and ECM1 in mesenchymal stem cells in psoriatic dermis.* Clin Exp Dermatol, 2016. **41**(5): p. 533-40.
108. Wall, M.E., et al., *Human adipose-derived adult stem cells upregulate palladin during osteogenesis and in response to cyclic tensile strain.* Am J Physiol Cell Physiol, 2007. **293**(5): p. C1532-8.
109. Leung, R., et al., *Filamin A regulates monocyte migration through Rho small GTPases during osteoclastogenesis.* J Bone Miner Res, 2010. **25**(5): p. 1077-91.
110. Mezawa, M., et al., *Filamin A regulates the organization and remodeling of the pericellular collagen matrix.* Faseb j, 2016.
111. Kelm, R.J., Jr., et al., *Osteonectin in matrix remodeling. A plasminogen-osteonectin-collagen complex.* J Biol Chem, 1994. **269**(48): p. 30147-53.
112. Daci, E., et al., *Increased bone formation in mice lacking plasminogen activators.* J Bone Miner Res, 2003. **18**(7): p. 1167-76.
113. Nair, R.R., J. Solway, and D.D. Boyd, *Expression cloning identifies transgelin (SM22) as a novel repressor of 92-kDa type IV collagenase (MMP-9) expression.* J Biol Chem, 2006. **281**(36): p. 26424-36.
114. Assinder, S.J., J.A. Stanton, and P.D. Prasad, *Transgelin: an actin-binding protein and tumour suppressor.* Int J Biochem Cell Biol, 2009. **41**(3): p. 482-6.

115. Kaartinen, M.T., et al., *Cross-linking of osteopontin by tissue transglutaminase increases its collagen binding properties*. J Biol Chem, 1999. **274**(3): p. 1729-35.
116. Choi, S.J., et al., *Identification of human asparaginyl endopeptidase (legumain) as an inhibitor of osteoclast formation and bone resorption*. J Biol Chem, 1999. **274**(39): p. 27747-53.
117. Annunen, P., H. Autio-Harminen, and K.I. Kivirikko, *The novel type II prolyl 4-hydroxylase is the main enzyme form in chondrocytes and capillary endothelial cells, whereas the type I enzyme predominates in most cells*. J Biol Chem, 1998. **273**(11): p. 5989-92.
118. Saad, F.A. and J.G. Hofstaetter, *Proteomic analysis of mineralising osteoblasts identifies novel genes related to bone matrix mineralisation*. Int Orthop, 2011. **35**(3): p. 447-51.
119. Gruenwald, K., et al., *Sc65 is a novel endoplasmic reticulum protein that regulates bone mass homeostasis*. J Bone Miner Res, 2014. **29**(3): p. 666-75.
120. Cabral, W.A., et al., *Prolyl 3-hydroxylase 1 deficiency causes a recessive metabolic bone disorder resembling lethal/severe osteogenesis imperfecta*. Nat Genet, 2007. **39**(3): p. 359-65.
121. Hudson, D.M. and D.R. Eyre, *Collagen prolyl 3-hydroxylation: a major role for a minor post-translational modification?* Connect Tissue Res, 2013. **54**(4-5): p. 245-51.
122. Baldridge, D., et al., *CRTAP and LEPRE1 mutations in recessive osteogenesis imperfecta*. Hum Mutat, 2008. **29**(12): p. 1435-42.
123. Barnes, A.M., et al., *Deficiency of cartilage-associated protein in recessive lethal osteogenesis imperfecta*. N Engl J Med, 2006. **355**(26): p. 2757-64.
124. Haag, J. and T. Aigner, *Identification of calponin 3 as a novel Smad-binding modulator of BMP signaling expressed in cartilage*. Exp Cell Res, 2007. **313**(16): p. 3386-94.
125. Flemming, A., et al., *A Conditional Knockout Mouse Model Reveals That Calponin-3 Is Dispensable for Early B Cell Development*. PLoS One, 2015. **10**(6): p. e0128385.
126. Brown, M.A., et al., *Genetic control of bone density and turnover: role of the collagen 1alpha1, estrogen receptor, and vitamin D receptor genes*. J Bone Miner Res, 2001. **16**(4): p. 758-64.
127. Trejo, P. and F. Rauch, *Osteogenesis imperfecta in children and adolescents-new developments in diagnosis and treatment*. Osteoporos Int, 2016.
128. Alexopoulos, L.G., et al., *Developmental and osteoarthritic changes in Col6a1-knockout mice: biomechanics of type VI collagen in the cartilage pericellular matrix*. Arthritis Rheum, 2009. **60**(3): p. 771-9.
129. Hong, D., et al., *Quantitative proteomic analysis of dexamethasone-induced effects on osteoblast differentiation, proliferation, and apoptosis in MC3T3-E1 cells using SILAC*. Osteoporos Int, 2011. **22**(7): p. 2175-86.
130. Yoon, K., R. Buenaga, and G.A. Rodan, *Tissue specificity and developmental expression of rat osteopontin*. Biochem Biophys Res Commun, 1987. **148**(3): p. 1129-36.
131. Sandberg, M., H. Autio-Harminen, and E. Vuorio, *Localization of the expression of types I, III, and IV collagen, TGF-beta 1 and c-fos genes in developing human calvarial bones*. Dev Biol, 1988. **130**(1): p. 324-34.

132. Malaval, L., et al., *Cellular expression of bone-related proteins during in vitro osteogenesis in rat bone marrow stromal cell cultures*. J Cell Physiol, 1994. **158**(3): p. 555-72.
133. Owen, T.A., et al., *Progressive development of the rat osteoblast phenotype in vitro: reciprocal relationships in expression of genes associated with osteoblast proliferation and differentiation during formation of the bone extracellular matrix*. J Cell Physiol, 1990. **143**(3): p. 420-30.
134. Poulsen, R.C., P.J. Moughan, and M.C. Kruger, *Long-chain polyunsaturated fatty acids and the regulation of bone metabolism*. Exp Biol Med (Maywood), 2007. **232**(10): p. 1275-88.
135. Bando, Y., et al., *Expression of epidermal fatty acid binding protein (E-FABP) in septoclasts in the growth plate cartilage of mice*. J Mol Histol, 2014. **45**(5): p. 507-18.
136. Storch, J. and A.E. Thumser, *The fatty acid transport function of fatty acid-binding proteins*. Biochim Biophys Acta, 2000. **1486**(1): p. 28-44.
137. Layne, M.D., et al., *Role of macrophage-expressed adipocyte fatty acid binding protein in the development of accelerated atherosclerosis in hypercholesterolemic mice*. Faseb j, 2001. **15**(14): p. 2733-5.
138. Srivastava, S.K., et al., *Aldose reductase inhibition suppresses oxidative stress-induced inflammatory disorders*. Chem Biol Interact, 2011. **191**(1-3): p. 330-8.
139. Srivastava, S., et al., *Lipid peroxidation product, 4-hydroxynonenal and its conjugate with GSH are excellent substrates of bovine lens aldose reductase*. Biochem Biophys Res Commun, 1995. **217**(3): p. 741-6.
140. Catala, A., *Lipid peroxidation of membrane phospholipids generates hydroxy-alkenals and oxidized phospholipids active in physiological and/or pathological conditions*. Chem Phys Lipids, 2009. **157**(1): p. 1-11.
141. Moriishi, T., et al., *Overexpression of BCLXL in Osteoblasts Inhibits Osteoblast Apoptosis and Increases Bone Volume and Strength*. J Bone Miner Res, 2016. **31**(7): p. 1366-80.
142. Brahim-Horn, M.C., et al., *Knockout of Vdac1 activates hypoxia-inducible factor through reactive oxygen species generation and induces tumor growth by promoting metabolic reprogramming and inflammation*. Cancer Metab, 2015. **3**: p. 8.
143. Morrison, D.J., M.A. English, and J.D. Licht, *WT1 induces apoptosis through transcriptional regulation of the proapoptotic Bcl-2 family member Bak*. Cancer Res, 2005. **65**(18): p. 8174-82.
144. Miyagi, S., et al., *The TIF1beta-HP1 system maintains transcriptional integrity of hematopoietic stem cells*. Stem Cell Reports, 2014. **2**(2): p. 145-52.
145. Polo, S.E., et al., *Regulation of DNA-end resection by hnRNPU-like proteins promotes DNA double-strand break signaling and repair*. Mol Cell, 2012. **45**(4): p. 505-16.
146. Angst, B.D., C. Marozzi, and A.I. Magee, *The cadherin superfamily: diversity in form and function*. J Cell Sci, 2001. **114**(Pt 4): p. 629-41.
147. Wheelock, M.J. and K.R. Johnson, *Cadherins as modulators of cellular phenotype*. Annu Rev Cell Dev Biol, 2003. **19**: p. 207-35.
148. Andreeva, A.V. and M.A. Kutuzov, *Cadherin 13 in cancer*. Genes Chromosomes Cancer, 2010. **49**(9): p. 775-90.

149. Brocker, C., et al., *Aldehyde dehydrogenase 7A1 (ALDH7A1) is a novel enzyme involved in cellular defense against hyperosmotic stress*. J Biol Chem, 2010. **285**(24): p. 18452-63.
150. Banfi, G., E.L. Iorio, and M.M. Corsi, *Oxidative stress, free radicals and bone remodeling*. Clin Chem Lab Med, 2008. **46**(11): p. 1550-5.
151. Boveris, A. and B. Chance, *The mitochondrial generation of hydrogen peroxide. General properties and effect of hyperbaric oxygen*. Biochem J, 1973. **134**(3): p. 707-16.
152. Hensley, K., et al., *Reactive oxygen species, cell signaling, and cell injury*. Free Radic Biol Med, 2000. **28**(10): p. 1456-62.
153. Fraser, J.H., et al., *Hydrogen peroxide, but not superoxide, stimulates bone resorption in mouse calvariae*. Bone, 1996. **19**(3): p. 223-6.
154. Suda, N., et al., *Participation of oxidative stress in the process of osteoclast differentiation*. Biochim Biophys Acta, 1993. **1157**(3): p. 318-23.
155. Sontakke, A.N. and R.S. Tare, *A duality in the roles of reactive oxygen species with respect to bone metabolism*. Clin Chim Acta, 2002. **318**(1-2): p. 145-8.
156. Addis, M.F., et al., *Generation of high-quality protein extracts from formalin-fixed, paraffin-embedded tissues*. Proteomics, 2009. **9**(15): p. 3815-23.
157. Geoui, T., et al., *Extraction of proteins from formalin-fixed, paraffin-embedded tissue using the Qproteome extraction technique and preparation of tryptic peptides for liquid chromatography/mass spectrometry analysis*. Curr Protoc Mol Biol, 2010. **Chapter 10**: p. Unit 10.27.1-12.
158. Sprung, R.W., Jr., et al., *Equivalence of protein inventories obtained from formalin-fixed paraffin-embedded and frozen tissue in multidimensional liquid chromatography-tandem mass spectrometry shotgun proteomic analysis*. Mol Cell Proteomics, 2009. **8**(8): p. 1988-98.
159. Guo, H., et al., *An efficient procedure for protein extraction from formalin-fixed, paraffin-embedded tissues for reverse phase protein arrays*. Proteome Sci, 2012. **10**(1): p. 56.
160. De Jonge, H.W., et al., *Embedding of large specimens in glycol methacrylate: prerequisites for multi-signal detection and high-resolution imaging*. Microsc Res Tech, 2005. **66**(1): p. 25-30.
161. Gerrits, P.O. and R.W. Horobin, *Glycol methacrylate embedding for light microscopy: Basic principles and trouble-shooting*. Journal of Histotechnology, 1996. **19**(4): p. 297-311.
162. Hanstede, J.G. and P.O. Gerrits, *The effects of embedding in water-soluble plastics on the final dimensions of liver sections*. J Microsc, 1983. **131**(Pt 1): p. 79-86.
163. Erben, R.G., *Embedding of bone samples in methylmethacrylate: an improved method suitable for bone histomorphometry, histochemistry, and immunohistochemistry*. J Histochem Cytochem, 1997. **45**(2): p. 307-13.
164. Cipriano, A.F., et al., *Cytocompatibility and early inflammatory response of human endothelial cells in direct culture with Mg-Zn-Sr alloys*. Acta Biomater, 2016.
165. Luthringer, B.J., F. Feyerabend, and R. Willumeit-Romer, *Magnesium-based implants: a mini-review*. Magnes Res, 2014. **27**(4): p. 142-54.
166. Staiger, M.P., et al., *Magnesium and its alloys as orthopedic biomaterials: a review*. Biomaterials, 2006. **27**(9): p. 1728-34.

167. Li, N. and Y.F. Zheng, *Novel Magnesium Alloys Developed for Biomedical Application: A Review*. Journal of Materials Science & Technology, 2013. **29**(6): p. 489-502.
168. Li, Z., et al., *The development of binary Mg-Ca alloys for use as biodegradable materials within bone*. Biomaterials, 2008. **29**(10): p. 1329-44.
169. Salahshoor, M. and Y.B. Guo, *Biodegradable Orthopedic Magnesium-Calcium (MgCa) Alloys, Processing, and Corrosion Performance*. Materials, 2012. **5**(1): p. 135-155.
170. Gray, J.J., *The interaction of proteins with solid surfaces*. Curr Opin Struct Biol, 2004. **14**(1): p. 110-5.
171. Elwing, H., *Protein absorption and ellipsometry in biomaterial research*. Biomaterials, 1998. **19**(4-5): p. 397-406.
172. Wohl, A.P., et al., *Extracellular Regulation of Bone Morphogenetic Protein Activity by the Microfibril Component Fibrillin-1*. J Biol Chem, 2016. **291**(24): p. 12732-46.
173. Arteaga-Solis, E., et al., *Material and mechanical properties of bones deficient for fibrillin-1 or fibrillin-2 microfibrils*. Matrix Biol, 2011. **30**(3): p. 188-94.
174. Smaldone, S., et al., *Fibrillin-1 Regulates Skeletal Stem Cell Differentiation by Modulating TGFbeta Activity Within the Marrow Niche*. J Bone Miner Res, 2016. **31**(1): p. 86-97.
175. Smaldone, S., et al., *Fibrillin-1 microfibrils influence adult bone marrow hematopoiesis*. Matrix Biol, 2016. **52-54**: p. 88-94.
176. Smaldone, S. and F. Ramirez, *Fibrillin microfibrils in bone physiology*. Matrix Biol, 2016. **52-54**: p. 191-7.
177. Walji, T.A., et al., *Characterization of metabolic health in mouse models of fibrillin-1 perturbation*. Matrix Biol, 2016.
178. Guo, P., et al., *Cartilage oligomeric matrix protein gene multilayers inhibit osteogenic differentiation and promote chondrogenic differentiation of mesenchymal stem cells*. Int J Mol Sci, 2014. **15**(11): p. 20117-33.
179. Guo, P., et al., *Effects of cartilage oligomeric matrix protein on bone morphogenetic protein-2-induced differentiation of mesenchymal stem cells*. Orthop Surg, 2014. **6**(4): p. 280-7.
180. Lim, S.S., et al., *Local delivery of COMP-angiopoietin 1 accelerates new bone formation in rat calvarial defects*. J Biomed Mater Res A, 2015. **103**(9): p. 2942-51.
181. Ishida, K., et al., *Cartilage oligomeric matrix protein enhances osteogenesis by directly binding and activating bone morphogenetic protein-2*. Bone, 2013. **55**(1): p. 23-35.
182. Chatakun, P., et al., *The effect of five proteins on stem cells used for osteoblast differentiation and proliferation: a current review of the literature*. Cell Mol Life Sci, 2014. **71**(1): p. 113-42.
183. Morgan, J.M., et al., *Regulation of tenascin expression in bone*. J Cell Biochem, 2011. **112**(11): p. 3354-63.
184. Chen, Y., Z.F. Chen, and F. He, *[Tenascin-C knockdown suppresses osteoblast differentiation and promotes osteoporosis in mice by inhibiting Wnt signaling]*. Nan Fang Yi Ke Da Xue Xue Bao, 2016. **36**(8): p. 1117-22.
185. Niemeier, A., et al., *Expression of LRP1 by human osteoblasts: a mechanism for the delivery of lipoproteins and vitamin K1 to bone*. J Bone Miner Res, 2005. **20**(2): p. 283-93.

186. Vinik, Y., et al., *The mammalian lectin galectin-8 induces RANKL expression, osteoclastogenesis, and bone mass reduction in mice*. *Elife*, 2015. **4**: p. e05914.
187. Zhou, W.P., et al., *THE INFLUENCE AND REGULATORY MECHANISM OF Y-BOX BINDING PROTEIN 1 IN OSTEOSARCOMA AND ITS SIGNIFICANCE*. *J Biol Regul Homeost Agents*, 2015. **29**(2): p. 485-91.
188. Fujiwara-Okada, Y., et al., *Y-box binding protein-1 regulates cell proliferation and is associated with clinical outcomes of osteosarcoma*. *Br J Cancer*, 2013. **108**(4): p. 836-47.
189. Xu, M., et al., *miR-382 inhibits osteosarcoma metastasis and relapse by targeting Y box-binding protein 1*. *Mol Ther*, 2015. **23**(1): p. 89-98.
190. McMichael, B.K. and B.S. Lee, *Tropomyosin 4 regulates adhesion structures and resorptive capacity in osteoclasts*. *Exp Cell Res*, 2008. **314**(3): p. 564-73.
191. McMichael, B.K., et al., *Tropomyosin isoforms localize to distinct microfilament populations in osteoclasts*. *Bone*, 2006. **39**(4): p. 694-705.
192. Liu, C.Y., et al., *Keratocan-deficient mice display alterations in corneal structure*. *J Biol Chem*, 2003. **278**(24): p. 21672-7.
193. Kao, W.W. and C.Y. Liu, *The use of transgenic and knock-out mice in the investigation of ocular surface cell biology*. *Ocul Surf*, 2003. **1**(1): p. 5-19.
194. Igwe, J.C., et al., *Keratocan is expressed by osteoblasts and can modulate osteogenic differentiation*. *Connect Tissue Res*, 2011. **52**(5): p. 401-7.
195. Merle, B. and P. Garnero, *The multiple facets of periostin in bone metabolism*. *Osteoporos Int*, 2012. **23**(4): p. 1199-212.
196. Heo, S.C., et al., *Periostin accelerates bone healing mediated by human mesenchymal stem cell-embedded hydroxyapatite/tricalcium phosphate scaffold*. *PLoS One*, 2015. **10**(3): p. e0116698.
197. Gerbaix, M., et al., *Periostin expression contributes to cortical bone loss during unloading*. *Bone*, 2015. **71**: p. 94-100.
198. Muhammad, S.I., et al., *Upregulation of genes related to bone formation by gamma-amino butyric acid and gamma-oryzanol in germinated brown rice is via the activation of GABAB-receptors and reduction of serum IL-6 in rats*. *Clin Interv Aging*, 2013. **8**: p. 1259-71.
199. Yu, H., et al., *Targeted disruption of TGFBI in mice reveals its role in regulating bone mass and bone size through periosteal bone formation*. *Calcif Tissue Int*, 2012. **91**(1): p. 81-7.
200. Lauing, K.L., et al., *Aggrecan is required for growth plate cytoarchitecture and differentiation*. *Dev Biol*, 2014. **396**(2): p. 224-36.
201. Wigner, N.A., et al., *Functional role of Runx3 in the regulation of aggrecan expression during cartilage development*. *J Cell Physiol*, 2013. **228**(11): p. 2232-42.
202. Lei, Y., et al., *Hydroxyapatite and calcified elastin induce osteoblast-like differentiation in rat aortic smooth muscle cells*. *Exp Cell Res*, 2014. **323**(1): p. 198-208.
203. Lee, E.R., et al., *Enzymes active in the areas undergoing cartilage resorption during the development of the secondary ossification center in the tibiae of rats ages 0-21 days: I. Two groups of proteinases cleave the core protein of aggrecan*. *Dev Dyn*, 2001. **222**(1): p. 52-70.
204. Salas, S., et al., *Molecular characterization of the response to chemotherapy in conventional osteosarcomas: predictive value of HSD17B10 and IFITM2*. *Int J Cancer*, 2009. **125**(4): p. 851-60.

205. Man, T.K., et al., *Expression profiles of osteosarcoma that can predict response to chemotherapy*. *Cancer Res*, 2005. **65**(18): p. 8142-50.
206. Jernberg, E., et al., *Characterization of prostate cancer bone metastases according to expression levels of steroidogenic enzymes and androgen receptor splice variants*. *PLoS One*, 2013. **8**(11): p. e77407.
207. Yilmaz, A.D., et al., *Association of Matrilin-3 Gene Polymorphism with Temporomandibular Joint Internal Derangement*. *Genet Test Mol Biomarkers*, 2016. **20**(10): p. 563-568.
208. Muttigi, M.S., et al., *Matrilin-3 Role in Cartilage Development and Osteoarthritis*. *Int J Mol Sci*, 2016. **17**(4).
209. Cheung, C.S., et al., *Human monoclonal antibody fragments targeting matrilin-3 in growth plate cartilage*. *Pharm Res*, 2015. **32**(7): p. 2439-49.
210. Kung, L.H., et al., *Increased classical endoplasmic reticulum stress is sufficient to reduce chondrocyte proliferation rate in the growth plate and decrease bone growth*. *PLoS One*, 2015. **10**(2): p. e0117016.
211. Shahzad, M., et al., *Expression of genes encoding matrilin-3 and cyclin-I during the impairment and recovery of chicken growth plate in tibial dyschondroplasia*. *Avian Dis*, 2014. **58**(3): p. 468-73.
212. Abe, T., et al., *Regulation of osteoclast homeostasis and inflammatory bone loss by MFG-E8*. *J Immunol*, 2014. **193**(3): p. 1383-91.
213. Sinnigen, K., et al., *Loss of milk fat globule-epidermal growth factor 8 (MFG-E8) in mice leads to low bone mass and accelerates ovariectomy-associated bone loss by increasing osteoclastogenesis*. *Bone*, 2015. **76**: p. 107-14.
214. Hajishengallis, G., *MFG-E8, a novel homeostatic regulator of osteoclastogenesis*. *Inflamm Cell Signal*, 2014. **1**(5): p. e285.
215. Ait-Oufella, H., et al., *Lactadherin deficiency leads to apoptotic cell accumulation and accelerated atherosclerosis in mice*. *Circulation*, 2007. **115**(16): p. 2168-77.
216. Hoemann, C.D., H. El-Gabalawy, and M.D. McKee, *In vitro osteogenesis assays: influence of the primary cell source on alkaline phosphatase activity and mineralization*. *Pathol Biol (Paris)*, 2009. **57**(4): p. 318-23.
217. Bab, I. and M. Chorev, *Osteogenic growth peptide: from concept to drug design*. *Biopolymers*, 2002. **66**(1): p. 33-48.
218. Shinozaki, T. and K.P. Pritzker, *Regulation of alkaline phosphatase: implications for calcium pyrophosphate dihydrate crystal dissolution and other alkaline phosphatase functions*. *J Rheumatol*, 1996. **23**(4): p. 677-83.
219. Lieder, R. and O.E. Sigurjonsson, *The Effect of Recombinant Human Interleukin-6 on Osteogenic Differentiation and YKL-40 Expression in Human, Bone Marrow-Derived Mesenchymal Stem Cells*. *Biores Open Access*, 2014. **3**(1): p. 29-34.
220. Haglund, L., et al., *Proteomic analysis of the LPS-induced stress response in rat chondrocytes reveals induction of innate immune response components in articular cartilage*. *Matrix Biol*, 2008. **27**(2): p. 107-18.
221. Zhou, Y., et al., *Chitinase 3-like 1 suppresses injury and promotes fibroproliferative responses in Mammalian lung fibrosis*. *Sci Transl Med*, 2014. **6**(240): p. 240ra76.
222. Laine, C.M., et al., *A novel splice mutation in PLS3 causes X-linked early onset low-turnover osteoporosis*. *J Bone Miner Res*, 2015. **30**(3): p. 510-8.
223. Fahiminiya, S., et al., *Osteoporosis caused by mutations in PLS3: clinical and bone tissue characteristics*. *J Bone Miner Res*, 2014. **29**(8): p. 1805-14.

224. van Dijk, F.S., et al., *PLS3 mutations in X-linked osteoporosis with fractures*. N Engl J Med, 2013. **369**(16): p. 1529-36.
225. Morsczeck, C., et al., *Proteomic analysis of osteogenic differentiation of dental follicle precursor cells*. Electrophoresis, 2009. **30**(7): p. 1175-84.
226. Widmer, C., et al., *Molecular basis for the action of the collagen-specific chaperone Hsp47/SERPINH1 and its structure-specific client recognition*. Proc Natl Acad Sci U S A, 2012. **109**(33): p. 13243-7.
227. Barbirato, C., et al., *Analysis of FKBP10, SERPINH1, and SERPINF1 genes in patients with osteogenesis imperfecta*. Genet Mol Res, 2016. **15**(3).
228. Marshall, C., et al., *A novel homozygous variant in SERPINH1 associated with a severe, lethal presentation of osteogenesis imperfecta with hydranencephaly*. Gene, 2016.
229. Valadares, E.R., et al., *What is new in genetics and osteogenesis imperfecta classification?* J Pediatr (Rio J), 2014. **90**(6): p. 536-41.
230. Zhang, Z.L., et al., *The identification of novel mutations in COL1A1, COL1A2, and LEPRE1 genes in Chinese patients with osteogenesis imperfecta*. J Bone Miner Metab, 2012. **30**(1): p. 69-77.
231. Urano, T., et al., *Single-nucleotide polymorphism in the hyaluronan and proteoglycan link protein 1 (HAPLN1) gene is associated with spinal osteophyte formation and disc degeneration in Japanese women*. Eur Spine J, 2011. **20**(4): p. 572-7.
232. Zhang, X., et al., *Epidermal growth factor receptor (EGFR) signaling regulates epiphyseal cartilage development through beta-catenin-dependent and -independent pathways*. J Biol Chem, 2013. **288**(45): p. 32229-40.
233. Morita, S., et al., *Expression of p53, p16, cyclin D1, epidermal growth factor receptor and Notch1 in patients with temporal bone squamous cell carcinoma*. Int J Clin Oncol, 2016.
234. Zhang, X., et al., *Epidermal growth factor receptor plays an anabolic role in bone metabolism in vivo*. J Bone Miner Res, 2011. **26**(5): p. 1022-34.
235. Li, Y., et al., *A fibrillar collagen gene, Col11a1, is essential for skeletal morphogenesis*. Cell, 1995. **80**(3): p. 423-30.
236. Mio, F., et al., *A functional polymorphism in COL11A1, which encodes the alpha 1 chain of type XI collagen, is associated with susceptibility to lumbar disc herniation*. Am J Hum Genet, 2007. **81**(6): p. 1271-7.
237. Hufnagel, S.B., et al., *A novel dominant COL11A1 mutation resulting in a severe skeletal dysplasia*. Am J Med Genet A, 2014. **164a**(10): p. 2607-12.
238. Abe, N., et al., *The complete primary structure of the long form of mouse alpha 1(IX) collagen chain and its expression during limb development*. Biochim Biophys Acta, 1994. **1204**(1): p. 61-7.
239. Nakata, K., et al., *Osteoarthritis associated with mild chondrodysplasia in transgenic mice expressing alpha 1(IX) collagen chains with a central deletion*. Proc Natl Acad Sci U S A, 1993. **90**(7): p. 2870-4.
240. Schminke, B., et al., *The pathology of bone tissue during peri-implantitis*. J Dent Res, 2015. **94**(2): p. 354-61.
241. Guo, D., et al., *Fluid shear stress changes cell morphology and regulates the expression of ATP6V1A and TCIRG1 mRNA in rat osteoclasts*. Mol Med Rep, 2010. **3**(1): p. 173-8.
242. Garcia-Gomez, A., et al., *RAF265, a dual BRAF and VEGFR2 inhibitor, prevents osteoclast formation and resorption. Therapeutic implications*. Invest New Drugs, 2013. **31**(1): p. 200-5.

243. Wallimann, T., et al., *Some new aspects of creatine kinase (CK): compartmentation, structure, function and regulation for cellular and mitochondrial bioenergetics and physiology*. *Biofactors*, 1998. **8**(3-4): p. 229-34.
244. Chen, J., et al., *RANKL up-regulates brain-type creatine kinase via poly(ADP-ribose) polymerase-1 during osteoclastogenesis*. *J Biol Chem*, 2010. **285**(47): p. 36315-21.
245. Jones, S.E. and C. Jomary, *Clusterin*. *International Journal of Biochemistry & Cell Biology*, 2002. **34**(5): p. 427-431.
246. Wilson, M.R. and S.B. Easterbrook-Smith, *Clusterin is a secreted mammalian chaperone*. *Trends in Biochemical Sciences*, 2000. **25**(3): p. 95-98.
247. Takayanagi, H., *Mechanistic insight into osteoclast differentiation in osteoimmunology*. *J Mol Med (Berl)*, 2005. **83**(3): p. 170-9.
248. Choi, B., et al., *Secretory clusterin inhibits osteoclastogenesis by attenuating M-CSF-dependent osteoclast precursor cell proliferation*. *Biochem Biophys Res Commun*, 2014. **450**(1): p. 105-9.
249. Karhukorpi, E.K., *Carbonic anhydrase II in rat acid secreting cells: comparison of osteoclasts with gastric parietal cells and kidney intercalated cells*. *Acta Histochem*, 1991. **90**(1): p. 11-20.
250. Marks, S.C., Jr., *Osteoclast biology: lessons from mammalian mutations*. *Am J Med Genet*, 1989. **34**(1): p. 43-54.
251. Shah, G.N., et al., *Carbonic anhydrase II deficiency syndrome (osteopetrosis with renal tubular acidosis and brain calcification): novel mutations in CA2 identified by direct sequencing expand the opportunity for genotype-phenotype correlation*. *Hum Mutat*, 2004. **24**(3): p. 272.
252. Vassalle, C. and A. Mazzone, *Bone loss and vascular calcification: A bi-directional interplay?* *Vascul Pharmacol*, 2016.
253. Berberi, A., et al., *Mesenchymal stem cells with osteogenic potential in human maxillary sinus membrane: an in vitro study*. *Clin Oral Investig*, 2016.
254. Okawa, R., et al., *Gene therapy improves dental manifestations in hypophosphatasia model mice*. *J Periodontal Res*, 2016.
255. Sage, A.P., et al., *Hyperphosphatemia-induced nanocrystals upregulate the expression of bone morphogenetic protein-2 and osteopontin genes in mouse smooth muscle cells in vitro*. *Kidney Int*, 2011. **79**(4): p. 414-22.
256. Singh, R., et al., *Modulation of infection-mediated migration of neutrophils and CXCR2 trafficking by osteopontin*. *Immunology*, 2016.
257. Kim, Y., et al., *Comparison of Osteogenesis between Adipose-Derived Mesenchymal Stem Cells and Their Sheets on Poly-epsilon-Caprolactone/beta-Tricalcium Phosphate Composite Scaffolds in Canine Bone Defects*. *Stem Cells Int*, 2016. **2016**: p. 8414715.
258. Li, M., et al., *Stimulatory effects of the degradation products from Mg-Ca-Sr alloy on the osteogenesis through regulating ERK signaling pathway*. *Sci Rep*, 2016. **6**: p. 32323.
259. Dabrowska, A.M., et al., *Fetuin-A (AHSG) and its usefulness in clinical practice. Review of the literature*. *Biomed Pap Med Fac Univ Palacky Olomouc Czech Repub*, 2015. **159**(3): p. 352-9.
260. Brylka, L. and W. Jahnen-Dechent, *The role of fetuin-A in physiological and pathological mineralization*. *Calcif Tissue Int*, 2013. **93**(4): p. 355-64.

261. Seto, J., et al., *Accelerated growth plate mineralization and foreshortened proximal limb bones in fetuin-A knockout mice*. PLoS One, 2012. **7**(10): p. e47338.
262. Mattinzoli, D., et al., *FGF23-regulated production of Fetuin-A (AHSG) in osteocytes*. Bone, 2016. **83**: p. 35-47.
263. Suleimenova, D., et al., *Gene expression profiles in guided bone regeneration using combinations of different biomaterials: a pilot animal study*. Clin Oral Implants Res, 2016.
264. Fink, H.A., et al., *Association of Fetuin-A With Incident Fractures in Community-Dwelling Older Adults: The Cardiovascular Health Study*. J Bone Miner Res, 2015. **30**(8): p. 1394-402.
265. Rajasekaran, S., et al., *Genetic susceptibility of lumbar degenerative disc disease in young Indian adults*. Eur Spine J, 2015. **24**(9): p. 1969-75.
266. Mototani, H., et al., *Identification of sequence polymorphisms in CALM2 and analysis of association with hip osteoarthritis in a Japanese population*. J Bone Miner Metab, 2010. **28**(5): p. 547-53.
267. Carafoli, E., *Intracellular calcium homeostasis*. Annu Rev Biochem, 1987. **56**: p. 395-433.
268. Mototani, H., et al., *A functional single nucleotide polymorphism in the core promoter region of CALM1 is associated with hip osteoarthritis in Japanese*. Hum Mol Genet, 2005. **14**(8): p. 1009-17.
269. Yang, Z., et al., *Dysregulated COL3A1 and RPL8, RPS16, and RPS23 in Disc Degeneration Revealed by Bioinformatics Methods*. Spine (Phila Pa 1976), 2015. **40**(13): p. E745-51.
270. Zhang, Z., J. Zhang, and J. Xiao, *Selenoproteins and selenium status in bone physiology and pathology*. Biochim Biophys Acta, 2014. **1840**(11): p. 3246-3256.
271. Thaler, R., et al., *Extra-cellular matrix suppresses expression of the apoptosis mediator Fas by epigenetic DNA methylation*. Apoptosis, 2010. **15**(6): p. 728-37.
272. Touw, I.P., *Game of clones: the genomic evolution of severe congenital neutropenia*. Hematology Am Soc Hematol Educ Program, 2015. **2015**: p. 1-7.
273. Xia, J., et al., *Prevalence of mutations in ELANE, GFI1, HAX1, SBDS, WAS and G6PC3 in patients with severe congenital neutropenia*. Br J Haematol, 2009. **147**(4): p. 535-42.
274. Horwitz, M.S., et al., *ELANE mutations in cyclic and severe congenital neutropenia: genetics and pathophysiology*. Hematol Oncol Clin North Am, 2013. **27**(1): p. 19-41, vii.
275. Shim, Y.J., et al., *Novel ELANE gene mutation in a Korean girl with severe congenital neutropenia*. J Korean Med Sci, 2011. **26**(12): p. 1646-9.
276. Dinand, V., et al., *Hepatic hemangioendothelioma in an infant with severe congenital neutropenia*. J Pediatr Hematol Oncol, 2012. **34**(4): p. 298-300.
277. Donadieu, J., et al., *Congenital neutropenia: diagnosis, molecular bases and patient management*. Orphanet J Rare Dis, 2011. **6**: p. 26.
278. Kim, H.J., et al., *Paternal Somatic Mosaicism of a Novel Frameshift Mutation in ELANE Causing Severe Congenital Neutropenia*. Pediatr Blood Cancer, 2015. **62**(12): p. 2229-31.
279. Kurnikova, M., et al., *Four novel ELANE mutations in patients with congenital neutropenia*. Pediatr Blood Cancer, 2011. **57**(2): p. 332-5.








280. Juranovic, T., et al., *Hematogones in the peripheral blood of a 5(1/2)-month-old boy with cyclic neutropenia due to heterozygous, novel ELANE gene mutation p.Q97P, c.290 A>C*. *Pediatr Dev Pathol*, 2014. **17**(5): p. 393-9.
281. Shu, Z., et al., *Clinical characteristics of severe congenital neutropenia caused by novel ELANE gene mutations*. *Pediatr Infect Dis J*, 2015. **34**(2): p. 203-7.
282. Nair, S.P., et al., *Molecular chaperones stimulate bone resorption*. *Calcif Tissue Int*, 1999. **64**(3): p. 214-8.
283. Hou, Y., et al., *[Expression of Cdc7 and mcm2 as a marker for proliferation and prognosis in diffuse large B cell lymphoma]*. *Zhonghua Zhong Liu Za Zhi*, 2011. **33**(12): p. 911-5.
284. Maslov, A.Y., et al., *Stem/progenitor cell-specific enhanced green fluorescent protein expression driven by the endogenous Mcm2 promoter*. *Stem Cells*, 2007. **25**(1): p. 132-8.
285. Lampert, I.A., et al., *The expression of minichromosome maintenance protein-2 in normal and abnormal megakaryocytes and comparison with the proliferative marker Ki-67*. *Br J Haematol*, 2005. **131**(4): p. 490-4.
286. Suzuki, S., et al., *Overexpression of MCM2 in myelodysplastic syndromes: association with bone marrow cell apoptosis and peripheral cytopenia*. *Exp Mol Pathol*, 2012. **92**(1): p. 160-6.
287. Zdolsek, J., J.W. Eaton, and L. Tang, *Histamine release and fibrinogen adsorption mediate acute inflammatory responses to biomaterial implants in humans*. *J Transl Med*, 2007. **5**: p. 31.
288. Mandracchia, V.J., K.J. John, and S.M. Sanders, *Wound healing*. *Clin Podiatr Med Surg*, 2001. **18**(1): p. 1-33.
289. Eriksson, C. and H. Nygren, *Polymorphonuclear leukocytes in coagulating whole blood recognize hydrophilic and hydrophobic titanium surfaces by different adhesion receptors and show different patterns of receptor expression*. *J Lab Clin Med*, 2001. **137**(4): p. 296-302.
290. Jenney, C.R. and J.M. Anderson, *Adsorbed serum proteins responsible for surface dependent human macrophage behavior*. *J Biomed Mater Res*, 2000. **49**(4): p. 435-47.
291. Tang, L. and J.W. Eaton, *Inflammatory responses to biomaterials*. *Am J Clin Pathol*, 1995. **103**(4): p. 466-71.
292. Wettero, J., T. Bengtsson, and P. Tengvall, *Complement activation on immunoglobulin G-coated hydrophobic surfaces enhances the release of oxygen radicals from neutrophils through an actin-dependent mechanism*. *J Biomed Mater Res*, 2000. **51**(4): p. 742-51.
293. Bergman, A.J. and K. Zygourakis, *Migration of lymphocytes on fibronectin-coated surfaces: temporal evolution of migratory parameters*. *Biomaterials*, 1999. **20**(23-24): p. 2235-44.
294. Groth, T., G. Altankov, and K. Klosz, *Adhesion of human peripheral blood lymphocytes is dependent on surface wettability and protein preadsorption*. *Biomaterials*, 1994. **15**(6): p. 423-8.
295. Guyton AC, H.J., *Textbook of Medical Physiology*. . 11th edition. ed. 2006, Philadelphia: Elsevier Saunders.
296. Morrissey, J.H., E. Bianco-Fisher, and M. Parizi-Robinson, *Factor VIIa-antithrombin complexes in plasma*. *Blood*, 2001. **98**(11): p. 526A-526A.
297. Dahlback, B., *Blood coagulation*. *Lancet*, 2000. **355**(9215): p. 1627-32.
298. Sase, T., et al., *Haemostatic abnormalities and thrombotic disorders in malignant lymphoma*. *Thromb Haemost*, 2005. **93**(1): p. 153-9.


















299. Alamelu, J., et al., *Acquired prothrombin deficiency in a patient with follicular lymphoma*. *Haemophilia*, 2008. **14**(3): p. 634-6.
300. Forastiero, R., *Bleeding in the antiphospholipid syndrome*. *Hematology*, 2012. **17 Suppl 1**: p. S153-5.
301. Houbouyan, L., et al., *[Antiprothrombinase anticoagulant and acquired prothrombin deficiency in childhood viral pathology. Spontaneous recovery]*. *Arch Fr Pediatr*, 1984. **41**(6): p. 417-20.
302. Degen, S.J. and W.Y. Sun, *The biology of prothrombin*. *Crit Rev Eukaryot Gene Expr*, 1998. **8**(2): p. 203-24.
303. Mumford, A.D., et al., *Bleeding symptoms and coagulation abnormalities in 337 patients with AL-amyloidosis*. *Br J Haematol*, 2000. **110**(2): p. 454-60.
304. Girolami, A., et al., *A family with factor X deficiency from Argentina: a compound heterozygosis because of the combination of a new mutation (Gln138Arg) with an already known one (Glu350Lys)*. *Blood Coagul Fibrinolysis*, 2016. **27**(6): p. 732-6.
305. Liu, W., et al., *[Acquired coagulation factor X deficiency: three cases report and literature review]*. *Zhonghua Xue Ye Xue Za Zhi*, 2014. **35**(7): p. 633-6.
306. Ashrani, A.A., et al., *Lupus anticoagulant associated with transient severe factor X deficiency: a report of two patients presenting with major bleeding complications*. *Br J Haematol*, 2003. **121**(4): p. 639-42.
307. Enjeti, A.K., M. Walsh, and M. Seldon, *Spontaneous major bleeding in acquired factor X deficiency secondary to AL-amyloidosis*. *Haemophilia*, 2005. **11**(5): p. 535-8.
308. Jones, K.S., *Effects of biomaterial-induced inflammation on fibrosis and rejection*. *Semin Immunol*, 2008. **20**(2): p. 130-6.
309. Tolosano, E., et al., *Defective recovery and severe renal damage after acute hemolysis in hemopexin-deficient mice*. *Blood*, 1999. **94**(11): p. 3906-14.
310. Vercellotti, G.M., et al., *Hepatic Overexpression of Hemopexin Inhibits Inflammation and Vascular Stasis in Murine Models of Sickle Cell Disease*. *Mol Med*, 2016. **22**.
311. Rank, G., et al., *Novel roles for erythroid Ankyrin-1 revealed through an ENU-induced null mouse mutant*. *Blood*, 2009. **113**(14): p. 3352-62.
312. Chen, Z., et al., *Mitigation of sensory and motor deficits by acrolein scavenger phenelzine in a rat model of spinal cord contusive injury*. *J Neurochem*, 2016. **138**(2): p. 328-38.
313. Okada, Y., et al., *TRPA1 is required for TGF-beta signaling and its loss blocks inflammatory fibrosis in mouse corneal stroma*. *Lab Invest*, 2014. **94**(9): p. 1030-41.
314. Lodeiro, M., et al., *Aggregation of the Inflammatory S100A8 Precedes Abeta Plaque Formation in Transgenic APP Mice: Positive Feedback for S100A8 and Abeta Productions*. *J Gerontol A Biol Sci Med Sci*, 2016.
315. Newton, R.A. and N. Hogg, *The human S100 protein MRP-14 is a novel activator of the beta 2 integrin Mac-1 on neutrophils*. *J Immunol*, 1998. **160**(3): p. 1427-35.
316. Boyd, J.H., et al., *S100A8 and S100A9 mediate endotoxin-induced cardiomyocyte dysfunction via the receptor for advanced glycation end products*. *Circ Res*, 2008. **102**(10): p. 1239-46.
317. Ehlermann, P., et al., *Increased proinflammatory endothelial response to S100A8/A9 after preactivation through advanced glycation end products*. *Cardiovasc Diabetol*, 2006. **5**: p. 6.

319. <http://www.dguv.de/ifa/gestis/gestis-biostoffdatenbank/index-2.jsp>.
320. <http://www.sigmaaldrich.com/germany.html>.

7 Risk and safety statement

According to Globally Harmonized System of Classification and Labelling of Chemicals (GHS), below is a list of potentially hazardous chemicals with the respective hazard and precautionary statements [319, 320].

Compound	GHS symbol	GHS hazard	Hazard statements	Precautionary statements
Methanol (LiChrosolv®)		GHS02 GHS06 GHS08	H225-H301 + H311 + H331- H370	P210-P240-P280-P302 + P352 -P304 + P340-P308 + P310-P403 + P233
Phenylmethyl- sulfonyl fluorid		GHS05 GHS06,	H301-H314	P280-P301 + P310 + P330-P303 + P361 + P353-P304 + P340 + P310-P305 + P351 + P338
Ammonium bicarbonate		GHS07	H302	P301 + P312 + P330
Protease inhibitor, Complete Tablet Mini, EDTA-free		GHS07	H315-H319	P264-P280-P302 + P352- P332 + P313-P337 + P313-P362 + P364
Dithiotrietol		GHS07	H302-H315- H319-H335	P261-P305 + P351 + P338
Iodoacetamide		GHS06 GHS08	H301-H317- H334	P261-P280-P301 + P310- P342 + P311
Formic acid		GHS02	H226-H302- H314-H331-	P210-P280-P301 + P330 + P331-P304 + P340-

	 	GHS06 GHS05	EUH071	P305 + P351 + P338- P308 + P310
Trifluoroacetic acid	 	GHS05 GHS07	H314-H332- H412	P273-P280-P305 + P351 + P338-P310
Acetonitril (LiChrosolv®)	 	GHS02, GHS07	H225- H302+H312+H 332-H319	P210-P240-P302 + P352- P305 + P351 + P338- P403 + P233
Oligo™ R3 Bulk Medium		GHS07	H335	P261- P304+ P340-P 312- P403+ P233- P405
Isopropanole	 	GHS02 GHS07	H225-H319- H336	P210-P261-P305 + P351 + P338
(2-Methoxyethyl)- acetate	  	GHS02 GHS07 GHS08	H226-H302 + H312 + H332- H360FD	P201-P210-P261-P280- P308 + P313-P370 + P378
Xylol	  	GHS02 GHS07 GHS08	H226-H304- H312 + H332- H315-H319- H335-H373- H412	P210-P260-P280-P301 + P310-P305 + P351 + P338-P370 + P378
Trypsin	 	GHS07 GHS08	H315-H319- H334-H317- H335	P264-P272-P280- P302+P352- P305+P351+P338-P312

GHS hazard statements

H225	Highly Flammable liquid and vapour
H226	Flammable liquid and vapour
H301	Toxic if swallowed
H302	Harmful if swallowed
H304	May be fatal if swallowed and enters airways
H311	May be fatal if swallowed and enters airways
H312	Harmful in contact with skin
H314	May be fatal if swallowed and enters airways
H315	Causes skin irritation
H317	May be fatal if swallowed and enters airways
H319	Causes serious eye irritation
H331	May be fatal if swallowed and enters airways
H332	Harmful if inhaled
H334	May be fatal if swallowed and enters airways
H335	May cause respiratory irritation
H336	May cause drowsiness or dizziness
H370	Causes damage to organs
H373	Causes damage to organs through prolonged or repeated exposure
H412	Harmful to aquatic life with long lasting effects
EUH071	Corrosive to the respiratory tract
H360FD	May damage fertility. May damage the unborn child

GHS precautionary statements

P201	Obtain special instructions before use
P210	Keep away from heat/sparks/open flames/hot surfaces. — No smoking
P240	Ground/bond container and receiving equipment
P260	Do not breathe dust/fume/gas/mist/vapours/spray
P261	Avoid breathing dust/fume/gas/mist/vapours/spray
P264	Wash hands thoroughly after handling
P272	Contaminated work clothing should not be allowed out of the workplace
P273	Avoid release to the environment
P280	Wear protective gloves/protective clothing/eye protection/face protection
P310	Immediately call a POISON CENTER or doctor/physician
P312	Call a POISON CENTER or doctor/physician if you feel unwell

P330	Rinse mouth
P405	Store locked upP301 + P310
P302 + P352	IF ON SKIN: wash with plenty of soap and water
P304 + P340	IF INHALED: Remove victim to fresh air and Keep at rest in a position comfortable for breathing
P301 + P310	IF SWALLOWED: Immediately call a POISON CENTER or doctor/physician
P301 + P312	IF SWALLOWED: call a POISON CENTER or doctor/physician IF you feel unwell
P304 + P340	IF INHALED: Remove victim to fresh air and Keep at rest in a position comfortable for breathing
P308 + P310	IF exposed or concerned: Immediately call a POISON CENTER or doctor/physician
P308 + P313	IF exposed or concerned: Get medical advice/attention
P332 + P313	IF SKIN irritation occurs: Get medical advice/attention
P337 + P313	IF eye irritation persists: Get medical advice/attention
P342 + P311	IF experiencing respiratory symptoms: call a POISON CENTER or doctor/physician
P362 + P364	Take off contaminated clothing and wash it before reuse
P370 + P378	In case of fire: Use ... for extinction
P403 + P233	Store in a well-ventilated place. Keep container tightly closed
P303 + P361 + P353	IF ON SKIN (or hair): Remove/Take off Immediately all contaminated clothing. Rinse SKIN with water/shower
P305 + P351 + P338	IF IN EYES: Rinse cautiously with water for several minutes. Remove contact lenses, if present and easy to do. Continue rinsing.
P301 + P330 + P331	IF SWALLOWED: Rinse mouth. Do NOT induce vomiting

8 Acknowledgement

First of all, I would like to sincerely thank my supervisor Prof. Hartmut Schlüter for giving me the opportunity to work in his group at *Universitätsklinikum Hamburg-Eppendorf* (UKE), guiding and teaching me how to be analytical in research.

Immense gratitude to Prof. Betzel who served as my co-supervisor and I am grateful for all his great scientific advices.

Financial support by the Helmholtz Virtual Institute MetBioMat is gratefully acknowledged.

I would like to thank the head of the MetBioMat project Prof. Regine Willumeit-Römer for her helpful advices and discussions during meetings and workshops.

Many thanks to the working group of Prof. Weinberg at *Medical University of Graz* (MUG), Prof. Hesse, Dr. Andreas Gasser, and Dr. Katharina Jähn at *Universitätsklinikum Hamburg-Eppendorf* (UKE), Anna Burmester and Adela-Helvia Martinez-Sanchez at Helmholtzzentrum Geesthacht (HZG) for preparing the bone samples for method development, bone tissue for the *in vivo* experiments, and cells used in the *in vitro* experiment respectively.

Manka, thanks a lot for your wonderful help in data interpretation and correction of my thesis, and all the nice and enjoyable time that we had. I am thankful to Parnian for German translation of the summary and for all the fantastic pleasant and good moments that we had during these years. I am also thankful to my sister Azam for all her support during these years.

Also, I am grateful to Marcus for his help in data processing and statistical analysis of the data. I would like to say thank you to all of our group members, Fritz, Sönke, David, Andrey, Refat, Pascal, Laura, Olga, Atef, and Yudong for the nice atmosphere in the lab.

Finally, I would like to thank my beloved family, my lovely mom and my great dad, my sisters and my brother, Azam, Elahe, Mahtab, and Reza for their support and endless love in my life.

9 Declaration

I hereby declare on oath, that I have written the present dissertation by my own and have not used other than the acknowledged resources and aids. The submitted written version corresponds to the version on the electronic storage medium. I hereby declare that I have not previously applied or pursued for a doctorate (Ph.D. studies).

Hamburg, 24.01.2017

city and date

signature